



TECHNISCHE  
UNIVERSITÄT  
WIEN

# Diplomarbeit

---

## Application of a High-Throughput Microfermentation System for the Screening of Protein Refolding

---

Ausgeführt am Institut für Verfahrenstechnik, Umwelttechnik und  
Technische Biowissenschaften der Technischen Universität Wien

unter Anleitung von

**Associate Prof. Dipl.-Ing. Dr.nat.techn. Oliver Spadiut**

und

**Dipl.-Ing. Julian Ebner**

**Diana Claudia Humer, MSc**

durch

**Viktor Rubus, BSc**

Wien, 05.09.2021

# 1 Acknowledgments

First of all, I would like to thank **Oliver Spadiut**, whose expertise, continuously constructive input and support made the completion of this challenging and unusual project possible. Your positive and straightforward attitude makes a huge difference in the academic world.

I would like to thank **Julian Ebner** for being my direct supervisor and leading the project in a determined but subtle way, always leaving room for my personal ideas and ready to give elaborate advice. I will not forget your standard phrase “Das wird toll!” at the beginning of experiments.

I would like to thank **Diana Humer** for her involvement in the organization of the project, despite being preoccupied by the final phase of her doctorate. Without your multichannel pipettes, I would still be pipetting.

I would like to thank **Robert Klausser** for his pragmatic support in the practical realization of countless experiments and the whole IBD research group for providing an enjoyable working atmosphere.

I would like to thank my family and friends for their support throughout my studies and for their understanding for my notoriously full calendar. I would especially like to thank my mother, **Katinka Gál**, for her endless support throughout my whole life, enabling all my achievements.

## 2 Abstract

Despite of manifold advantages of recombinant protein production in form of inclusion bodies (IBs), the two additionally required unit operations for IB processing, solubilization and refolding, present a bottleneck in the downstream process (DSP) due to their high complexity and low yields. To date, these unit operations are highly empirical and dependent on the protein of interest (POI), opposing the Quality-by-Design (QbD) paradigm. In this thesis, process analytical tools (PATs) for the in-process monitoring (IPM) and in-process control (IPC) of both unit operation steps are presented. Furthermore, a novel technique for the screening of protein refolding was developed that enables the control of critical process parameters (CPPs), which cannot be controlled by prevalent techniques.

The current analytical method of choice for the analysis of the solubilization process is sodium dodecyl sulfate polyacrylamide gel electrophoresis (SDS-PAGE) but a low selectivity, a low accuracy and a time-consuming application are making it unsuitable for the IPM and IPC of the solubilization process. An at-line reversed-phase liquid chromatography (RPLC) method for the monitoring of the target protein concentration during solubilization is presented. Compared to SDS-PAGE, the method exhibits a considerably shorter analysis time (8.1 min), a higher accuracy and meets all crucial criteria for the application as an IPM tool.

Versatile high throughput small-scale techniques for the screening of protein refolding parameters using a design of experiments (DoE) approach were reported recently. However, these techniques are incapable of controlling the CPPs refolding temperature and oxygen input. Additionally, the associated analytical tools for the characterization of the refolding process and the capabilities for the realization of fed-batch refolding are severely limited. To solve these problems, the feasibility of the application of the BioLector<sup>®</sup> Pro microfermentation system for the screening of protein refolding parameters was assessed for two proteins: green fluorescent protein (GFP) and horseradish peroxidase (HRP). The device has capabilities for the in-line monitoring of pH, dO<sub>2</sub> and fluorescence, while its microfluidic technology enables continuous feeding and pH regulation. The comparison to a conventional screening approach revealed that the screening outcome is fundamentally different, but the approach utilizing the BioLector<sup>®</sup> system is hypothesized to be more accurate and useful for screening experiments. Furthermore, the in-line analytics exhibit profound problems, and it was found that the microfluidic technology is not functional at an ambient temperature of 4 °C. Based on the findings of this feasibility study, six proposals are formulated with the goal to improve the application of the BioLector<sup>®</sup> Pro for the screening of protein refolding.

### 3 Table of Contents

1	Acknowledgments .....	1
2	Abstract.....	2
3	Table of Contents .....	3
4	Abbreviations .....	5
5	Introduction.....	6
6	At-Line RPLC Approach for Improved Analysis of the Solubilization Process.....	13
6.1	Introduction .....	13
6.2	Publication.....	14
6.3	Conclusion.....	32
7	Application of the BioLector® Pro for the Screening of Protein Refolding.....	33
7.1	Introduction .....	33
7.2	Materials and Methods .....	36
7.2.1	Chemicals and Software .....	36
7.2.2	Recombinant Production of IBs .....	36
7.2.2.1	GFP .....	36
7.2.2.2	HRP .....	36
7.2.3	Homogenization and Wash .....	36
7.2.3.1	GFP .....	36
7.2.3.2	HRP .....	37
7.2.4	Solubilization.....	37
7.2.4.1	GFP .....	37
7.2.4.2	HRP .....	37
7.2.5	Protein Refolding.....	37
7.2.5.1	Conventional Small-Scale Screening Experiments .....	37
7.2.5.1.1	GFP .....	37
7.2.5.1.2	HRP.....	38
7.2.5.2	BioLector® Pro Screening Experiments.....	39
7.2.5.2.1	GFP .....	39
7.2.5.2.2	HRP.....	40
7.2.6	Analytics.....	40
7.2.6.1	Off-line fluorescence .....	40
7.2.6.2	HRP Activity .....	40
7.2.6.3	In-Line Analytics .....	41
7.3	Results and Discussion .....	42

7.3.1	Comparison to Conventional Approach .....	42
7.3.1.1	Green Fluorescence Protein.....	42
7.3.1.2	Horseradish Peroxidase.....	45
7.3.1.3	Summary .....	51
7.3.2	Advantages of In-Line Analytics for Screening of Protein Refolding .....	52
7.3.2.1	In-Line Fluorescence Detection.....	52
7.3.2.2	In-Line pH Detection .....	56
7.3.2.2.1	Green Fluorescence Protein.....	57
7.3.2.2.2	Horseradish Peroxidase.....	58
7.3.2.2.3	Summary.....	59
7.3.2.3	In-Line dO <sub>2</sub> Detection.....	59
7.3.2.3.1	Green Fluorescence Protein.....	59
7.3.2.3.2	Horseradish Peroxidase.....	64
7.3.2.3.3	Summary.....	69
7.3.3	Advantages of a Continuous Feed for Screening of Protein Refolding .....	70
8	Conclusions of the Thesis.....	72
8.1	Goal One.....	72
8.2	Goal Two.....	72
8.3	Goal Three.....	72
8.4	Goal Four .....	73
9	Outlook.....	74
10	References.....	76

## 4 Abbreviations

---

ABTS	2,2'-azino-bis (3-ethylbenzothiazoline-6-sulfonic acid)
CH	Cysteine
CPP	Critical process parameter
CQA	Critical quality attributes
CSSC	Cystine
dO <sub>2</sub>	Dissolved oxygen [%]
DSP	Downstream process
DTT	Dithiothreitol
FDA	Food and drug administration
GFP	Green fluorescent protein
GSH	Reduced Glutathione
GSSG	Oxidized Glutathione
HIC	Hydrophobic interaction chromatography
HPLC	High Performance Liquid Chromatography
HRP	Horseradish peroxidase
IB	Inclusion body
IEC	Ion exchange chromatography
IPC	In-process control
IPM	In-process monitoring
IPTG	Isopropyl- $\beta$ -D-thiogalactopyranoside
LC	Liquid Chromatography
MLR	Multiple linear regression
MTP	Microtiter plate
PAT	Process analytical technology
POI	Protein of interest
PTM	Post-translational modification
QbD	Quality-by-Design
q <sub>s</sub>	Specific substrate uptake rate [g/g/h]
RB	Refolding buffer
RPLC	Reversed-phase liquid chromatography
SB	Solubilization buffer
SDS-PAGE	Sodium dodecyl sulfate polyacrylamide gel electrophoresis
SEC	Size exclusion chromatography
USP	Upstream process

---

## 5 Introduction

Inclusion Bodies (IBs) are insoluble agglomerations of partially folded-, misfolded- or unfolded proteins [1-3]. They are a frequent product of recombinant expression of heterologous proteins in bacteria like *Escherichia coli* and their formation is enhanced by the usage of strong promoters, which can lead to yields beyond 50 % of the total cellular protein. The central reasons for IB formation are high protein formation rates that transcend the protein folding rates of the host cell and the inability to form post-translational modifications (PTMs) required for the folding of heterologous proteins. An example for the latter phenomenon is the inhibition of disulfide bond formation due to the reducing characteristics of the cytoplasm [2]. The spheric, porous IBs are mainly formed in the polar regions of the rod-shaped *E. coli* cells and their diameter lies in a range of 50 - 800 nm [3].

Usually, the expression of a correctly folded POI in the soluble phase is aspired and achieved by optimizing the expression system, by expressing the POI as a fusion protein, by lowering the growth temperature or by adding various additives to the cultivation medium [1, 3, 4]. However, the perception of bacterial IBs shifted into a more positive direction in the last decades. This shift was caused on one hand by further research into the complex nature of IBs, which among others uncovered the presence of biological activity within IBs, and on the other hand by the development of applications as immobilized catalysts, scaffolds for tissue engineering or implantable depots for therapeutic proteins [3, 5]. Moreover, the expression in form of IBs has several advantages: (i) high purity, (ii) simple isolation, (iii) steric protection from proteolytic degradation caused by proteases, (iv) high expression levels and (v) the possibility to express proteins with toxic effects on the host organism in their native form [1]. Hence, the listed advantages can outweigh the disadvantage of a cumbersome protein refolding step, which is necessary for the downstream processing of IBs. Ultimately, the expression of recombinant proteins in form of IBs can even lead to more profitable downstream processing, therefore a wide range of recombinant products are produced as IBs nowadays. Prominent examples are  $\beta$ -Galactosidase, insulin or the major capsid protein of human papillomavirus type 16 (HPV 16 vaccine) [4].

The industrial production of biologically active proteins in form of IBs requires additional unit operations during the downstream process (DSP). At first the IBs are produced by a host organism during the upstream process (USP). Subsequently, the cells are harvested by centrifugation followed by cell lysis, isolation and subsequent washing of the isolated IBs. Afterwards the IBs are solubilized using chaotropic agents (e.g. guanidine hydrochloride, urea) or detergents resulting in denatured proteins. For proteins containing cysteines, the addition of reducing agents is imperative to break inter- or intramolecular disulfide bonds during the solubilization step. The solubilization step is followed by a protein refolding step, where the denatured protein is converted into its native, correctly folded form. Several methods for protein refolding can be applied (e.g. simple dilution, dialysis- or chromatographic methods), which are all based on an identical concept: (partial) removal of denaturing agents and optional addition of agents

which support the molecular refolding process. Due to their simplicity and low instrumental requirements, batch and fed-batch refolding based on dilution are the most common approaches for protein refolding. After the refolding process, the refolded proteins are subject to a purification step to reach the desired final purity [4, 6-10].

On the molecular level, there are several steps within the refolding process where the denatured protein is converted into its native form. In the initial phase of the process, intermediate structures are rapidly formed upon reduction of the denaturing agents, which is driven by the formation of secondary structures and interactions between hydrophobic patches. This is followed by a comparably slow conversion of the intermediate structures into the native protein structure. Simultaneously, the first order protein refolding reaction of the intermediate competes with an irreversible, second order aggregation reaction, leading to diminished refolding yields [6-8, 11]. Because of the nature of the second order reaction, in which two molecules are involved on the molecular level, the kinetics of aggregation reactions are promoted by high protein concentrations, hence the refolding yield is favored by low protein concentrations [8, 10]. However, considering the cost, time and effort of high dilutions caused by high buffer volumes and subsequent concentration steps in industrial scale applications, higher protein concentrations are desired for protein refolding processes. Thus, the optimal space-time yield of refolded protein needs to be determined empirically during the development of refolding processes [8, 12].

Proteins containing disulfide bridges in their tertiary structure require the presence of a redox system, which is composed of a reducing- and an oxidizing agent within the refolding buffer (RB). The purpose of the reducing agent is to break non-native disulfide bonds while the oxidizing agent promotes the formation of native and non-native disulfide bridges by increasing the oxidation rate. The presence of both antagonists causes a cycle of random pairing and separation of cysteine residues within the protein, resulting in the formation of the native disulfide bridges due to the corresponding, energetically favored native protein structure. This effect, known as “disulfide shuffling”, has shown to increase the refolding yield in comparison to an unpaired reducing agent. Prominent examples for redox systems are reduced- and oxidized glutathione (GSH/GSSG), dithiothreitol and oxidized glutathione (DTT/GSSG) or cysteine and cystine (CH/CSSC) [6, 8, 13]. An example for a recombinant protein that is expressed as IBs, has a high biopharmaceutical relevance and its refolding process is highly dependent on a redox system is the human growth factor rhVEGF [14].

Despite of the many advantages of IBs, the two additionally required unit operations, solubilization and refolding, present a bottleneck in IB processing due to their high complexity and low yields. Furthermore, these unit operations are highly empirical and depend heavily on the characteristics of the POI, opposing QbD principles [4, 14-17]. The core concept of the QbD approach is the assurance of product quality by a profound apprehension of the product and the ability to control the corresponding formulation and manufacturing variables adequately. The implementation of this approach for biopharmaceutical production processes was introduced by the International Conference



on Harmonization and is nowadays anticipated by major pharmaceutical regulatory organs [16].

Currently, sodium dodecyl sulfate polyacrylamide gel electrophoresis (SDS-PAGE) is performed for the analysis of the solubilization process, due to its high tolerance to harsh conditions that are presented by the high concentration of chaotropic agents during solubilization [18, 19]. Its separation principle, based on size, favors the analysis of proteins derived from microbial sources, considering impurities. Additionally, different stainings (e.g. Coomassie blue staining, silver staining) with diverse advantages have been established and sensitivity can be further increased by applying immunoblotting techniques [20]. However, the QbD paradigm for biopharmaceutical products requires PATs for IPC, for which SDS-PAGE is not suitable because of its time-consuming application [16]. Liquid Chromatography (LC) methods, on the other hand, require very low sample preparation- and analysis times, while displaying high accuracy for the analysis of biopharmaceuticals [21-23]. Hydrophobic interaction chromatography (HIC), ion exchange chromatography (IEC) and size exclusion chromatography (SEC) are established for recombinant protein analysis, but the high concentration of chaotropic agent required for solubilization still poses an obstacle for these methods [24, 25]. Reversed-phase liquid chromatography (RPLC) has been reported to tolerate the harsh conditions of the solubilization process [20]. Regarding the compatibility with mass spectrometry, robustness and high selectivity, RPLC appears to be a suitable technique for the in-process monitoring and respectively in-process control of protein solubilization processes [26, 27].

A major target of the QbD paradigm is an extensive knowledge on the product and its manufacturing process. Hence, the development of all unit operations of the production process must be invariably systematic, especially regarding the identification of process parameters that influence critical quality attributes (CQA). The design of experiments (DoE) approach is a reliable tool for the efficient selection of experiments and to systematically optimize such CPPs [16, 28]. The main advantages of a multivariate DoE approach over a univariate approach are the lower number of required experiments and the ability to observe interactions between the investigated parameters [28]. For protein refolding based on dilution (batch or fed-batch refolding), manifold process parameters need to be optimized. An overview of these process parameters is displayed in Table 1 [6, 8, 11, 28-32].

Table 1: Overview of process parameters subject to optimization during protein refolding [6, 8, 11, 28-32].

<b>Batch Refolding Process Parameters</b>
Protein concentration
Refolding time
pH value
Concentration of several buffer components and additives
Reducing- and oxidizing agent (redox system)
Denaturant (chaotrope; e.g. urea)
Aggregation inhibitor (moderate chaotrope; e.g. L-Arg)
Stabilizer (kosmotrope; e.g. sucrose)
Foldases and chaperones
Lipids for micelle and liposome formation
Buffer substance (e.g. Tris)
Concentration of coenzymes and cofactors
Oxygen input via $dO_2$ and reaction chamber gas composition
Temperature
Hydrostatic pressure
Geometry of refolding vessel (e.g. Reynolds number)
<b>Additional Process Parameters for Fed-Batch Refolding</b>
Supply of denatured protein or additives via feed
Feed profile (pulsed or continuous)
Characteristics of feed profiles (e.g intervals between pulses)

For the screening of these parameters several small-scale approaches have been reported. Humer et al. described screening experiments in 2 mL scale using reaction tubes for HRP. The quantification of the refolding results was conducted by off-line protein activity assays after the refolding process [12]. Wang et al. performed high-throughput screening experiments in 200  $\mu$ L scale using 96-well plates in combination with off-line differential scanning fluorimetry analysis, distributed over four measurements throughout the refolding process. For the validation of this approach, four proteins were used: interleukin-17A, the inhibitory receptor ligand of programmed death receptor 1, mouse double minute 2 homolog, and the receptor binding domain of hemagglutinin [33]. Vincentelli et al. developed automated screening experiments in 100  $\mu$ L scale to further increase the throughput. This approach was validated by 24 different proteins [34].

Although these approaches enable a high number of experiments within a short amount of time, they are not suitable for the screening of many CPPs. The CPPs which cannot be controlled adequately in these setups are the refolding temperature, the oxygen input and the hydrostatic pressure, while the screening of feed profiles is heavily restricted. The ability for the screening of pulsed feed profiles is extraordinarily laborious if no automation is applicable, while the screening for continuous feed profiles is entirely

impossible. The geometry of the refolding vessel can naturally only be investigated in appropriate larger scale vessels [28].

Furthermore, the analytical tools of these setups for the characterization of the refolding process are very limited and require sampling, which limits the number of measurements throughout the process considerably at this scale. Hence, there is a demand for IPM and IPC, not only for the solubilization process, but also for the refolding process. First, to gain more profound knowledge on the highly empirical protein refolding process and thereby improving the quality of the screening experiments as defined by the QbD paradigm. Second, to improve similarity to large-scale stirred tank reactors, in which large-scale refolding is performed, in order to improve the scale-up process by having the ability to compare CPPs between different scales.

Although having numerous differences in comparison to protein refolding, fermentation processes have been confronted with similar challenges. In the field of upstream processing, screening experiments are generally conducted in shake flasks or microtiter plates (MTPs) in uncontrolled batch modes. In extreme cases this can result in a complete failure of the scale-up. This led to the development of microfermentation systems with working volumes below 1 mL that were capable of applying a feed via microfluidic systems and to monitor fermentation parameters using optical, non-invasive optodes [35]. One of the available high-throughput microfermentation systems that is routinely used in laboratories is the BioLector<sup>®</sup> System of m2p-labs GmbH (Baesweiler, Germany). Among other models the BioLector<sup>®</sup> Pro was presented in 2016. It is capable of monitoring pH, dO<sub>2</sub>, biomass and fluorescence. The 48-well MTPs can be continuously shaken at different levels and the temperature of the reaction chamber, as well as the gas composition within the chamber, can be monitored and controlled. Additionally, a built-in microfluidic system enables continuous feeding and pH regulation in 32 individually operated wells, handling nanoliter amounts of liquid. In this case, the remaining 16 wells of the 48-well MTP are serving as reservoirs for the pH-control or feeding reagents. Alongside the round-well MTPs, flower-shaped-well MTPs are available, which increase the oxygen transfer rate significantly and decrease spilling and foaming of the contained liquid [36]. All the characteristics mentioned above have the potential to benefit screening experiments for protein refolding and to solve challenges that were mentioned in the previous paragraphs, yet the BioLector<sup>®</sup> Pro has not been reported to be applied for this cause.

Based on the previously summarized information, **four goals** were defined to be investigated throughout this thesis. The **first goal** of this thesis was the development of a suitable method applicable for the IPM and IPC of the solubilization process. The developed method should be compared to SDS-PAGE analysis in terms of analysis time and the precision in reflecting the subsequent refolding results accurately. Furthermore, the application of the implemented method for IPC should be demonstrated on HRP IBs originating from two different fermentations. While the first goal concerns the solubilization unit operation, the following goals comprise several aspects of the evaluation of the application of the BioLector<sup>®</sup> Pro microfermentation system for the

screening of protein refolding parameters during the refolding unit operation. The **second goal** was to develop a protocol for the screening of protein refolding parameters using the BioLector<sup>®</sup> Pro and to determine whether different results, compared to an already established conventional screening approach, are obtained. The **third goal** was to investigate the benefits of the in-line detection of fluorescence, pH and dO<sub>2</sub> of the BioLector<sup>®</sup> Pro for the screening of protein refolding parameters. The **fourth goal** was to investigate the benefits of a constant feed for the screening of protein refolding parameters.

The investigation of the solubilization unit operation was performed with HRP, while the investigation concerning the refolding unit operation was conducted with two different proteins: HRP and GFP. The choice of the model proteins is primarily based on the fact that refolding protocols have already been established for the selected proteins at TU Wien. This forms the basis for a profound comparison of the conventional screening approach to the BioLector<sup>®</sup> Pro. Further reasons and the characteristics of the proteins are presented in the following chapters.

**GFP** is a single domain fluorescent protein consisting of 238 amino acids and a molecular weight of 27 kDa [37]. Its extraction was first reported in 1962 from *Aequorea victoria*, in which it acts as a luminescent protein, but during these times no important applications were identified for GFP [38, 39]. The significant role of GFP in the field of molecular biology was introduced in the beginning of the 1990s for versatile applications, e.g., as a reporter gene, for two-hybrid screening or for labelling purposes [40]. The structure of GFP is based on 11  $\beta$ -strands forming a  $\beta$ -barrel surrounding a central  $\alpha$ -helix, whereas short helical segments can be found on the barrel ends. No cofactors are involved in the structure of GFP and no disulfide bridges can be found in GFP, only two cysteine residues are present in their reduced form [38, 40]. The chromophore is based on the dipeptide tyrosine-glycine with wild type excitation peaks at 395 nm and at 475 nm, while the emission peak can be found at 508 nm [38, 40, 41]. The fluorescent properties of GFP are highly dependent on the native conformation of its  $\beta$ -barrel structure, which is pH-dependent. No impairment of the GFP fluorescence was reported in the pH range 7.5 - 11.0 [32]. Due to the simple structure of GFP, fast protein refolding kinetics were reported and the absence of disulfide bridges makes the application of a redox system during protein refolding unnecessary. Furthermore, the fluorescent characteristics of GFP enable a simple quantitative analysis of the refolding process, making it well suited for the characterization of protein refolding using the BioLector<sup>®</sup> Pro, due to its ability for in-line fluorescence detection [30-32].

**HRP C** is the most abundant isoenzyme present in the roots of the horseradish plant (*Armoracia rusticana*) [42]. During this thesis, the HRP C isoenzyme is investigated and will be abbreviated as HRP. The enzyme is classified as an oxidoreductase consisting of 308 amino acids, containing heme and two calcium ions as cofactors [42-44]. Additionally, four disulfide bridges are present in the native structure of HRP, requiring a redox system during protein refolding [12, 42-44]. HRP that is produced by *A. rusticana* is generally glycosylated at eight of nine asparagine residues and has a molecular weight of 44 kDa.

Recombinant HRP expressed in *E. coli* in the form of IBs on the other hand is unglycosylated and has a molecular weight of 34.5 kDa [12, 45, 46]. To date, the industrial demand for HRP is covered by HRP extracted from *A. rusticana*. Since the isolation from plant material has several disadvantages, recombinant production processes were investigated extensively in the past. The most recent protocol for the recombinant production of HRP from *E. coli* IBs was published by Humer et al. in 2020 [12]. The range of application for HRP is very versatile. Due to its ability to catalyze the transformation of various substrates, it is mainly used as a reporter enzyme for nucleic acid-, antibody- and protein labelling or as a biosensor for the detection of hydrogen peroxide and other substances (e.g. glucose, ethanol) [47-51]. Additionally, it is used in the field of environmental biotechnology for the bioremediation of pollutants, in the textile industry for decolorization and in the chemical industry for organic polymer synthesis and biocatalysis [12, 52-55]. For protein refolding, HRP represents a protein with a challenging tertiary structure. Because of the four disulfide bridges and the requirement for a coenzyme and a cofactor, the tertiary structure of HRP is more complex than the structure of GFP. Furthermore, a redox system is required, which makes the refolding process more demanding but also more interesting for the characterization of the BioLector® Pro for protein refolding.

## 6 At-Line RPLC Approach for Improved Analysis of the Solubilization Process

### 6.1 Introduction

The current analytical method of choice for the analysis of the IB solubilization process is SDS-PAGE, mainly due to its high tolerance to harsh conditions, but its time-consuming application makes it unsuitable for IPM and IPC [16, 18, 19]. RPLC has also been reported to tolerate the harsh conditions, but in contrast to SDS-PAGE it requires very low sample preparation- and analysis times, while showing high accuracy, high selectivity, high robustness and compatibility with mass spectrometry [20-23, 26, 27]. All these advantages are making RPLC predestined to be applied for IPM and IPC during the IB solubilization process. In chapter 6 of this thesis, the implementation of an at-line RPLC method for the IPM and IPC of the solubilization process is presented to ensure compliance to QbD principles. The developed method is verified using HRP as a model protein. In order to evaluate whether the at-line RPLC method meets the criteria of an IPM tool, the DTT concentration and the solubilization time were varied as factors in form of a DoE approach using the concentration of monomeric HRP and the volumetric activity after refolding as the quality attributes of interest (=response of DoE). The method is additionally compared to SDS-PAGE in terms of analysis time and the precision in reflecting the subsequent refolding results accurately.



DTT is a reducing agent that is required during solubilization for the reduction of cysteine residues with the purpose to prevent aggregation caused by intermolecular disulfide bridge formation [6, 8, 12, 13]. The solubilization time has a grave influence on the concentration of monomeric protein in the solubilizate, hence low solubilization times are generally beneficial [12]. Based on the aggregation kinetics, low protein concentrations during protein refolding are favoring high refolding yields [8, 10]. However, due to several factors that are discussed in chapter 5, high protein concentrations are often desired in large scale industrial applications, thus the highest space-time yield of refolded protein needs to be determined empirically during the development of the process [8, 12]. This empirically determined protein concentration is generally controlled by the wet IB weight during the solubilization and by a fixed dilution during the refolding step. However, this strategy is susceptible to variations of the HRP titer in wet IB weight and the solubilization yield. To counteract these variations, we demonstrate the application of the previously implemented at-line RPLC method for the IPC of the protein concentration during the subsequent protein refolding process.

## 6.2 Publication

The following chapter is provided in form of an article with the title “At-Line Reversed Phase Liquid Chromatography for In-Process Monitoring of Inclusion Body Solubilization”, published in the journal “Bioengineering” in July 2021 [56]. The supplementary materials can be found subsequently to the publication.

Article

# At-Line Reversed Phase Liquid Chromatography for In-Process Monitoring of Inclusion Body Solubilization

Julian Ebner <sup>1</sup>, Diana Humer <sup>1</sup>, Robert Klausser <sup>1</sup>, Viktor Rubus <sup>1</sup>, Reinhard Pell <sup>2</sup>, Oliver Spadiut <sup>1</sup>  and Julian Kopp <sup>1,\*</sup> 

- <sup>1</sup> Research Division Integrated Bioprocess Development, Institute of Chemical, Environmental and Bioscience Engineering, Vienna University of Technology, 1060 Vienna, Austria; julian.ebner@tuwien.ac.at (J.E.); diana.humer@tuwien.ac.at (D.H.); robert.klausser@tuwien.ac.at (R.K.); viktor.rubus@tuwien.ac.at (V.R.); oliver.spadiut@tuwien.ac.at (O.S.)
- <sup>2</sup> SANDOZ GmbH, Mondseestrasse 11, 4866 Unterach, Austria; reinhard.pell@gmx.at
- \* Correspondence: julian.kopp@tuwien.ac.at; Tel.: +43-1-5880-1166-485

**Abstract:** Refolding is known as the bottleneck in inclusion body (IB) downstream processing in the pharmaceutical industry: high dilutions leading to large operating volumes, slow refolding kinetics and low refolding yields are only a few of the problems that impede industrial application. Solubilization prior to refolding is often carried out empirically and the effects of the solubilize on the subsequent refolding step are rarely investigated. The results obtained in this study, however, indicate that the quality of the IB solubilize has a severe effect on subsequent refolding. As the solubilize contains chaotropic reagents in high molarities, it is commonly analyzed with sodium dodecyl sulfate polyacrylamide gel electrophoresis (SDS-PAGE). SDS-PAGE, however, suffers from a long analysis time, making at-line analytical implementation difficult. In this study, we established an at-line reversed phase liquid chromatography method to investigate the time-dependent quality of the solubilize. To verify the necessity of at-line solubilization monitoring, we varied the essential solubilization conditions for horseradish peroxidase IBs. The solubilization time was found to have a major influence on subsequent refolding, underlining the high need for an at-line analysis of solubilization. Furthermore, we used the developed reversed phase liquid chromatography method for an in-process control (IPC). In conclusion, the presented reversed phase liquid chromatography method allows a proper control of IB solubilization applicable for tailored refolding.

**Keywords:** inclusion bodies; inclusion body solubilization; tailored refolding; reversed phase liquid chromatography; process analytical technology tools; in-process monitoring; in-process control



**Citation:** Ebner, J.; Humer, D.; Klausser, R.; Rubus, V.; Pell, R.; Spadiut, O.; Kopp, J. At-Line Reversed Phase Liquid Chromatography for In-Process Monitoring of Inclusion Body Solubilization. *Bioengineering* **2021**, *8*, 78. <https://doi.org/10.3390/bioengineering8060078>

Academic Editor: Susan Sharfstein

Received: 7 May 2021

Accepted: 5 June 2021

Published: 7 June 2021

**Publisher's Note:** MDPI stays neutral with regard to jurisdictional claims in published maps and institutional affiliations.



**Copyright:** © 2021 by the authors. Licensee MDPI, Basel, Switzerland. This article is an open access article distributed under the terms and conditions of the Creative Commons Attribution (CC BY) license (<https://creativecommons.org/licenses/by/4.0/>).

## 1. Introduction

To date, approximately 20–30% of all approved biopharmaceuticals are produced in microbial hosts [1,2]. Insoluble aggregates, better known as inclusion bodies (IBs), produced by the gram-negative bacterium *Escherichia coli*, present a dominant fraction of the microbial production segment [3]. This is mainly because cultivation with *E. coli* can be carried out at very low costs in short fermentation run-times and high target protein concentrations at a high purity can be achieved [4–6]. Early downstream steps in IB processing, however, are notorious for their high complexity and low yields [7,8]. In particular, refolding is regarded as a major bottleneck in IB processing. Solubilization and refolding strategies are commonly developed empirically with protocols being highly dependent on the target protein [9,10]. Protein hydrophobicity, for instance, affects the required molarity of the chaotropic agent and pH in solubilization and refolding [11]. The addition of reducing agents during solubilization is required for proteins containing disulfide bonds [8], subsequently influencing the amount of oxidizing compounds to be added in refolding [12]. Refolding yields are highly dependent on the protein in question as well as the protein concentration during the refolding process: only 15–25% of refolding



yields are reported for many therapeutic proteins [13] compared with a refolding yield of 97% for the enzyme lysozyme [14].

Singh et al. reported that mild solubilization boosts the refolding yield [15]. The reduction of chaotropic reagent molarity was compensated by either highly alkaline conditions or via the addition of solubilization-enhancing chemicals (i.e., n-propanol) [16,17]. The analyses in these studies, however, were performed with the commonly known sodium dodecyl sulfate polyacrylamide gel electrophoresis (SDS-PAGE) [17]. SDS-PAGE is frequently used for a solubilize analysis as it tolerates the harsh conditions [18,19]. Various staining protocols (e.g., silver staining or Coomassie staining) with a different selectivity and treatment time have been established [20] and subsequent immunoblotting can further increase the sensitivity of gel-based analytical methods [21].

Unfortunately, this gel-based method is not suitable for in-process control (IPC) as the sample treatment, method running time and staining protocols are very time-consuming. However, according to quality by design (QbD) principles in pharmaceutical manufacturing, an IPC must be applied [22] and, for this purpose, process analytical technology (PAT) tools are of a great advantage as they allow a timely process intervention [23,24]. High molarities of chaotropic reagents required for solubilization, however, interfere with the measuring principles of many available PAT tools (i.e., near-infrared and Raman spectroscopy) [25,26].

Several liquid chromatography (LC) separation principles can tolerate the high molarities of the chaotropic agents required for the sample dissolution [27,28]. LC is implemented for the quantification of diverse biopharmaceuticals due to the straightforward and facile sample preparation as well as a rapid and accurate analysis [29–31]. Hydrophobic interaction chromatography (HIC), ion exchange chromatography (IEX) and size exclusion chromatography (SEC) are frequently used in a recombinant protein analysis [32,33]; however, high molarities of the chaotropic reagent required in IB solubilization again complicate the implementation of these chromatographic techniques. Reversed phase liquid chromatography (RPLC) is a denaturing chromatographic technique tolerating these harsh conditions [18]. Furthermore, RPLC is known for its robustness, high selectivity and compatibility with a mass spectrometric analysis [34,35] making it a highly suitable technique for in-process monitoring in IB processing.

In this study, we implemented an RPLC method applicable for an at-line solubilize analysis. In this context, at-line defines a measurement that is performed in close proximity to the process stream as specified by regulatory agencies [36]. To demonstrate the need for in-process monitoring, we used HRP (horseradish peroxidase) as a model protein. HRP contains four disulfide bonds, thus requiring a complex solubilization and refolding strategy. We hypothesize that RPLC is faster and more precise than SDS-PAGE to determine the optimal solubilization conditions for tailored refolding. Hence, the solubilization conditions for HRP were varied and an SDS-PAGE analysis was compared with an RPLC analysis. The obtained results confirmed the effect of the solubilize on the subsequent refolding step. In addition, the in-process control based on at-line RPLC measurements was demonstrated. The results of this study demonstrate that solubilize quality influences the refolding yield and RPLC is suitable for the IPC of IB solubilization.

## 2. Materials and Methods

### 2.1. Production and Isolation of HRP IB

HRP was produced in *E. coli* BL21 (DE3) (Life Technologies, Carlsbad, CA, USA) with details stated in previous publications [37,38]. After a successful HRP expression [37,39,40], the cell broth was harvested via centrifugation and the biomass was stored at  $-20^{\circ}\text{C}$ .

Cell disruption was carried out at 1200 bar for 3 passages using a high-pressure homogenizer (PANDA+ 2000, GEA, Biberach, Germany). After centrifugation at 10,000 rpm,  $4^{\circ}\text{C}$  and 20 min (Eppendorf, Hamburg, Germany), the soluble fraction was discarded. The resulting IB pellet was washed two times with a buffer (50 mM Tris, pH 8, 500 mM NaCl,

2 M Urea). The IB pellets were then resuspended in water, aliquoted to a defined wet IB weight, centrifuged (20,379 rcf, 4 °C, 20 min) and stored at −20 °C until further use.

## 2.2. Solubilization and Refolding

### 2.2.1. In-Process Monitoring

The aliquoted IBs were thawed and resuspended in an HRP solubilization buffer (50 mM Tris/HCl pH 8; 6 M Urea). After the resuspension, DTT (1 M DTT stock) was added to a final concentration of 0 mM, 7.11 mM and 14.22 mM, respectively. The solubilization was performed at RT and a slight agitation and the samples were drawn after 0.5 h, 2 h, 4 h, 6 h, 8 h and 21 h. The samples were centrifuged (20,379 rcf, 4 °C, 20 min) and the supernatant was used for refolding, the RPLC analysis and diluted 1:2 in 2x Laemmli buffer for the SDS-PAGE analysis. For refolding, the solubilize was diluted 1:40 in a pre-cooled HRP refolding buffer (20 mM Tris/HCl pH 8.5; 2 M Urea; 2 mM CaCl<sub>2</sub>; 7% *v/v* glycerol) containing either 0 mM, 1.27 mM or 2.54 mM GSSG (glutathione disulfide) [37]. Refolding was performed for 48 h at 4 °C on a rocker-shaker. Hemin was added 24 h after the refolding start to a final concentration of 20 μM (1 mM Hemin stock in 100 mM KOH). After refolding, the enzyme activity was measured as described previously [37].

### 2.2.2. Demonstration of At-Line RPLC for IPC

In order to demonstrate the applicability of the at-line RPLC method for the IPC, we produced two different IB batches. Fermentations for both batches were conducted as described here [39] only the specific feeding rate ( $q_s$ ) during the induction was varied. Batch 1 was conducted at a  $q_s$  of 0.25 g/g/h during the induction whereas Batch 2 was performed at a  $q_s$  of 0.35 g/g/h during the induction. The harvest, cell disruption, IB wash, aliquoting and storage were done identically for both batches.

The inclusion bodies from both batches were solubilized at a concentration of 100 g wet IB/L solubilization mix. The solubilization buffer consisted of 50 mM glycine pH 10; 6 M Urea. DTT was added to a final concentration of 7.11 mM (1 M DTT stock). The solubilization was performed for 0.5 h at RT on a rocker-shaker. After centrifugation (20,379 rcf, 4 °C, 20 min), the supernatant was analyzed using the described RPLC method. Batch 1 solubilize was diluted 1:40 in a refolding buffer (20 mM glycine pH 10; 2 M Urea; 2 mM CaCl<sub>2</sub>; 7% *v/v* glycerol; 1.27 mM GSSG). For IB Batch 2, two different refolding approaches were performed: the solubilize was diluted 1:40 (= "fixed dilution") and the dilution was adapted based on the RPLC results in order to achieve the same monomeric HRP concentration as in Batch 1. In this case, the dilution was reduced to 1:17 due to a lower concentration of the target protein HRP in IB Batch 2.

## 2.3. Analytical Techniques

### 2.3.1. Reversed Phase Liquid Chromatography Measurements

The RPLC measurements were performed using a Dionex UltiMate 3000 system with a quaternary solvent delivery pump, an auto-sampler with a sample thermostat and a UV detector (Thermo Fisher, Waltham, MA, USA). The wavelength for the UV detection was set to 280 nm in order to monitor the protein absorption allowing the quantification of the target protein and its impurities. The instrument control and data acquisition were carried out via Chromeleon 7.2 software (Thermo Fisher). Prior to the RPLC measurement, all samples were centrifuged (20,379 rcf, 4 °C, 20 min) to separate the aggregates from the soluble fraction. We used a BioResolve RP mAb Polyphenyl column (dimensions 100 mm × 3 mm, particle size 2.7 μm) (Waters Corporation, MA, USA) connected to a pre-column (3.9 mm × 5 mm, 2.7 μm) of the same stationary phase. The mobile phase was composed of ultrapure water (MQ; eluent A) and acetonitrile (eluent B) both supplemented with 0.1% (*v/v*) trifluoroacetic acid. Ultrapure water was acquired from a Milli-Q system from Merck Millipore (Darmstadt, Germany). Acetonitrile (HPLC-grade) and trifluoroacetic acid (TFA, >99.9%) were obtained from Carl Roth (Karlsruhe, Germany). For the analysis, a recently published RPLC method, which had been developed

and validated according to QbD principles, was modified in terms of gradient, column temperature and flow rate [18]. The method was optimized empirically, reducing the overall running time to 8.1 min in order to allow for short analysis times during solubilization. The runs were conducted at 78 °C and a flow rate of 1.2 mL/min using the gradient displayed in Table 1.

**Table 1.** Gradient used for the RPLC analysis, with eluent A being ultrapure water and eluent B acetonitrile both supplemented with 0.1% (v/v) trifluoroacetic acid.

Time (min)	Percent Eluent B (%)
0	25
3.1	62
5.1	62
5.2	25
8.1	25

The HRP concentration in the solubilize was determined using a bovine serum albumin (BSA) standard calibration ranging from 0.0625 g/L to 1.0000 g/L. The BSA was used for the quantification as no non-glycosylated standard was available for HRP.

### 2.3.2. SDS-PAGE Measurements

For the SDS-PAGE analysis, the samples were mixed with 2× concentrated Laemmli buffer to achieve a 1× concentration of Laemmli buffer in the final dilution. The used buffer solution did not contain β-mercaptoethanol (non-reducing conditions) in order to analyze the solubilization quality in regard to disulfide bridge formation. The samples were heated to 95 °C for 10 min. A total of 5 μL of each sample was loaded onto pre-cast SDS gels (4–15%, Bio-Rad, Hercules, CA, USA). The gels were run in a Mini-PROTEAN Tetra System (Bio-Rad) for 30 min at 180 V and stained with Coomassie Blue. The protein bands were evaluated densitometrically using ImageLab software (Bio-Rad).

### 2.3.3. HRP Enzymatic Activity Assay

The HRP enzyme activity was measured with a Tecan Infinite M200 PRO (Männedorf, Switzerland) using flat-bottom polystyrene 96-well plates, as described previously [37]. The samples after refolding were diluted in the range of 1:2–1:25 in a dilution buffer (20 mM Bis-Tris; pH 7; 7% v/v glycerol) depending on their volumetric activity. A total of 170 μL of ABTS solution (50 mM KH<sub>2</sub>PO<sub>4</sub>; pH 5; 5 mM ABTS) was mixed with 10 μL of the respective diluted sample in the well. The reaction was started by adding 20 μL hydrogen peroxide (the final concentration in the well was 1 mM). Immediately after the start of the reaction, the change in the absorbance at 420 nm was recorded at 30 °C for 2 min. The volumetric enzyme activity was calculated using Equation (1):

$$A \left[ \frac{U}{mL} \right] = \frac{V_{total} * \Delta \frac{A}{min} * Dilution}{V_{sample} * d * \epsilon} \quad (1)$$

$V_{total}$ —total well volume (μL).

$\Delta A/min$ —change in absorption ( $\Delta_{Abs}$  420 nm/min).

$Dilution$ —dilution of the sample.

$V_{sample}$ —volume of the sample (μL).

$d$ —length of the beam path through the well ( $d = 0.58$  cm).

$\epsilon$ —extinction coefficient ( $\epsilon_{420} = 36 \text{ mM}^{-1} \text{ cm}^{-1}$ ).

## 2.4. Experimental Design

The experiments were conducted using a full factorial design, as shown in Table 2, varying the solubilization time and DTT concentrations in a multivariate data approach. All combinations of the solubilization time and DTT concentration are listed in Supplementary

Table S1. As responses for this design of experiment (DoE), the concentration of monomeric HRP was quantified with SDS-PAGE and RPLC. Additionally, all solubilization conditions were refolded at a GSSG concentration of either 0 mM, 1.27 mM or 2.54 mM GSSG to verify the effect on the refolding yield.

**Table 2.** Full factorial experimental design for HRP solubilization. The listed DTT concentrations were used in combination with each listed time-point.

Time (h)	DTT Concentrations (mM)
0.5	0
2	7.11
4	14.22
6	-
8	-
21	-

### 2.5. Multivariate Data Assessment of Solubilization and Refolding

An analysis of the used design of experiments (DoEs) was done using a multivariate data assessment program (MODDE 12, Umetrics, Sweden) with the model being based on a multiple linear regression. The results were analyzed for the statistical relevance of the model by the measure of fit ( $R^2$ ) and the model predictability ( $Q^2$ ).

## 3. Results and Discussion

### 3.1. In-Process Monitoring

In order to be applicable as an in-process monitoring method for solubilization, the respective analytical method had to meet three criteria:

1. The ability to quantify a defined quality attribute;
2. The quality attribute had to influence the refolding behavior;
3. Timely measurement of the respective quality attribute.

In order to determine whether at-line RPLC met the criteria of an in-process monitoring tool, DTT concentration and the solubilization time of HRP IBs were varied in a DoE approach (Table 2). DTT was required during solubilization in order to keep the cysteines (eight contained in HRP) in a reduced state and therefore prevent aggregation caused by an intermolecular disulfide bridge formation. It was expected that DTT concentration and the solubilization time would influence the titer of monomeric HRP in the solubilizate.

The key quality attribute (=DoE response) was defined as the concentration of monomeric HRP. We hypothesized that the enzymatic activity after refolding would directly correlate with the concentration of monomeric HRP in the solubilizate. The aggregated HRP was believed to result in a structure not applicable for refolding whereas monomeric HRP was defined as completely reduced and denatured during solubilization. Therefore, a monomeric HRP titer was chosen as the target response for the DoE. To test whether both RPLC and SDS-PAGE could predict the targeted solubilization for tailored refolding, all solubilizates were refolded and the volumetric activity (U/mL) after refolding was recorded.

Figure 1 shows that the solubilizate containing no DTT displayed an additional peak before the HRP target peak (at a 4.1 min retention time). This peak could already be monitored after 0.5 h of solubilization and increased with longer solubilization times. A complete degradation of the target peak could be observed after 21 h of solubilization independent of the supplied DTT concentration. The pellets resulting from the centrifugation prior to the RPLC analysis after 21 h solubilization increased compared with pellets received from shorter solubilization times, indicating an enhanced protein aggregate formation [7].

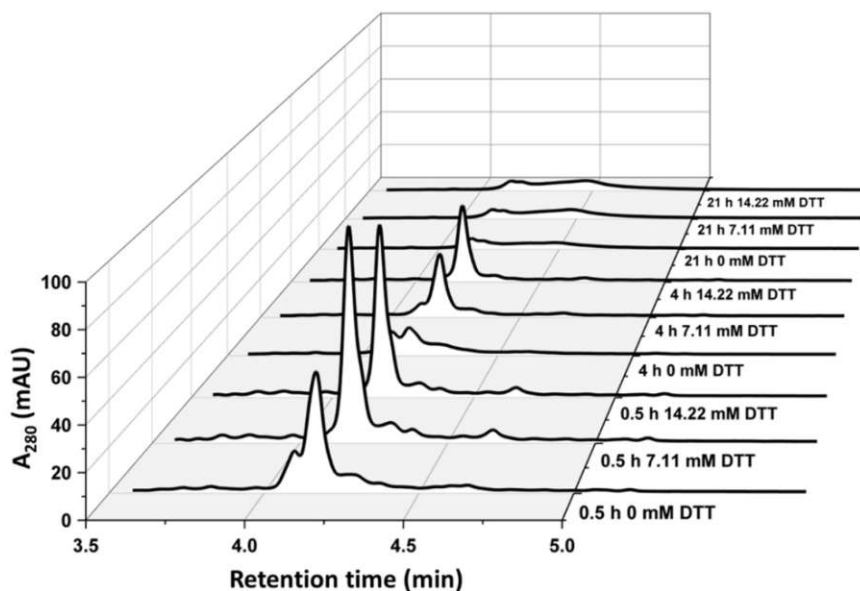


**Figure 1.** RPLC chromatograms at 280 nm quantifying monomeric HRP eluting at 4.18 min. The results demonstrate the trends of solubilization at three applied DTT concentrations (0 mM, 7.11 mM and 14.22 mM) for 0.5 h of solubilization, 4 h of solubilization and 21 h of solubilization. After 21 h of solubilization, a strong degradation of the target peak in the solubilizate is visible.

For the SDS-PAGE analysis, the HRP target band was found at 34 kDa (Figure 2). We hypothesized that the protein band at approximately 68 kDa was a product dimer due to an intermolecular disulfide bridge formation. The 68 kDa band tended to increase with extended solubilization times, especially beyond 4 h and for experiments without DTT. In good agreement with the RPLC measurements, we found that HRP was substantially degraded after 21 h of solubilization (Figure 2C). It was therefore concluded that both factors varied for this DoE (DTT concentration and solubilization time) had an influence on the quality attribute “monomeric HRP concentration” in the solubilizate. Furthermore, SDS-PAGE and RPLC were able to measure these changes, with RPLC being applicable as an at-line monitoring tool due to its short analysis time of less than 10 min.

A multivariate data approach was applied in order to quantify the effects of the varied DTT concentrations and solubilization times on the monomeric HRP concentration during solubilization. The contour plots (i.e., model responses) of the multivariate data analysis for SDS-PAGE and RPLC in solubilization and the enzymatic activity after refolding are shown in Figure 3. All concentrations of HRP during solubilization (including respective purity) for the shown experiment are listed in Supplementary Table S1 for both SDS-PAGE and RPLC. The results for 21 h of solubilization (Figures 1 and 2, Supplementary Table S1) were excluded from the model as they led to a response distortion due to product degradation. The model terms ( $R^2$  and  $Q^2$ ) are summarized in Supplementary Figure S1. Furthermore, ANOVA plots for the responses and significant factors used for the models are shown in Supplementary Figures S2 and S3, respectively.

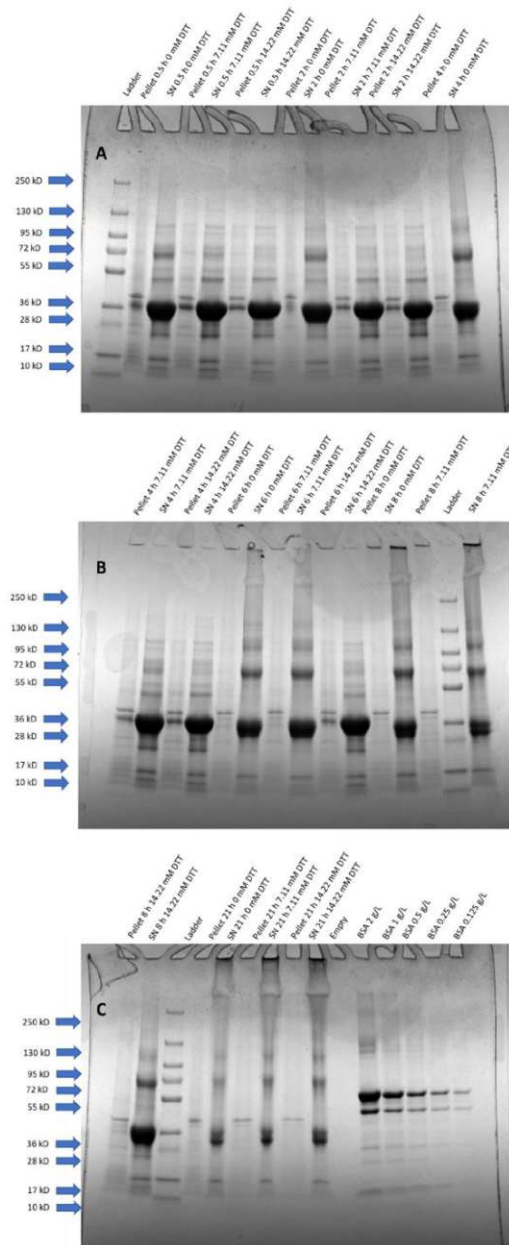


**Figure 2.** SDS-PAGE analysis of HRP solubilizes with varying DTT concentrations and time factors as depicted in Table 2; non-glycosylated HRP is visible at 34 kDa. The potential dimer formed due to the intermolecular disulfide bridge formation can be seen at 68 kDa. The samples are displayed in the following order from (A–C): pellet and supernatant (SN) for each time-point varying the three altered DTT concentrations. Additionally to samples, in (C), a standard protein calibration with BSA was performed. Protein ladders were added to confirm protein size.

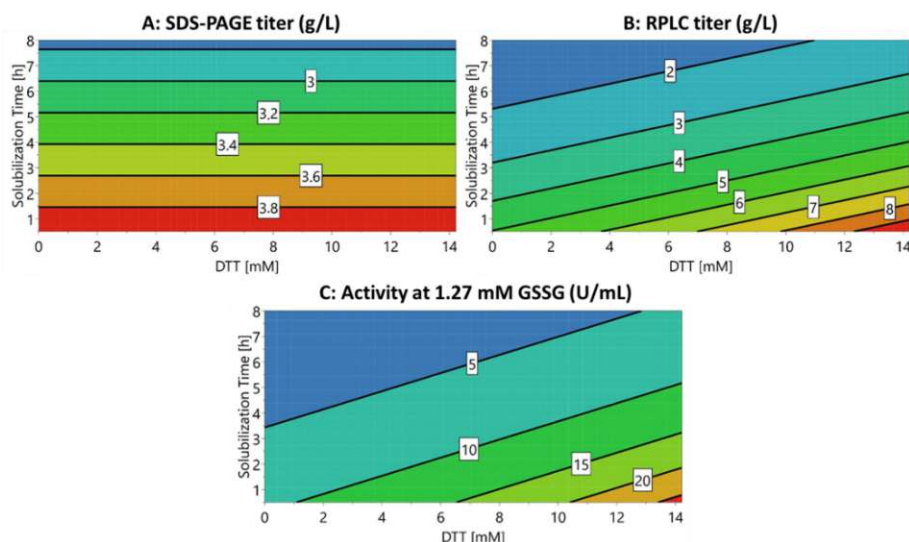


**Figure 3.** MODDE contour plots with the two factors of DTT concentration on the X-axis and the solubilization time on the Y-axis. The following responses are shown: (A) Monomeric HRP concentration in the solubilizate (g/L) analyzed using SDS-PAGE. (B) Monomeric HRP concentration in the solubilizate (g/L) analyzed using RPLC. (C) Effect of the different solubilization conditions on the volumetric activity (U/mL) after refolding, which was performed at constant GSSG conditions of 1.27 mM.

The results obtained for the model responses varied between the SDS-PAGE and the RPLC analysis for the conducted DoE (Figure 3A,B). Surprisingly, the SDS-PAGE analysis indicated that the monomeric HRP concentration was solely dependent on the solubilization time (Figure 3A). The raw data of both SDS-PAGE and RPLC (Figures 1 and 2) showed that short solubilization times below 4 h were superior over longer solubilization times. However, the raw data also indicated that high DTT concentrations were beneficial for the concentration of monomeric HRP during solubilization whereas lower DTT concentrations led to a lower solubilization yield. This effect was especially true for longer solubilization times. The model prediction for the SDS-PAGE analysis was very low in comparison with the RPLC analysis (Supplementary Figure S1). We hypothesized that this trend occurred due to different separation principles leading to non-linear model responses. The model response for the RPLC analysis with the monomeric HRP concentration indicated that both DTT concentration and the solubilization time had a significant influence (Figure 3B).

The effects on the product purity during solubilization can be found in Supplementary Table S1 and Figure S4 for both SDS-PAGE and RPLC, indicating the same trends as for the monomeric HRP concentration shown in Figure 3A,B. The differences in the total titer between the SDS-PAGE analysis and RPLC might result from the high sample concentrations chosen for SDS-PAGE. This was done to determine the impurities and monomeric HRP titer in the SDS-PAGE analysis. For the RPLC analysis, monomeric HRP and purity could be well assessed within one chromatogram.

To assess which analytical method was better suited for refolding yield prediction, the volumetric activity (U/mL) after refolding was determined (Figure 3C). The GSSG concentration was varied according to previous experiments [37]; however, no alterations in the model trend were obtained (Supplementary Table S1). The effects are exemplarily shown for 1.27 mM GSSG in Figure 3C. The enzyme activity after refolding was found to be highest at short solubilization durations (0.5 h, Figure 3C) and an increase in DTT concentration led to increased enzyme activity. Hence, the enzyme activity showed the same trends as

RPLC solubilize prediction (Figure 3B,C) while solubilizes quantified via SDS-PAGE led to a different prediction than enzymatic activity after refolding (Figure 3A,C).

Therefore, the presented RPLC method met the criteria required for an at-line monitoring tool for the solubilization of HRP IBs. In comparison with the commonly used SDS-PAGE, the models based on the RPLC data were able to predict the influence of DTT concentration and time during solubilization on the subsequent refolding step and the refolding yield correctly. Furthermore, due to the versatility and short analysis time [18], RPLC could be applied as a suitable technique for the in-process control of IB processes.

### 3.2. Demonstration of At-Line RPLC for IPC

The refolding yield highly depends on the protein concentration during refolding with lower protein concentrations favoring higher refolding yields [6,9]. The protein concentration that leads to a maximum space-time yield of a correctly folded protein is empirically determined during process development of refolding [37]. The protein concentration in solubilization is commonly controlled by a fixed amount of wet IB weight dissolved in a solubilization buffer and a subsequent fixed dilution in the refolding buffer [10]. However, this approach is highly dependent on a rigid HRP titer per wet IB weight as well as a constant solubilization yield. It guarantees the desired concentration of the target product during solubilization and the subsequent refolding. In-process monitoring of the target protein concentration in the solubilize is necessary to counteract batch to batch variations derived from upstream processing (USP) and varying yields during solubilization.

In order to evaluate if the presented RPLC method was suited for the IPC, we conducted solubilization and refolding experiments comparing two IB batches. Early DSP until the refolding step were kept constant for both IB batches. The refolding was performed by two different approaches:

1. Solubilizates were diluted at a fixed ratio of 1:40, as previously determined [37];
2. Solubilizates were diluted according to the product quantity assessed by RPLC (Table 3).

**Table 3.** HRP concentration in the solubilize was determined via RPLC. Furthermore, the dilution in the refolding buffer as well as the activity after refolding are given for the two different IB batches. Two different dilutions were done for Batch 2: (1) solubilize was diluted with a fixed dilution (1:40) and (2) dilution was adapted to achieve the same HRP concentration as for Batch 1 (1:17).

IB Batch	c(HRP) (g/L) in Solubilization	Applied Dilution	Activity (U/mL) after Refolding
Batch 1, Fixed Dilution	5.27 ± 0.11	1:40	89.7 ± 6.0
(1) Batch 2, Fixed Dilution	2.35 ± 0.05	1:40	41.9 ± 2.8
(2) Batch 2, IPC via RPLC	2.35 ± 0.05	1:17	79.8 ± 5.4

As shown in Table 3, the concentration of monomeric HRP in the solubilize varied from Batch 1 (5.27 g/L) to Batch 2 (2.35 g/L). This led to an over 50% decrease of enzymatic activity after refolding for Batch 2 if the empirically determined fixed dilution of 1:40 was applied. When using the RPLC method as an in-process control tool, the dilution for Batch 2 could be adapted to 1:17. While the refolding yield for Batch 2 only decreased minimally when adjusting the dilution from 1:40 to 1:17 (Table 3), the refolding buffer volume could be reduced by more than 50%. Therefore, using a correction via RPLC, the 54% variation caused by USP could be reduced to only 11%. However, for the IPC in solubilization and refolding, the following factors still needed to be considered to elucidate the activity deviation of 11%:

1. The corrected dilution in refolding led to a variation in the redox system because a higher DTT carry-over occurred at lower dilutions. This shift of the redox system potentially influences the refolding yield [37].
2. For the demonstration purpose of the IPC via RPLC, drastic deviations from the USP were targeted (i.e. 54% of titer deviation). However, the protein concentration



adjustment in refolding via at-line RPLC from solubilization might be even less error-prone for smaller deviations.

3. Furthermore, standard deviations resulting from the RPLC measurements and enzymatic assay could explain further deviations (Table 3).

In the case of HRP IBs, the presented RPLC method was applied successfully as an IPC tool. Based on the rapid analysis time of the developed RPLC method, the deviations caused by the USP could be monitored at-line and the dilution was adapted to minimize the deviations during the refolding step. In addition, the received IB fingerprint (i.e., impurity monitoring) obtained via RPLC could provide valuable information using a reference impurity pattern for industrial applications.

#### 4. Conclusions

The solubilization of IBs prior to refolding is essential to obtain the desired protein conformation and protein concentrations in refolding. In this study, we developed an at-line RPLC method to monitor the target protein concentration during the solubilization unit operation of IB processing. DTT concentration and the solubilization time were varied for HRP IBs and the monomeric HRP concentration was recorded using SDS-PAGE and RPLC. The short analysis time (8.1 min), facile sample preparation and the high accuracy of RPLC (as demonstrated for the generic method [18]) allowed for a precise prediction of the monomeric HRP concentration on the refolding yield. The results thus favored the RPLC analysis over the SDS-PAGE analysis as the former could also be used for in-process monitoring.

Moreover, we demonstrated the IPC making use of the developed RPLC method, determining USP alterations. As downstream operations are performed sequentially in industry, subsequent unit operations are influenced by initial deviations. In this study, the protein concentration in refolding could be adapted by adjusting the dilution factor based on the at-line RPLC analysis. This allowed for a more robust refolding process against the deviations contrived from the USP and a reduction of the refolding buffer compared with empirical dilutions thus facilitating a more economic process.

Concluding, the developed RPLC method can be applied to accelerate process development in IB solubilization and for in-process monitoring therefore allowing IPC, which facilitates tailored IB refolding.

**Supplementary Materials:** The following are available online at <https://www.mdpi.com/article/10.3390/bioengineering8060078/s1>, Table S1: Conditions and raw data for the HRP solubilization DoE. Figure S1: Showing the measure of fit ( $R^2$ ) of the model and the model predictability ( $Q^2$ ) for the multivariate data analysis (based on multiple linear regression) conducted. SDSHRP conducts for titer measurements in solubilization performed with SDS-PAGE whereas SDSpurity shows the model for SDS impurity measurement in solubilization. It can be seen that these models show a low model predictability and a low measure of fit compared to other models in supplementary Figure S2. RPHRP and RPpurity copes for solubilization models of HRP titer and impurities respectively. Models after refolding are abbreviated according to their GSSG concentration i.e., 0 mM GSSG in refolding = vAct 0 mM GSSG, 1.27 mM GSSG in refolding = vAct 1.27 mM GSSG and 2.54 mM GSSG in refolding = vAct 2.54 mM GSSG; All model except for SDS-PAGE prediction (i.e. SDSHRP and SDSImp) show a  $R^2$  close to 0.8 and  $Q^2$  close to 0.7 and can thus be regarded as models describing input data appropriately. Figure S2: ANOVA plots are displayed for utilized responses. SDSHRP displays the concentration of monomeric HRP measured using SDS-PAGE, whereas SDSpurity shows the purity of the monomeric HRP analyzed via SDS-PAGE. RPHRP displays the concentration of monomeric HRP measured using RPLC and RPpurity shows the purity of monomeric HRP measured using RPLC analysis. vAct 1.27 mM GSSG shows the volumetric activity [U/mL] after refolding with 1.27 mM GSSG contained in the refolding buffer. For each response, SD-regression shows the variation of the response explained by the model while the RSD shows the variation of the response which is not explained by the model. Both values are adjusted for the respective degrees of freedom.  $RSD \cdot \sqrt{F(\text{crit})}$  shows RDS multiplied by the square root of the critical F (statistically significant at the 95% confidence level). Figure S3: Significant factors contributing for the models

for the used responses. SDSHRP displays the concentration of monomeric HRP measured using SDS-PAGE, whereas SDSpurity shows the purity of the monomeric HRP analyzed via SDS-PAGE. RPHRP displays the concentration of monomeric HRP measured using RPLC and RPhpurity shows the purity of monomeric HRP measured using RPLC analysis. vAct 1.27 mM GSSG shows the volumetric activity [U/mL] after refolding with 1.27 mM GSSG contained in the refolding buffer. Abbreviated factors are: Tim is the solubilization time [h], DTT is the DTT concentration during solubilization [mM]. For both SDS-PAGE responses (SDSHRP and SDSpurity), only the solubilization time was identified as a significant factor. For the RPLC responses as well as the volumetric activity after refolding both the DTT concentration during solubilization and the solubilization time were significant factors. Figure S4: Comparison of the two quality attributes monomeric HRP concentration [g/L] and purity [%] measured with SDS-PAGE and RPLC, respectively. MODDE contour plots with the two factors DTT concentration on the X-axis and the solubilization time on the Y-axis. The following responses are shown: A: Monomeric HRP concentration in the solubilize [g/L] analyzed using SDS-PAGE. B: Purity [%] of the monomeric HRP concentration in the solubilize analyzed via SDS-PAGE. C: Monomeric HRP concentration in the solubilize [g/L] analyzed using RPLC. D: Purity [%] of the monomeric HRP concentration in the solubilize analyzed via RPLC.

**Author Contributions:** J.E., O.S. and J.K. founded the idea of this study and planned the experimental design. J.E. carried out the data treatment and the statistical analysis. J.E., D.H., R.K. and V.R. conducted the experiments. R.P. and J.K. developed the RPLC method. J.E., O.S. and J.K. wrote the manuscript. All authors have read and agreed to the published version of the manuscript.

**Funding:** This research was funded by Austrian Research Promotion Agency (Österreichische Forschungsförderungsgesellschaft = FFG), grant number 874206. Furthermore, the authors acknowledge TU Wien Bibliothek for financial support through its Open Access Funding Programme.

**Institutional Review Board Statement:** Not applicable.

**Informed Consent Statement:** Not applicable.

**Data Availability Statement:** The data presented in this study are available on request from the corresponding author. The data are not publicly available due to cooperation with an industrial partner.

**Acknowledgments:** The authors acknowledge the TU Wien Bibliothek for financial support through its Open Access Funding Program. Furthermore, the authors want to thank the Austrian Research Promotion Agency (FFG) for their funding facilitating this study (874206).

**Conflicts of Interest:** The authors declare that the research was conducted in the absence of any commercial or financial relationships that could be interpreted as a potential conflict of interest.

## References

- Walsh, G. Biopharmaceutical benchmarks 2018. *Nat. Biotechnol.* **2018**, *36*, 1136–1145. [[CrossRef](#)] [[PubMed](#)]
- Baeshen, M.N.; Al-Hejin, A.M.; Bora, R.S.; Ahmed, M.M.; Ramadan, H.A.; Saini, K.S.; Baeshen, N.A.; Redwan, E.M. Production of Biopharmaceuticals in *E. coli*: Current Scenario and Future Perspectives. *J. Microbiol. Biotechnol.* **2015**, *25*, 953–962. [[CrossRef](#)] [[PubMed](#)]
- Slouka, C.; Kopp, J.; Spadiut, O.; Herwig, C. Perspectives of inclusion bodies for bio-based products: Curse or blessing? *Appl. Microbiol. Biotechnol.* **2018**. [[CrossRef](#)] [[PubMed](#)]
- Rinas, U.; Garcia-Fruitós, E.; Corchero, J.L.; Vázquez, E.; Seras-Franzoso, J.; Villaverde, A. Bacterial Inclusion Bodies: Discovering Their Better Half. *Trends Biochem. Sci.* **2017**, *42*, 726–737. [[CrossRef](#)]
- García-Fruitós, E.; Vázquez, E.; Díez-Gil, C.; Corchero, J.L.; Seras-Franzoso, J.; Ratera, I.; Veciana, J.; Villaverde, A. Bacterial inclusion bodies: Making gold from waste. *Trends Biotechnol.* **2012**, *30*, 65–70. [[CrossRef](#)]
- Jungbauer, A. Continuous downstream processing of biopharmaceuticals. *Trends Biotechnol.* **2013**, *31*, 479–492. [[CrossRef](#)] [[PubMed](#)]
- Palmer, I.; Wingfield, P.T. Preparation and extraction of insoluble (inclusion-body) proteins from *Escherichia coli*. *Curr. Protoc. Protein Sci.* **2012**. [[CrossRef](#)] [[PubMed](#)]
- Humer, D.; Spadiut, O. Wanted: More monitoring and control during inclusion body processing. *World J. Microbiol. Biotechnol.* **2018**, *34*, 158. [[CrossRef](#)]
- Eiberle, M.K.; Jungbauer, A. Technical refolding of proteins: Do we have freedom to operate? *Biotechnol. J.* **2010**, *5*, 547–559. [[CrossRef](#)]

10. Walther, C.; Mayer, S.; Jungbauer, A.; Dürauer, A. Getting ready for PAT: Scale up and inline monitoring of protein refolding of Npro fusion proteins. *Process. Biochem.* **2014**, *49*, 1113–1121. [[CrossRef](#)]
11. Wagner, J.R.; Sorgentini, D.A.; Añón, M.C. Relation between Solubility and Surface Hydrophobicity as an Indicator of Modifications during Preparation Processes of Commercial and Laboratory-Prepared Soy Protein Isolates. *J. Agric. Food Chem.* **2000**, *48*, 3159–3165. [[CrossRef](#)] [[PubMed](#)]
12. Uchimura, H.; Kim, Y.; Mizuguchi, T.; Kiso, Y.; Saito, K. Quantitative evaluation of refolding conditions for a disulfide-bond-containing protein using a concise <sup>18</sup>O-labeling technique. *Protein Sci.* **2011**, *20*, 1090–1096. [[CrossRef](#)]
13. Datar, R.V.; Cartwright, T.; Rosen, C.-G. Process Economics of Animal Cell and Bacterial Fermentations: A Case Study Analysis of Tissue Plasminogen Activator. *Biotechnology* **1993**, *11*, 349–357. [[CrossRef](#)]
14. Ma, F.-H.; An, Y.; Wang, J.; Song, Y.; Liu, Y.; Shi, L. Synthetic Nanochaperones Facilitate Refolding of Denatured Proteins. *ACS Nano* **2017**, *11*, 10549–10557. [[CrossRef](#)]
15. Singh, A.; Upadhyay, V.; Panda, A.K. Solubilization and Refolding of Inclusion Body Proteins. In *Insoluble Proteins: Methods and Protocols*; García-Fruitós, E., Ed.; Springer: New York, NY, USA, 2015; pp. 283–291.
16. Singh, S.M.; Panda, A.K. Solubilization and refolding of bacterial inclusion body proteins. *J. Biosci. Bioeng.* **2005**, *99*, 303–310. [[CrossRef](#)]
17. Singh, S.M.; Sharma, A.; Upadhyay, A.K.; Singh, A.; Garg, L.C.; Panda, A.K. Solubilization of inclusion body proteins using n-propanol and its refolding into bioactive form. *Protein Expr. Purif.* **2012**, *81*, 75–82. [[CrossRef](#)]
18. Kopp, J.; Zauner, F.B.; Pell, A.; Hausjell, J.; Humer, D.; Ebner, J.; Herwig, C.; Spadiut, O.; Slouka, C.; Pell, R. Development of a generic reversed-phase liquid chromatography method for protein quantification using analytical quality-by-design principles. *J. Pharm. Biomed. Anal.* **2020**, 113412. [[CrossRef](#)]
19. Sasse, J.; Gallagher, S.R. Staining Proteins in Gels. *Curr. Protoc. Mol. Biol.* **2009**, *85*, 10.16.11–10.16.27. [[CrossRef](#)] [[PubMed](#)]
20. Gallagher, S.; Sasse, J. Protein Analysis by SDS-PAGE and Detection by Coomassie Blue or Silver Staining. *Curr. Protoc. Pharmacol.* **1998**, *2*, A.3B.1–A.3B.10. [[CrossRef](#)]
21. Kurien, B.T.; Scofield, R.H. Western blotting. *Methods* **2006**, *38*, 283–293. [[CrossRef](#)] [[PubMed](#)]
22. Pramod, K.; Tahir, M.A.; Charoo, N.A.; Ansari, S.H.; Ali, J. Pharmaceutical product development: A quality by design approach. *Int. J. Pharm. Investig.* **2016**, *6*, 129–138. [[CrossRef](#)]
23. Kopp, J.; Slouka, C.; Spadiut, O.; Herwig, C. The Rocky Road from Fed-Batch to Continuous Processing with *E. coli*. *Front. Bioeng. Biotechnol.* **2019**, *7*, 328. [[CrossRef](#)]
24. Esmonde-White, K.A.; Cuellar, M.; Uerpmann, C.; Lenain, B.; Lewis, I.R. Raman spectroscopy as a process analytical technology for pharmaceutical manufacturing and bioprocessing. *Anal. Bioanal. Chem.* **2017**, *409*, 637–649. [[CrossRef](#)]
25. Ferrari, M.; Mottola, L.; Quaresima, V. Principles, techniques, and limitations of near infrared spectroscopy. *Can. J. Appl. Physiol.* **2004**, *29*, 463–487. [[CrossRef](#)]
26. Eberhardt, K.; Stiebing, C.; Matthäus, C.; Schmitt, M.; Popp, J. Advantages and limitations of Raman spectroscopy for molecular diagnostics: An update. *Expert Rev. Mol. Diagn.* **2015**, *15*, 773–787. [[CrossRef](#)]
27. Gustavsson, R.; Mandenius, C.-F. Soft sensor control of metabolic fluxes in a recombinant *Escherichia coli* fed-batch cultivation producing green fluorescence protein. *Bioprocess. Biosyst. Eng.* **2013**, *36*, 1375–1384. [[CrossRef](#)]
28. Chemmalil, L.; Prabhakar, T.; Kuang, J.; West, J.; Tan, Z.; Ehamparanathan, V.; Song, Y.; Xu, J.; Ding, J.; Li, Z. Online/at-line measurement, analysis and control of product titer and critical product quality attributes (CQAs) during process development. *Biotechnol. Bioeng.* **2020**, *117*, 3757–3765. [[CrossRef](#)]
29. Sandra, K.; Vandenhede, I.; Sandra, P. Modern chromatographic and mass spectrometric techniques for protein biopharmaceutical characterization. *J. Chromatogr. A* **2014**, *1335*, 81–103. [[CrossRef](#)]
30. Fekete, S.; Guillarme, D. Ultra-high-performance liquid chromatography for the characterization of therapeutic proteins. *TrAC Trends Anal. Chem.* **2014**, *63*, 76–84. [[CrossRef](#)]
31. Fekete, S.; Veuthey, J.-L.; Guillarme, D. Modern Column Technologies for the Analytical Characterization of Biopharmaceuticals in Various Liquid Chromatographic Modes. *Spec. Issues* **2015**, *34*, 6–13.
32. Baca, M.; De Vos, J.; Bruylants, G.; Bartik, K.; Liu, X.; Cook, K.; Eeltink, S. A comprehensive study to protein retention in hydrophobic interaction chromatography. *J. Chromatogr. B* **2016**, *1032*, 182–188. [[CrossRef](#)]
33. Fekete, S.; Goyon, A.; Veuthey, J.-L.; Guillarme, D. Size Exclusion Chromatography of Protein Biopharmaceuticals: Past, Present and Future. *Am. Pharm. Rev.* **2018**, 1–4.
34. Kochling, J.; Wu, W.; Hua, Y.; Guan, Q.; Castaneda-Merced, J. A platform analytical quality by design (AQbD) approach for multiple UHPLC-UV and UHPLC-MS methods development for protein analysis. *J. Pharm. Biomed. Anal.* **2016**, *125*, 130–139. [[CrossRef](#)]
35. Fekete, S.; Veuthey, J.-L.; Guillarme, D. New trends in reversed-phase liquid chromatographic separations of therapeutic peptides and proteins: Theory and applications. *J. Pharm. Biomed. Anal.* **2012**, *69*, 9–27. [[CrossRef](#)]
36. Rathore, A.S.; Bhambure, R.; Ghare, V. Process analytical technology (PAT) for biopharmaceutical products. *Anal. Bioanal. Chem.* **2010**, *398*, 137–154. [[CrossRef](#)]
37. Humer, D.; Ebner, J.; Spadiut, O. Scalable High-Performance Production of Recombinant Horseradish Peroxidase from *E. coli* Inclusion Bodies. *Int. J. Mol. Sci.* **2020**, *21*, 4625. [[CrossRef](#)]

38. Humer, D.; Spadiut, O. Improving the Performance of Horseradish Peroxidase by Site-Directed Mutagenesis. *Int. J. Mol. Sci.* **2019**, *20*, 916. [[CrossRef](#)]
39. Slouka, C.; Kopp, J.; Hutwimmer, S.; Strahammer, M.; Strohm, D.; Eitenberger, E.; Schwaighofer, A.; Herwig, C. Custom made inclusion bodies: Impact of classical process parameters and physiological parameters on inclusion body quality attributes. *Microb. Cell Fact.* **2018**, *17*, 148. [[CrossRef](#)]
40. Kopp, J.; Kittler, S.; Slouka, C.; Herwig, C.; Spadiut, O.; Wurm, D.J. Repetitive Fed-Batch: A Promising Process Mode for Biomanufacturing with *E. coli*. *Front. Bioeng. Biotechnol.* **2020**, *8*, 1312. [[CrossRef](#)]

# At-line reversed phase liquid chromatography for in-process monitoring of inclusion body solubilization

Julian Ebner <sup>1</sup>, Diana Humer <sup>1</sup>, Robert Klausser <sup>1</sup>, Viktor Rubus <sup>1</sup>, Reinhard Pell <sup>2</sup>, Oliver Spadiut <sup>1</sup>  
Julian Kopp <sup>1,\*</sup>

<sup>1</sup> Research Division Integrated Bioprocess Development, Institute of Chemical, Environmental and Bioscience Engineering, Vienna University of Technology, 1060 Vienna, Austria; julian.ebner@tuwien.ac.at (J.E.); diana.humer@tuwien.ac.at (D.H.); robert.klausser@tuwien.ac.at (R.K.); viktor.rubus@tuwien.ac.at (V.R.); oliver.spadiut@tuwien.ac.at (O.S.)

<sup>2</sup> SANDOZ GmbH, Mondseestrasse 11, 4866 Unterach, Austria; reinhard.pell@gmx.at

\* Correspondence: julian.kopp@tuwien.ac.at

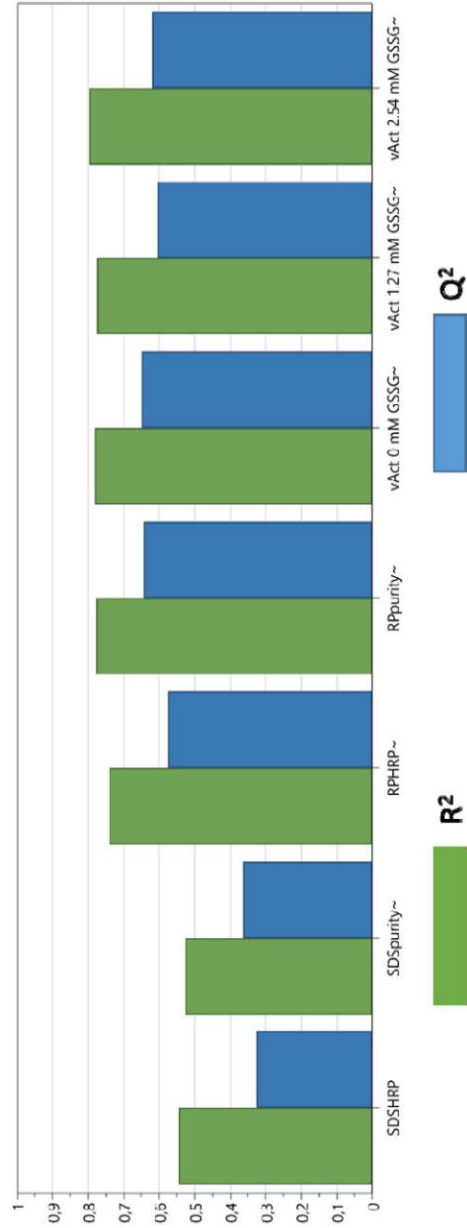
## Supplementary Table S1:

Conditions and raw data for the HRP solubilization DoE. Product purity was assessed as area- percentage for RPLC and SDS-PAGE using equation 1:

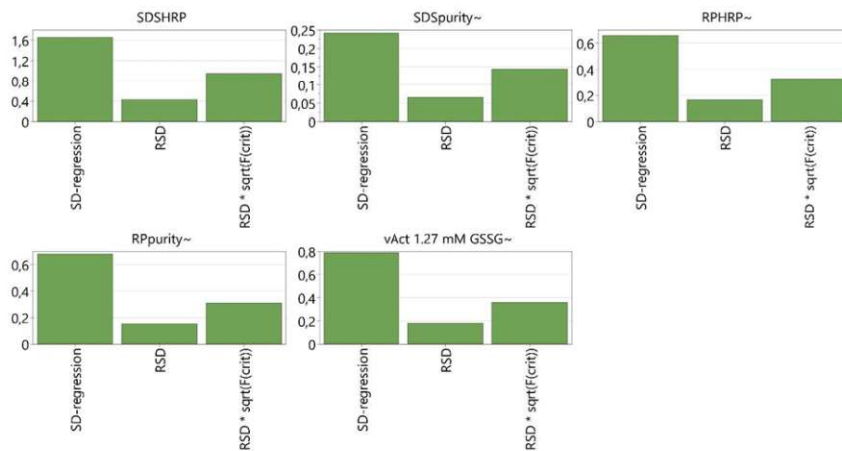
$$EQ1: \text{Solubilize purity [\%]} = \frac{\text{Target protein}_{Area[-]}}{\text{Target protein}_{Area[-]} + \text{Impurities}_{Area[-]}}$$

The volumetric activities were measured after refolding the listed solubilization conditions with a concentration of 1.27 mM CSSG. Measurements were performed in triplicates and standard deviation was <12% in all cases.

DTT [mM]	Solubilization time [h]	HRP (SDS-PAGE) [g/L]	Purity HRP (SDS-PAGE) [%]	HRP (RP-HPLC) [g/L]	Purity HRP (RP-HPLC) [%]	Volumetric activity [U/mL]
0	0.5	3.97	53.2	4.98	41.4	5.0
7.11	0.5	3.28	50.4	8.04	51.8	19.1
14.22	0.5	4.18	58.0	6.30	56.8	17.0
0	2	4.16	59.6	3.90	36.1	6.6
7.11	2	3.77	52.3	6.12	55.1	17.5
14.22	2	3.52	43.3	6.19	53.7	21.3
0	4	3.23	48.1	2.29	18.0	5.6
7.11	4	3.35	36.4	5.56	41.1	11.0
14.22	4	3.48	39.2	6.24	45.1	16.3
7.11	6	3.20	50.3	1.64	11.5	3.8
14.22	6	3.81	32.9	5.86	45.0	11.5
0	8	2.54	37.3	1.62	12.4	2.8
7.11	8	1.88	29.8	0.80	6.8	1.6
14.22	8	3.14	42.3	2.52	18.9	4.4
0	21	0.87	28.5	0.59	7.1	1.1
7.11	21	0.89	19.6	0.67	6.3	0.6
14.22	21	1.12	19.5	0.68	7.6	0.6

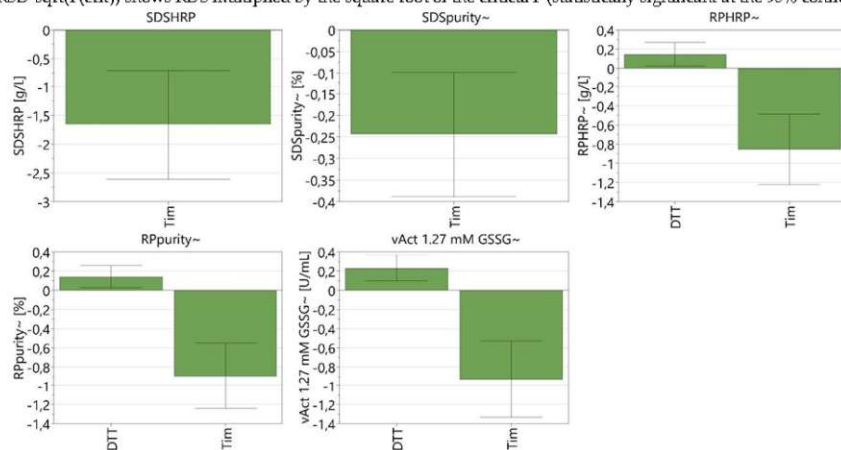


**Supplementary Figure S1.** Showing the measure of fit ( $R^2$ ) of the model and the model predictability ( $Q^2$ ) for the multivariate data analysis (based on multiple linear regression) conducted. SDSHRP conducts for titer measurements in solubilization performed with SDS-PAGE whereas SDSpurity shows the model for SDS impurity measurement in solubilization. It can be seen that these models show a low model predictability and a low measure of fit compared to other models in supplementary figure 2. RPHRP and RPhurity copes for solubilization models of HRP titer and impurities respectively. Models after refolding are abbreviated according to their GSSG concentration i.e. 0mM GSSG in refolding = vAct 0 mM GSSG, 1.27 mM GSSG in refolding = vAct 1.27 mM GSSG and 2.54 mM GSSG in refolding = vAct 2.54 mM GSSG; All model except for SDS-PAGE prediction (i.e. SDSHRP and SDSImp) show a  $R^2$  close to 0.8 and  $Q^2$  close to 0.7 and can thus be regarded as models describing input data appropriately.



**Supplementary Figure S2.** ANOVA plots are displayed for utilized responses. SDSHRP displays the concentration of monomeric HRP measured using SDS-PAGE, whereas SDSpurity shows the purity of the monomeric HRP analyzed via SDS-PAGE. RPHRP displays the concentration of monomeric HRP measured using RPLC and RPpurity shows the purity of monomeric HRP measured using RPLC analysis. vAct 1.27 mM GSSG shows the volumetric activity [U/mL] after refolding with 1.27 mM GSSG contained in the refolding buffer. For each response, SD-regression shows the variation of the response explained by the model while the RSD shows the variation of the response which is not explained by the model. Both values are adjusted for the respective degrees of freedom.

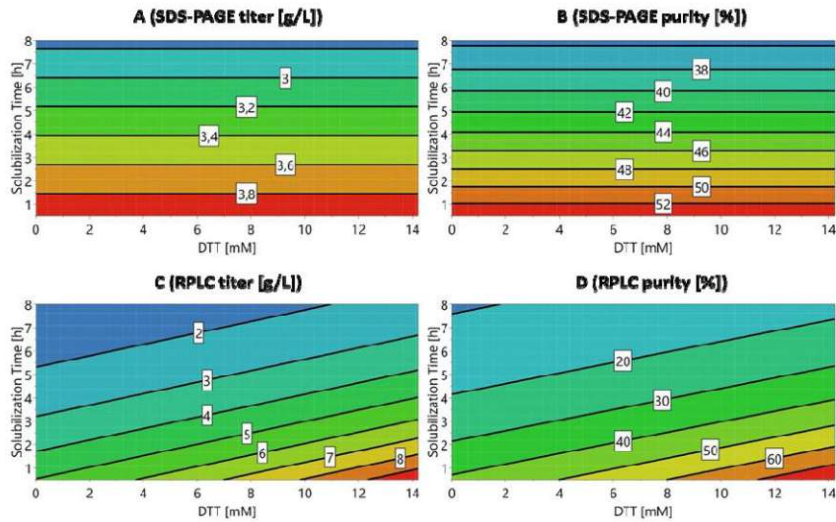
RSD\*sqrt(F(crit)) shows RDS multiplied by the square root of the critical F (statistically significant at the 95% confidence level).



**Supplementary Figure S3.** Significant factors contributing for the models for the used responses. SDSHRP displays the concentration of monomeric HRP measured using SDS-PAGE, whereas SDSpurity shows the purity of the monomeric HRP analyzed via SDS-PAGE. RPHRP displays the concentration of monomeric HRP measured using RPLC and RPpurity shows the purity of monomeric HRP measured using RPLC analysis. vAct 1.27 mM GSSG shows the volumetric activity [U/mL] after refolding with

1.27 mM GSSG contained in the refolding buffer. Abbreviated factors are: Tim is the solubilization time [h], DTT is the DTT concentration during solubilization [mM]. For both SDS-PAGE responses (SDSHRP and SDSpurity), only the solu-

bilization time was identified as a significant factor. For the RPLC responses as well as the volumetric activity after refolding both the DTT concentration during solubilization and the solubilization time were significant factors.



**Supplementary Figure S1.** Comparison of the two quality attributes monomeric HRP concentration [g/L] and purity [%] measured with SDS-PAGE and RPLC, respectively. MODDE contour plots with the two factors DTT concentration on the X-axis and the solubilization time on the Y-axis. The following responses are shown: A: Monomeric HRP concentration in the solubilizate [g/L] analyzed using SDS-PAGE. B: Purity [%] of the monomeric HRP concentration in the solubilizate analyzed via SDS-PAGE. C: Monomeric HRP concentration in the solubilizate [g/L] analyzed using RPLC. D: Purity [%] of the monomeric HRP concentration in the solubilizate analyzed via RPLC.



### 6.3 Conclusion

The publication presents a recently implemented at-line RPLC method for the monitoring of the target protein concentration during the solubilization unit operation of IB processing. All crucial criteria for the application as an IPM tool have been met. The analytical method can quantify the monomeric HRP concentration as the defined quality attribute and the quality attribute has been shown to correlate with the refolding yield. Additionally, the analysis of the quality attribute is conducted within a considerably shorter time (8.1 min) and with a higher accuracy compared to the established approach using SDS-PAGE.

Furthermore, the application of the developed at-line RPLC method for the IPC of the target protein concentration during the subsequent refolding unit operation was demonstrated. Variations of the HRP titer in wet IB weight and the solubilization yield were identified in a timely fashion in order to adapt the dilution factor and to control the HRP concentration during protein refolding.

In conclusion, the implemented RPLC method can be applied for the rapid and accurate development of IB solubilization processes and for the IPM of the solubilization process, to enable IPC for the improvement of protein refolding.

## 7 Application of the BioLector<sup>®</sup> Pro for the Screening of Protein Refolding

### 7.1 Introduction

Protein solubilization is an elementary step in the processing of IBs, with the goal to obtain the required protein conformation and concentration for the subsequent protein refolding unit operation. Thus, the proper IPM and IPC of key process parameters during solubilization, as described in the previous chapters, forms the basis for successful protein refolding. However, the screening experiments required for the development of protein refolding processes according to QbD principles still pose substantial challenges.

Several small-scale techniques for the screening of protein refolding parameters using a DoE approach were reported recently [12, 33, 34]. The scale of the experiments varies from 100 - 2,000  $\mu$ L and as refolding vessels MTPs or reaction tubes were used. Although some of these techniques are suitable for the parallel screening of large experiment numbers, they are incapable of controlling the CPPs refolding temperature and oxygen input, while the capabilities for the application of fed-batch refolding are severely limited. Applying a pulsed feed is laborious if no automation is applicable and the application of a continuous feed is entirely impossible.

Furthermore, the analytical tools of these setups for the characterization of the refolding process are limited and require sampling, which limits the number of measurements throughout the process considerably at this scale. Hence, there is a demand for IPM and IPC, not only for the solubilization process, but also for the refolding process. First, to gain more profound knowledge on the highly empirical protein refolding process and thereby improving the quality of the screening experiments, as defined by the QbD paradigm. Second, to improve similarity to larger scale stirred tank reactors, in which refolding is performed at an industrial scale, to improve the scale-up process by having the ability to compare crucial process parameters between different scales.

In order to solve the issues discussed above, the application of the BioLector<sup>®</sup> Pro microfermentation system for the screening of protein refolding parameters was investigated in chapter 7. The refolding temperature and the oxygen input into the refolding solution can be monitored and controlled via the gas composition of the reaction chamber. Furthermore, the device is able to monitor pH,  $dO_2$ , biomass and fluorescence using optical, non-invasive optodes and other optical systems [35]. Moreover, a built-in microfluidic system allows continuous feeding and pH regulation in 32 separately operated wells, handling nanoliter amounts of liquid [36]. All the characteristics mentioned above have the potential to benefit screening experiments for protein refolding and to solve challenges that were mentioned in the previous paragraphs, yet the BioLector<sup>®</sup> Pro has not been reported to be applied for this cause.

The in-line monitoring of fluorescence during protein refolding is useful to quantify refolding processes of fluorescent proteins, whose fluorescence emission depends on the

native tertiary protein structure. Several fluorescent proteins with versatile excitation- and emission wavelengths have been reported (e.g. GFP, mCherry, mRuby) for live cell imaging or similar applications in the field of molecular biology [57]. Unfortunately, the number of fluorescent proteins of industrial relevance is still vanishingly low. Thus, the demand for fluorescence detection for protein refolding is negligible but has promising potential to be combined with labelling techniques using fluorescent chromophores [17, 33]. For example, dyes as ANS (1-anilinonaphthalene-8-sulfonate) and Nile Red have been reported for the monitoring of differences in surface hydrophobicity, with the goal to detect aggregate formation during protein refolding [17].

The in-line monitoring of the pH value has multiple advantages for protein refolding screening experiments. For the conventional screening approach, the pH during refolding is controlled by the prior adjustment of the pH value and its consistency during refolding is ensured by the addition of buffer substances to the RB. Therefore, the main drawback of this method is that the pH value of the RB may change, if a solubilizate of different pH is added without being noticed and without means to counteract. The ability of the BioLector® system for in-line pH detection via optodes enables the identification of pH value changes due to solubilizate addition. In combination with the capability to apply a continuous feed, control of the pH-value is possible. The implementation of this system for protein refolding, has the potential to control the pH-dependent kinetics of redox systems during refolding. Thus, leading to an expansion of possibilities for screening experiments and forming the basis for the implementation of a fine-tuning of redox kinetics for protein refolding.

The in-line monitoring of  $dO_2$  is suitable for tracking the oxygen consumption throughout the refolding process. This aspect is particularly appealing for the refolding of proteins, whose refolding relies on redox systems, which naturally interact with oxygen [14]. In combination with the in-line monitoring of the redox potential, the in-line monitoring of  $dO_2$  has been established as a soft sensor for product quality and product yield during refolding processes. For that purpose, the resulting  $dO_2$  profiles are correlated with more specific and more accurate, but also more elaborate and costly HPLC analysis [4, 14, 17]. Subsequently, the  $dO_2$  profiles can be applied for the mitigation of batch-to-batch variability and for a variable control of operation time and target protein concentration [14]. Based on the capability of the BioLector® Pro for the in-line monitoring of  $dO_2$ , there is a high potential to implement  $dO_2$  monitoring for screening experiments in early DSP development, to gain specific insight into protein refolding and to facilitate the corresponding scale-up processes.

The microfluidic technology of the BioLector® Pro was expected to be the most substantial advantage of the system over conventional screening approaches. Aside of the prevalent 48-well plates, microfluidic well plates are available. These well plates also have 48 wells, but the first two rows, consisting of 8 wells each, serve as reservoirs that are connected via micro channels to the remaining wells. The microfluidic technology applies pressurized air to operate membrane valves underneath the reservoir wells in order to pump liquids through the micro channels of the chip [35, 36]. According to the technical

data sheet of the microfluidic wells, the volume of one pump stroke, which depends on the viscosity of the liquid, amounts to 120 nL for H<sub>2</sub>O and the maximum pump rate per reservoir well is approx. 80 µL/h, but since one well is connected to two reservoir wells (with the underlying idea to use one for a medium feed and the second for an acid/base feed during fermentation screenings), the max. pump rate can be doubled. Minimal pump rates below 1 µL/h are possible, with 0.6 µL/h being reported for an aqueous 500 g/L glucose solution [36].

The kinetics of the second order aggregation reaction, which competes against the first order protein refolding reaction, has been shown to be promoted by high initial protein concentrations [8, 10]. Although the increasing concentration of denatured protein has a negative influence on the refolding yield due to promoting aggregation, it was reported for several proteins that the presence of protein in form of its native tertiary structure does not reduce the refolding yield and therefore does not contribute to aggregation reactions [31, 58]. These findings support the idea of adding the solubilizate to the RB over a longer period of time as a pulsed feed, resulting in low denatured protein concentrations, preventing aggregation and thereby promoting the refolding reaction. Pulsed fed-batch refolding has been proven to increase the refolding yield in comparison to batch refolding for several proteins (e.g. GFP and hen egg white lysozyme) [31, 58, 59]. The reduction of pulse volume and the time period in between the pulses of a pulsed feed inherently leads to a continuous feed. In contrast to a pulsed feed, a continuous feed can be easily applied with established reactor-scale setups. However, a continuous protein feed yielded inferior refolding results in comparison to a pulsed protein feed for fed-batch refolding. This effect was reported for GFP and hen egg white lysozyme [30, 59]. In addition to a target protein feed, also buffer components and cofactors are subjected to a feed. Based on the hypothesis that the required coenzyme hemin stimulates self-aggregation and aggregation with unfolded or misfolded proteins due to its hydrophobic characteristics, its steady addition using a continuous feed yielded improved refolding results in comparison to a batch addition [12].

The microfluidic technology enables the application of a continuous feed for protein refolding screening experiments. Hence its application for this purpose needs to be investigated in order to be systematically applied in future screenings. Furthermore, the BioLector<sup>®</sup> Pro can be integrated into a robotic liquid handling system to enable the application of a pulsed feed. In contrast to the BioLector<sup>®</sup> system, the conventional approaches only allow screening for pulsed feed and its characteristics [12, 33, 34]. However, a pulsed feed using conventional methods is very laborious and does not capitalize on the possibilities of larger-scale reactors for the application of a continuous feed.

## 7.2 Materials and Methods

### 7.2.1 Chemicals and Software

Hemin from bovine ( $\geq 90\%$ ) and 2,2'-azino-bis (3-ethylbenzothiazoline-6-sulfonic acid) diammonium salt (ABTS) were purchased from Sigma-Aldrich (St. Louis, MO, USA). All other chemicals were purchased from Carl Roth (Karlsruhe, Germany). The process control and data collection during the fermentation was performed by Lucillus process information and management system (Biospectra; Schlieren, Switzerland). The design and analysis of the DoEs were performed with Umetrics<sup>®</sup> MODDE<sup>®</sup> Pro (Version 12.1) by Sartorius Stedim Data Analytics AB (Umeå, Sweden).

### 7.2.2 Recombinant Production of IBs

#### 7.2.2.1 GFP

The recombinant production of GFP using the production host *E. coli* BL21(DE3) was performed in a 10 L Biostat Cplus stainless steel reactor (Sartorius; Göttingen, Germany). The pre-culture was cultivated in a 2.5 L Ultra Yield<sup>®</sup> Flask (Thomson Instrument Company; Encinitas, CA, USA) in 0.5 L DeLisa medium at 37 °C and 200 rpm overnight [60]. The pre-culture was transferred into the bioreactor containing 3 L DeLisa medium and a batch fermentation was performed for 6.5 h at 35 °C, 1000 rpm, while the pH value was continuously adjusted to 6.7 with an aqueous 12.5 % NH<sub>3</sub> solution and the dO<sub>2</sub> was kept at approximately 100 % air saturation. During the subsequent fed-batch phase, which lasted 16.5 h, the specific substrate uptake rate ( $q_s$ ) was set to 0.25 g/g/h. After the induction with 0.5 mM isopropyl- $\beta$ -D-thiogalactopyranoside (IPTG), the induction phase was performed for 9 h, with  $q_s$  set to 0.35 g/g/h. Process analytics were conducted as reported in previous studies [61-64]. Subsequently, the biomass was harvested by centrifugation (17,568 rcf, 30 min, 4 °C) and stored at -20 °C until further use.

#### 7.2.2.2 HRP

The recombinant production of the HRP variant C1A was performed analogously to chapter 7.2.2.1, apart from a different  $q_s$  of 0.3 g/g/h during the induction phase. Due to a malfunction of the mass flow controller of the bioreactor, the dO<sub>2</sub> dropped to 0 % for ~2 h during the fed-batch phase, hence the time period of that phase was extended to 19 h.

### 7.2.3 Homogenization and Wash

#### 7.2.3.1 GFP

The biomass was resuspended with an IKA T10 basic ULTRA-TURRAX (Staufen, Germany) in 5 mL homogenization buffer per g wet biomass (homogenization buffer: 100 mM Tris/HCl; pH 7.4; 10 mM ethylenediaminetetraacetic acid (EDTA)) and was homogenized via high-pressure homogenization utilizing a GEA Niro Soavi Panda PLUS (Düsseldorf, Germany) at >1300 bar, while cooled, for three passages. The homogenized suspension was centrifuged (17,568 rcf, 4 °C, 30 min), the supernatant was discarded, the cell debris

was resuspended (ULTRA-TURRAX) in 10 mL H<sub>2</sub>O per g wet cell debris and centrifuged again (17,568 rcf, 4 °C, 30 min). Subsequently, the supernatant was discarded, the washed cell debris was resuspended (ULTRA-TURRAX) in 10 mL H<sub>2</sub>O per g wet cell debris, divided in 1 mL-, 5 mL and 50 mL aliquots using pre-weighed 2 mL-, 15 mL- and 50 mL reaction tubes. The aliquots were centrifuged (20,379 rcf, 4 °C, 20 min), the supernatant was discarded and the IB pellets were stored at -20 °C until further use.

#### 7.2.3.2 HRP

The homogenization of the biomass from the HRP fermentation and the wash of the HRP IBs were performed analogously to chapter 7.2.3.1. Instead of H<sub>2</sub>O, a HRP wash buffer was used for the first wash step (HRP wash buffer: 50 mM Tris/HCl; pH 8; 0.5 M NaCl; 2 M urea). This protocol was previously reported by Humer et al. [12].

### 7.2.4 Solubilization

#### 7.2.4.1 GFP

For solubilization, the IB pellet was thawed and its wet IB weight was determined. Afterwards, the thawed pellet was suspended in GFP SB (solubilization buffer) to reach a wet IB concentration of 100 g/L (GFP SB: 40 mM citric acid; 10 mM Na<sub>2</sub>HPO<sub>4</sub>; pH 2.5; 5 M urea) utilizing an ULTRA-TURRAX at power levels 2 - 5. After suspension, β-mercaptoethanol was added to a final concentration of 10 mM, to serve as a reducing agent during solubilization and the subsequent refolding. Next, the solubilization mix was incubated for 0.5 h at room temperature and slight agitation, followed by a centrifugation (20,379 rcf, 4 °C, 20 min). The supernatant (described as solubilizate throughout the thesis) was instantly used for refolding and the remaining pellet was discarded.

#### 7.2.4.2 HRP

The solubilization process for HRP was performed analogously to chapter 7.2.4.1. However, a HRP SB, whose composition varied based on the DoE design space, was used for the suspension of the IB pellet (HRP SB: 50 mM Bis-Tris/HCl (pH 7) or Tris/HCl (pH 8.5) or glycine (pH 10); pH 7 or 8.5 or 10; 6 M urea). Instead of β-mercaptoethanol, CH was added to the solubilization mix as reducing agent, to reach a final concentration of 10, 30 or 50 mM, depending on the design space of the DoE.

### 7.2.5 Protein Refolding

#### 7.2.5.1 Conventional Small-Scale Screening Experiments

##### 7.2.5.1.1 GFP

The conventional small-scale batch-refolding experiments, based on a previously reported approach, were conducted in 2 mL reaction tubes [12]. First, the appropriate GFP RBs were prepared with varying buffer substance concentration, L-Arg concentration

and pH value, dependent on the design space of the DoE (GFP RB: 0.05 M or 0.5 M or 1 M Tris/HCl; 0 M or 0.33 M L-Arg; pH 8 or 9; 0.25 M sucrose; 2 mM EDTA).

Subsequently, certain volumes of the GFP RBs, in accordance with the dilutions that are required to attain the initial protein concentrations of the design space, were transferred into 2 mL reaction tubes and cooled at 4 °C. To start the refolding process, the volumes of solubilizate, that were required to attain a final volume of 2 mL, were added to the corresponding pre-cooled GFP RBs. The reaction tubes were closed, instantly inverted several times to ensure sufficient mixing and incubated at 4 °C and slight agitation overnight (approx. 15 h).

For GFP, one DoE was designed using a full factorial design. As factors, the pH value of the RB, the buffer substance concentration, the initial protein concentration and the L-Arg concentration were varied, with the normalized off-line/in-line fluorescence after refolding as response. Four replicates of the center points were performed. The factor levels are depicted in Table 2.

Table 2: Factor levels of the GFP DoE with in-line/off-line fluorescence after refolding as response.

<b>pH of RB (-)</b>	<b>Buffer Substance Concentration (M)</b>	<b>Initial Protein Concentration (g/L)</b>	<b>L-Arg Concentration (M)</b>
8	0.05	0.25	0
9	0.5	0.5	0.33
-	1	1	-

#### 7.2.5.1.2 HRP

For HRP, the conventional small-scale batch-refolding experiments are also based on the previously reported approach [12]. First, the appropriate HRP RBs were prepared with varying CSSC concentrations and pH values, dependent on the design space of the DoEs (HRP RB: 20 mM Bis-Tris/HCl (pH 7) or Tris/HCl (pH 8.5) or glycine (pH 10); pH 7 or 8.5 or 10; 0 M or 0.375 M or 0.75 M CSSC; 2 mM CaCl<sub>2</sub>; 2 M urea; 7 % (v/v) glycerol). Afterwards, 1.95 mL of the HFP RBs were transferred into 2 mL reaction tubes and cooled at 4 °C. To start the refolding process, 50 µL solubilizate were transferred to the pre-cooled HRP RBs to reach a final volume of 2 mL. Throughout all experiments, a 1:40 dilution was performed. The reaction tubes were closed, immediately inverted several times to ensure sufficient mixing and incubated at 4 °C and slight agitation. After 15 h incubation overnight (approx. 15 h), 40 µL of a 1 mM hemin stock solution in 100 mM KOH were added to the refolding mix to reach a final hemin concentration of 20 µM and the incubation was continued for further 2 h.

For HRP, two DoEs were designed using a full factorial design. HRP DoE 1 was performed with the refolding protocol utilizing the standard dilution approach. As factors, the pH value of the SB, the pH value of the RB, the CH concentration of the SB and the CSSC concentration of the RB were varied, with the volumetric activity after refolding as

response. The factor levels are depicted in Table 3. Four replicates were performed at the center point of all factors.

*Table 3: Factor levels of the HRP DoE 1 with volumetric activity after refolding as response.*

<b>pH of SB</b> <b>(-)</b>	<b>pH of RB</b> <b>(-)</b>	<b>CH Concentration in SB</b> <b>(mM)</b>	<b>CSSC Concentration in RB</b> <b>(mM)</b>
7	7	10	0
8.5	8.5	50	0.5
10	10	-	-

HRP DoE 2 was performed with the optimized refolding protocol utilizing the reverse dilution approach. Furthermore, one of the four factors, the pH value of the RB, was removed from the DoE and an additional level is added to each of the factors CH- and CSSC concentration, in order to reduce the complexity of the design and facilitate its analysis. Hence, the pH value of the SB, the CH concentration of the SB and the CSSC concentration of the RB were varied, with the volumetric activity after refolding as response. The factor levels are depicted in Table 4. Four replicates were performed for all 3 levels of the factor pH of SB at the center points of the remaining two factors. The rationale behind the optimization of the four factors is extensively discussed in chapter 7.3.1.2.

*Table 4: Factor levels of the HRP DoE 2 with volumetric activity after refolding as response.*

<b>pH of SB</b> <b>(-)</b>	<b>CH Concentration in SB</b> <b>(mM)</b>	<b>CSSC Concentration in RB</b> <b>(mM)</b>
7	10	0
8.5	30	0.375
10	50	0.75

### 7.2.5.2 BioLector® Pro Screening Experiments

In addition to the refolding experiments, blanks for both model proteins were conducted in order to gain further information on the impact of refolding on the in-line analytics signals. The blanks are performed identically to the screening experiments described in the following two chapters, the only difference was that no IBs were added during the solubilization process.

#### 7.2.5.2.1 GFP

The DoE for the small-scale batch-refolding experiments using the BioLector® Pro for GFP was identical to the conventional small-scale experiments (chapter 7.2.5.1.1). However, the experiments were conducted in the wells of a BioLector® 48 round-well plate at 10 °C, varying agitation levels between 200 - 400 rpm and sealed with an oxygen-permeable membrane. Since the active cooling system of the BioLector® Pro can only reduce the



temperature within the reaction chamber to 5 °C below ambient temperature, the device was installed in a cold room at an ambient temperature of ~4 °C. In contrast to the reaction tubes of the conventional small-scale approach, the wells of the round well plate cannot be mixed individually, hence the refolding experiments are mixed altogether after the solubilizate is added to all experiments and the agitation within the reaction chamber is started. Due to the complex experimental designs, the solubilizate addition is a lengthy process for 48 wells (30 - 45 min).

#### 7.2.5.2.2 HRP

The two DoEs for the small-scale batch-refolding experiments using the BioLector® Pro for HRP were identical to the conventional small-scale experiments (chapter 7.2.5.1.2). However, the experiments were conducted in the wells of a BioLector® 48 round-well plate at 10 °C, varying agitation levels between 200 - 400 rpm and sealed with an oxygen-permeable membrane. In contrast to the GFP experiments utilizing the BioLector® Pro, the inability for instant mixing of the individual wells after solubilizate addition and the consequent insufficient homogeneity were problematic and led to unsatisfactory results. Hence, the standard dilution, where the solubilizate was transferred into the RB, was replaced by a reverse dilution, during which the RB was added to the afore prepared solubilizate in the wells. The optimization process is further discussed in chapter 7.3.1.2.

### 7.2.6 Analytics

#### 7.2.6.1 Off-line fluorescence

The off-line fluorescence measurements were conducted with a Tecan Spark® (Männedorf, Switzerland) microplate reader using black, flat-bottom 96-well plates. The excitation wavelength was set at 485 nm (bandwidth 20 nm) and the emission wavelength at 535 nm (bandwidth 25 nm). Before measurement, samples were diluted 1:10 in GFP dilution buffer (GFP dilution buffer: 50 mM Tris/HCl; pH 8.5).

#### 7.2.6.2 HRP Activity

The HRP activity measurements were conducted with a Tecan Spark® (Männedorf, Switzerland) microplate reader using transparent, flat-bottom 96-well plates. Depending on the concentration of correctly folded HRP, samples from the screening experiments were diluted 1:1 - 1:25 in HRP dilution buffer (HRP dilution buffer: 20 mM Bis-Tris/HCl; pH 7). For the activity assay, 175 µL of an ABTS solution (8 mM ABTS; 50 mM Na<sub>2</sub>HPO<sub>4</sub>/citric acid; pH 5) were mixed with 5 µL diluted sample in the well and subsequently 20 µL of an aqueous 10 mM H<sub>2</sub>O<sub>2</sub> solution were added to start the reaction. Instantly afterwards, the absorption at 420 nm was detected over a time span of 4 min at 30 °C. The volumetric activity was calculated using the linear slope of the absorption as a function of time as shown in formula 1.

$$Act_v = \frac{V_{total} * \Delta Abs_{420} / min * DF}{V_{sample} * d * \epsilon} \quad (1)$$

- Act<sub>v</sub> ..... Volumetric activity after refolding (U/mL)  
V<sub>total</sub> ..... Total volume of assay (200 µL)  
ΔAbs<sub>420</sub>/min ..... Change in absorption at 420 nm per minute (-)  
DF ..... Dilution factor of sample (-)  
V<sub>sample</sub> ..... Volume of sample (5 µL)  
d ..... Length of beam path through the liquid of the assay (0.58 cm)  
ε ..... Extinction coefficient of ABTS (36 mM<sup>-1</sup>cm<sup>-1</sup> [65])

### 7.2.6.3 In-Line Analytics

The in-line detection of fluorescence, pH and dO<sub>2</sub> was conducted for experiments using the BioLector® Pro with MTP-R48-BOH2 round well plates. The gain of in-line fluorescence measurements was varied between 1 - 4, the gain used for pH detection was 8 and the gain used for dO<sub>2</sub> detection was 4. Preset calibrations for 25 °C were used.

## 7.3 Results and Discussion

### 7.3.1 Comparison to Conventional Approach

To evaluate the application of the BioLector<sup>®</sup> Pro microfermentation system for the screening of protein refolding parameters, screening experiments were performed in 2 mL reaction tubes, as they are performed conventionally, and in the 48-well MTP of the BioLector<sup>®</sup> Pro. Subsequently, the results are compared to assess whether screening experiments performed in the microfermentation system yield identical results as the conventional method described by Humer et al. [12].

#### 7.3.1.1 Green Fluorescence Protein

For the assessment of the comparability of the conventional method with the BioLector<sup>®</sup> Pro for GFP, screening experiments using the DoE approach were designed. The response of the resulting multiple linear regression (MLR) is the normalized off-line fluorescence after refolding and the four factors are the pH value of the RB, the buffer substance concentration, the initial protein concentration and the L-arginine concentration.

Since the fluorescence of GFP depends on the native structure of the protein, the concentration of refolded protein can be quantified directly by fluorescence measurements. The fluorescence must be normalized to assess the influence of protein concentration adequately because otherwise the refolding experiments with the highest initial protein concentration would yield the highest absolute fluorescence and the impact of this factor would undermine the significance of the other factors of the MLR model. Since the fluorescence of GFP has been reported to be pH-dependent without being suppressed in the pH range 7.5 – 11 and with refolding optima in the pH range 7.5 - 8.5, the variation range for the pH of the RB is limited [32]. The buffer substance (Tris-HCl) has been used for refolding at a concentration of 1 M in previously conducted refolding experiments [30, 31]. This high concentration is economically unsustainable and raises the question, whether it can be reduced with no or minimal loss of refolding efficiency, especially in combination with L-Arg, which itself has buffering capabilities in combination with HCl. L-Arg is a moderate chaotropic substance with the function to suppress aggregation and the ability to enable protein refolding at the same time due to its less chaotropic character in comparison to strong chaotropes (e.g. urea) [8, 66]. Based on the aggregation kinetics, low protein concentrations during protein refolding are favoring high refolding yields [8, 10]. However, due to several factors that are discussed in chapter 5, high protein concentrations are often desired in large scale industrial applications [8, 12].

In Figure 1 the contour plots of the MLR models based on the screening experiments are depicted and the corresponding coefficient plots are shown in Figure 2.

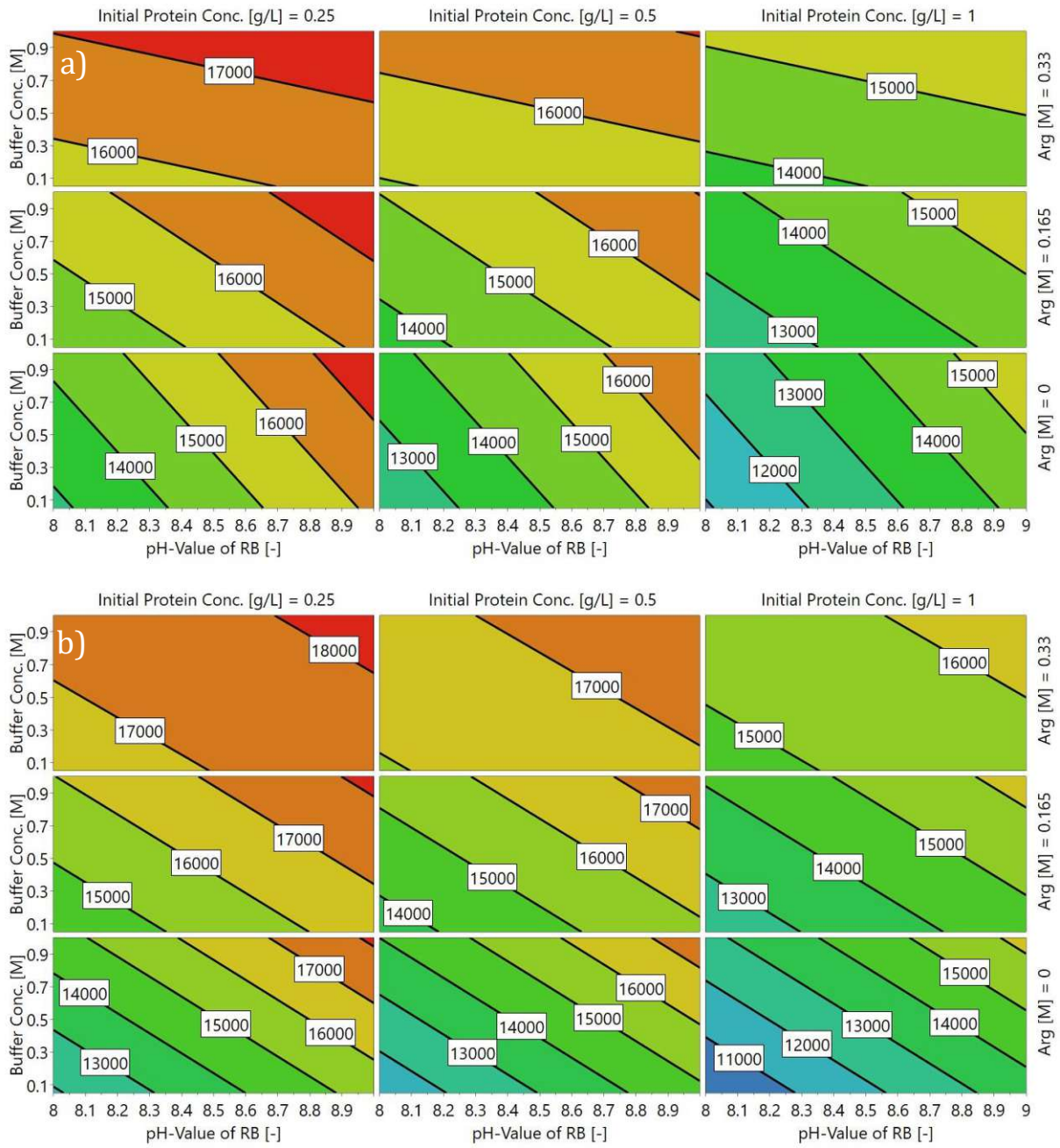


Figure 1: Contour plots of the MLR models based on the GFP screening experiments, conducted in the BioLector® Pro (a) and in reaction tubes (b). The response is the normalized off-line fluorescence (RFU) and the factors are the pH-value of the RB (-), the buffer substance concentration (M), the initial protein concentration (g/L) and the L-Arg concentration (M).

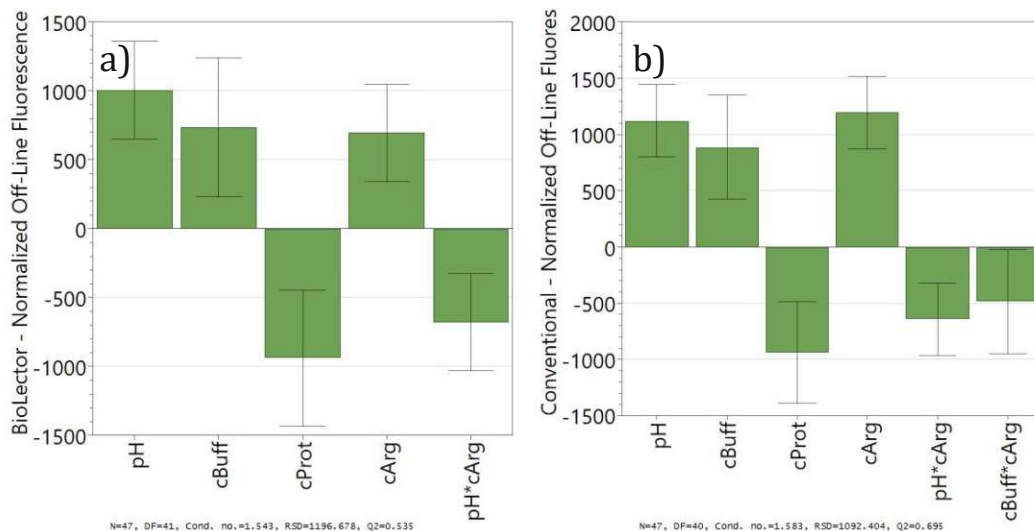


Figure 2: Coefficient plots of the MLR models based on the GFP screening experiments, conducted in BioLector® Pro (a) and in reaction tubes (b). The response is the normalized off-line fluorescence (RFU) and the factors are the pH-value of the RB (-), the buffer substance concentration (M), the initial protein concentration (g/L) and the L-Arg concentration (M).

The contour plots based on the two different approaches are nearly identical. All four factors are significant for the MLR and while the factors pH-value, buffer substance concentration and L-Arg concentration have a positive effect on the response, the factor initial protein concentration has a negative effect. Additionally, an increasing L-Arg concentration seems to reduce the required buffer substance concentration by acting as a buffer substance itself.

Slight deviation between the MLR models of the two approaches can only be seen in the interaction terms, with the interaction term of the pH-value and the L-Arg concentration being barely significant for the conventional approach and not significant for refolding conducted in the BioLector® Pro. Furthermore, a slightly higher response has been obtained via the conventional approach, exceeding 18,000 RFU.

In Figure 3 the detected off-line fluorescence values of each experimental condition are plotted against each other.

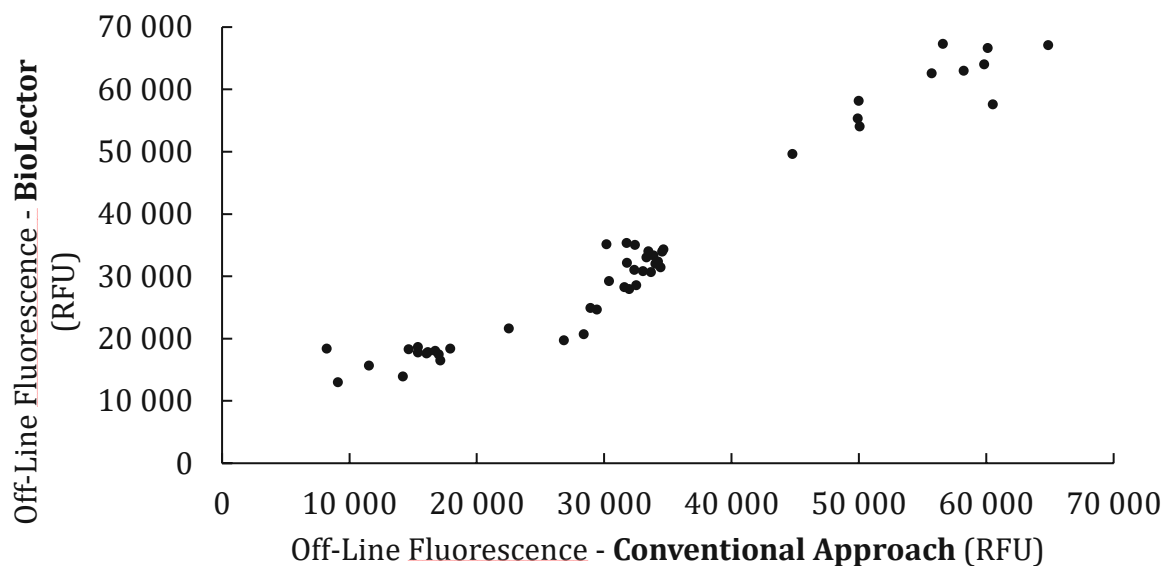


Figure 3: Off-line fluorescence of 48 experiments after refolding - BioLector<sup>®</sup> Pro vs. conventional approach.

The previous observations from the MLR models are underlined by the high similarity of the raw data of both approaches. The clustering is caused by the three levels of initial protein concentration resulting in absolute differences in the intensity of the emitted fluorescence. Despite of marginally low differences, the protein refolding screening experiments conducted in the BioLector<sup>®</sup> Pro are identical to the conventional approach for GFP as the target protein.

### 7.3.1.2 Horseradish Peroxidase

To assess the comparability of the conventional method with the BioLector<sup>®</sup> Pro for HRP, the same concept as for GFP was applied. The response of the resulting MLR is the volumetric activity after refolding and the four factors are the pH value of the SB, the pH value of the RB, the CH concentration in the SB and the CSSC concentration in the RB.

The volumetric activity after refolding has been reported to quantify refolding results, since the enzymatic activity of HRP requires, aside from its cofactors hemin and two calcium ions, its native tertiary structure [12, 56]. Since HRP contains four native disulfide bridges, a redox system is required during refolding to facilitate their formation [12, 42-44]. For HRP refolding, CH and CSSC were used throughout this thesis as redox partners due to their higher cost-effectiveness in comparison to the established redox partners DTT and GSSG. Similar CH/CSSC concentration ranges are covered by the design space of the screening experiments as reported for DTT/GSSG [12, 67].

Furthermore, it has been reported that the pH value has no effect on HRP refolding in the pH range 7 - 10 for univariate experiments, in which the concentration of the redox partners (DTT/GSSG) was kept constant [68]. However, the reaction kinetics of DTT/GSSG or CH/CSSC redox systems are pH-dependent [12, 69, 70]. Since high pH-

values increase the reaction constants, the pH value of the SB and RB were varied in the pH range 7 - 10.

Hence the number of factors is too high and the number of levels is partially too low, the resulting data of HRP DoE 1 could not be fitted using the statistical tool MLR. The factor pH value of RB had to be removed from the design space to yield valid MLR models that reflect the trends of the raw data accurately. In Figure 4 the contour plots of the MLR models at RB pH 10 are illustrated. This data represents the corresponding MLR models at other RB pH values very well (data not shown).

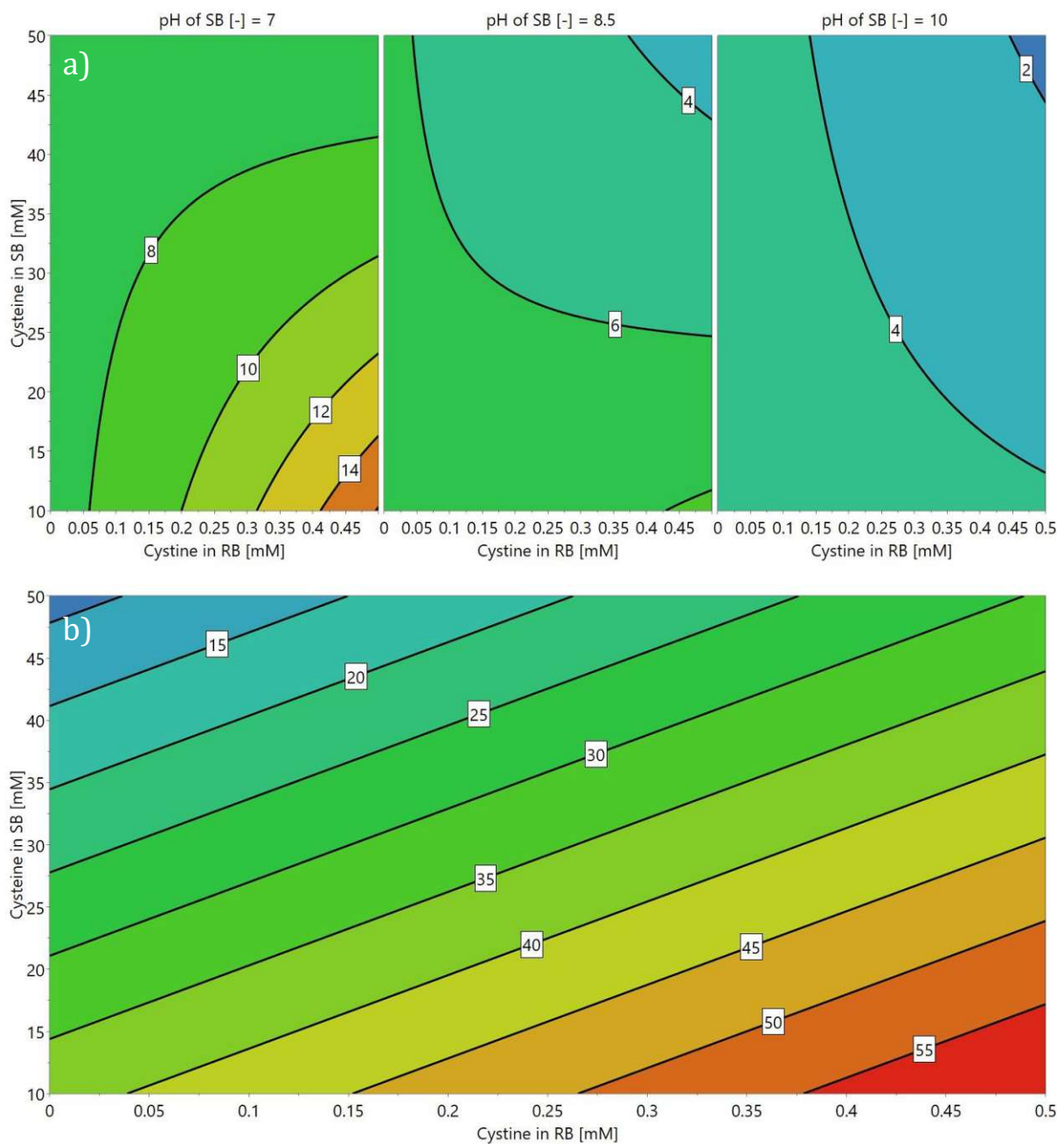


Figure 4: Contour plots of the MLR models based on the HRP DoE 1, conducted in the BioLector<sup>®</sup> Pro (a) and in reaction tubes (b) for RB pH 10. The response is the volumetric activity (U/mL) and the factors are the pH-value of the SB (-), the pH-value of the RB (-) and the concentration of the redox partners CH/CSSC in the SB/RB (mM).

It is clearly observable that the MLR models of the two different refolding approaches yield divergent results. The pH value of the SB is insignificant according to the conventional method, while it is significant using the BioLector®. The trend of low CH and high CSSC concentrations being beneficial for the refolding of HRP can only be seen at a SB pH of 7. Additionally, square terms are present in the MLR of the BioLector® approach, while there are none present in the other model. Furthermore, an astoundingly high difference can be observed in the detected volumetric activities after refolding. The maximal response using the BioLector® amounts to approximately 27 % of the maximal response yielded by the conventional refolding method.

In harsh contrast to the comparison using GFP as model protein, the results of screening experiments using the BioLector® Pro are profoundly divergent for HRP. It was hypothesized that these profound differences might have multiple reasons:

- i. **Insufficient mixing** caused by the prevalent dilution method combined with a delay until agitation is initiated. The long waiting time is caused by the lengthy addition of solubilizate to the MTP wells due to complex experimental designs (approx. 40 min). Especially in the crucial initial phase of protein refolding, at which refolding kinetics are the fastest, irreversible aggregate formation at a substantial scale could impair the refolding process. Furthermore, the screening experiments cannot be mixed individually within the BioLector® well in contrast to single reaction tubes.
- ii. **Foam formation** that was observed while shaking at 400 rpm. Protein refolding requires a suitable matrix on the molecular level, whose characteristics are shaped by the components of the refolding buffer. Hence, refolding on the gas/liquid interface of foam bubbles facilitates aggregation and results in diminished refolding yields.
- iii. **Different refolding temperature**, which was set to 10 °C within the reaction chamber of the BioLector® in comparison to the conventional approach, for which the experiments were cooled in a fridge at 4 °C. The fact that the temperature of the BioLector® reaction chamber is controlled precisely in contrast to the conventional approach, is believed to have a negligible impact on the divergent results.
- iv. The **material of the BioLector® round well plate** (polystyrene), that could enhance adsorption in comparison to the material of the reaction tubes (polypropylene). The more hydrophobic residue of the monomeric unit could exhibit a higher affinity to the intermediate refolding products, whose hydrophobic segments are not sterically covered within the protein structure in contrast to proteins in their native form.
- v. The **oxygen input during refolding** that was controlled during the BioLector® experiments via the gas composition of the reaction chamber and enabled by the oxygen-permeable sealing foil covering the MTP. The ratio of oxygen in the gas composition of the reaction chamber was held constant at ambient atmospheric level at approximately 21 % [71]. In contrast to the BioLector® experiments, there was no oxygen input into the closed reaction tubes and the amount of oxygen



present within the 2 mL reaction tubes was very low, since the refolding volume itself was 2 mL.

The three latter reasons (iii – v) raised in the last paragraph cannot be further adapted to the requirements of protein refolding screening experiments. According to the available data sheets, the active cooling system of the BioLector® Pro is only capable to reduce the temperature within the reaction chamber to maximally 5 °C below ambient temperature. Thus, the device was installed and used in a cold room in which the temperature of the reaction chamber can be controlled at 10 °C reliably. In order to adjust the oxygen input by changing the gas composition in the BioLector® reaction chamber, external nitrogen and oxygen sources need to be connected to the device, which is a challenging task inside a cold room that is not equipped properly for this purpose and therefore couldn't be realized in the scope of this thesis.

To decrease foam formation (ii), the shaking speed was reduced from 400 rpm to 200 rpm in the subsequent optimization experiments. Thereby, foam formation was reduced distinctively (assessed optically) but could not be eradicated completely. The issues of insufficient mixing and delayed agitation (i) showed promising potential for optimization and were further investigated. For this purpose, four dilution methods were defined. For the “no mixing” method the solubilizate was transferred without immediate mixing into the RB. During “reverse dilution” the solubilizate was transferred into the MTP wells before the RB is added. The dilution method “pipette mixing” describes mixing by repeatedly (5x) pipetting the RB up- and down the volume of the pipette tip after the solubilizate addition. Furthermore, the impact of starting the refolding experiments in reaction tubes followed by instant mixing through shaking and a subsequent transfer of the refolding experiment into the wells of the BioLector® MTP the was investigated (“start in reaction tubes”).

For the assessment of the impact of these dilution methods on protein refolding efficiency, experiments were conducted in which the four dilution methods were varied. Additionally, two agitation delay times (0 min and 45 min) were investigated to assess the impact of the delay on protein refolding. Due to the different nature of the two screening approaches, the prevalent dilution method for the BioLector® approach is “no mixing”, while for the conventional approach it is “start in reaction tubes”. The results are depicted in Table 5 for the BioLector® approach and in Table 6 for the conventional approach.

Table 5: Results of *BioLector*<sup>®</sup> refolding experiments conducted for the optimization of the dilution method and the analysis of the agitation delay.

Dilution Method (-)	0 min Agitation Delay		45 min Agitation Delay	
	Average Volumetric Activity (U/mL)	Relative Standard Deviation (%)	Average Volumetric Activity (U/mL)	Relative Standard Deviation (%)
No Mixing	4.7	7.3	6.5	4.7
Pipette Mixing	15.4	19.1	16.9	9.0
Start in Reaction Tubes	39.9	8.0	60.7	5.1
Reverse Dilution	29.4	16.6	60.0	4.7

Table 6: Results of *conventional refolding experiments* conducted for the optimization of the dilution method and the analysis of the agitation delay.

Dilution Method (-)	0 min Agitation Delay		45 min Agitation Delay	
	Average Volumetric Activity (U/mL)	Relative Standard Deviation (%)	Average Volumetric Activity (U/mL)	Relative Standard Deviation (%)
No Mixing	30.7	27.1	42.1	52.4
Pipette Mixing	61.2	12.9	61.4	4.4
Start in Reaction Tubes	72.1	3.1	70.9	2.5
Reverse Dilution	69.9	5.0	71.8	2.4

Surprisingly, the obtained results of the *BioLector*<sup>®</sup> experiments showed that after refolding, higher volumetric activities are detected if the agitation start is delayed by 45 min. It is hypothesized that this phenomenon is caused by less foam formation and oxygen input during the crucial initial phase of protein refolding. The “pipette mixing” dilution method yields only slightly higher volumetric activities than the “no mixing” method, while “reverse dilution” and “start in reaction tubes” equivalently lead to the highest volumetric activities. Given the lower effort required for “reverse dilution”, it is the most effective and suitable dilution method for *BioLector*<sup>®</sup> screening experiments. However, the volumetric activities achieved by the most efficient dilution method with the *BioLector*<sup>®</sup> are still marginally lower than those achieved by the conventional approach. It is hypothesized that this is resulting from the remaining uncontrollable differences (iii – v) between the two approaches that were described beforehand.

The results of the conventional screening experiments present a different picture. The delay of agitation does not make a significant difference for protein refolding and the

methods with the putatively worst mixing characteristics (“no mixing” and “pipette mixing”) yield higher volumetric activities than the BioLector® experiments. It is very likely that this is caused by the handling of individual reaction tubes, leading to unintentional mixing of the experiments. Additionally, the standard deviation of the “no mixing” experiments is remarkably high, which is a hint for an extraordinarily low robustness resulting in low reproducibility for this dilution method.

Based on the findings of the previous optimization experiments, the protocol for the BioLector® screening experiments was adapted and the DoE was repeated (HRP DoE 2) in order to re-evaluate the comparability of the two approaches. Moreover, one of the four factors, the pH value of the RB, was removed from the DoE and an additional level is added to each of the factors CH- and CSSC concentration in order to reduce the complexity of the design and facilitate its analysis. The resulting raw data yielded significant results but displayed low differences at many points of the design space, hence the application of a MLR leads to the incorporation of variance into the modeled trends and does not reflect the raw data correctly. For this reason, the raw data is displayed graphically in Figure 5 exemplary for the SB with pH 8.5. The trends of the raw data for the SB pH levels 7 and 10 depict identical trends (data not shown).

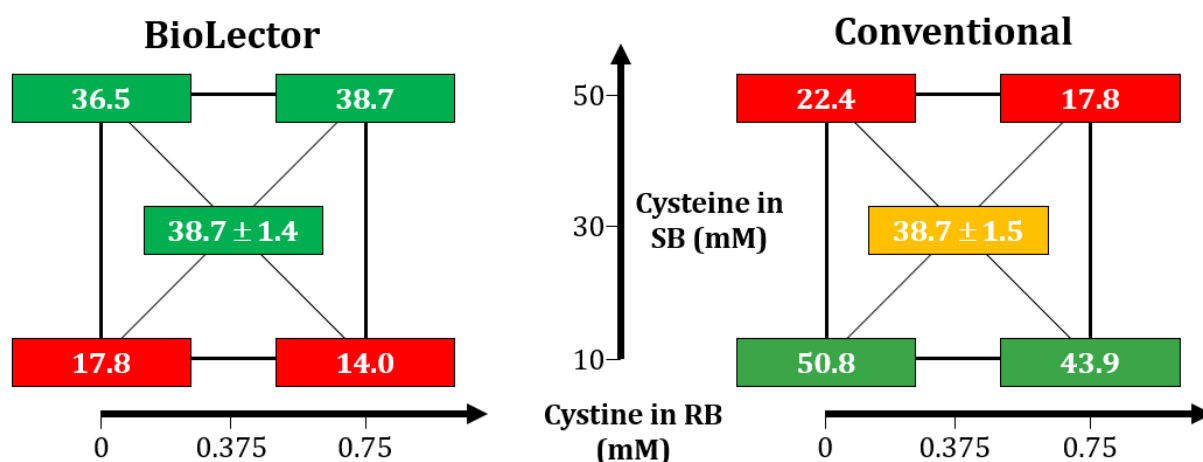


Figure 5: Graphical illustration of the raw data of HRP DoE 2 conducted in the BioLector® Pro (left) and in reaction tubes (right) at RB pH 10. The response is the volumetric activity (U/mL) and the factors are the pH value of the SB (-) and the concentration of the redox partners CH/CSSC in the SB/RB (mM).

It is clearly observable that the range of detected volumetric activities is similar for both approaches, forming the basis for an objective comparison. This underlines the success of the prior optimization of the dilution method for the BioLector® experiments.

While the CSSC concentration of the RB seems to have no effect on the refolding of HRP, clear but divergent trends are visible concerning the CH concentration of the RB. High CH concentrations in the range 30 – 50 mM result in the highest volumetric activities for the BioLector® approach and are therefore improving the refolding process. On the contrary,

a low CH concentration of 10 mM yields the highest volumetric activities after refolding for the conventional approach. As a consequence of this outcome, it is hypothesized that the controlled and constant oxygen input of the BioLector<sup>®</sup> leads to a shift in the required redox system. A higher oxygen input inevitably increases the oxidation rate of CH available in the RB and thereby also the amount of CH required for effective protein refolding. Since the oxygen input in large-scale stirred tank reactors can be controlled, the ability of the BioLector<sup>®</sup> Pro to control and include this factor into the design of screening experiments is an advantage for the scale-up process, enabling the comparison of this crucial process parameter between different scales and increasing the robustness of the experiments.

To verify whether the observed divergent results of the two approaches are truly caused by the oxygen input, nitrogen- and oxygen sources need to be implemented in the cold room to actively control the gas composition in the reaction chamber of the BioLector<sup>®</sup> Pro. This intricate task could not be accomplished in the scope of this thesis and bears potential for further investigations.

### 7.3.1.3 Summary

A refolding protocol for the BioLector<sup>®</sup> system was developed and established. Therefore, the conventional refolding protocol, especially in terms of the dilution method, was adapted to the characteristics BioLector<sup>®</sup> system since the wells of its MTP cannot be mixed individually after solubilize addition. As a result, reverse dilution was implemented because it proved to be the most effective dilution method for refolding experiments conducted using the BioLector<sup>®</sup> Pro.

In conclusion, the novel approach for the screening of protein refolding, utilizing the BioLector<sup>®</sup> Pro, yields different results as the conventional approach in terms of parameter optimization. It is hypothesized, that the reasons for this can be found in a set of parameters that characteristically differ for the two investigated approaches, such as differences in foam formation, refolding temperature, vessel material and oxygen input. The divergent results only occur for the refolding of HRP but not for GFP. This is probably due to the simple structure of GFP, leading to too fast refolding kinetics and too robust refolding for the discussed parameters to have a significant impact on the refolding process. Furthermore, the results imply that the impact of the oxygen input on the redox system is the main driver of the diverging results.

Given that the BioLector<sup>®</sup> Pro has the ability to control refolding temperature and oxygen input (via dO<sub>2</sub> and reaction chamber gas composition), its results are believed to be more accurate and helpful for the main purpose of small-scale screening experiments, which is the optimization of process parameters for industrial scale refolding. Since the temperature and the oxygen input can also be controlled at these larger scales, the BioLector<sup>®</sup> Pro enables the optimization of these parameters and ensures comparability at different scales, improving the scale-up process. Additionally, the increased control

over process parameters that cannot be controlled by a conventional screening approach generally improves the robustness and quality of the screening.

### 7.3.2 Advantages of In-Line Analytics for Screening of Protein Refolding

In the previous chapter, the comparability of the BioLector® with the conventional approach for protein refolding screening experiments is discussed, especially in regard to the ability of the BioLector® to control additional refolding parameters that have a substantial impact on refolding. However, the BioLector® further features analytical tools for the in-line monitoring of fluorescence, pH and dO<sub>2</sub>, bearing high potential to be applied for protein refolding screening experiments to meet the demands for IPM and IPC according to QbD [36].

#### 7.3.2.1 In-Line Fluorescence Detection

The monitoring of fluorescence during protein refolding is useful to quantify refolding processes of fluorescent proteins and has promising potential to be combined with labelling techniques using fluorescent chromophores [17, 33]. To investigate the advantages of in-line fluorescence detection for protein refolding, the parameter was monitored during the BioLector® GFP screening experiments. The in-line fluorescence profiles of three experiments displaying high fluorescence and of three experiments displaying low fluorescence after refolding are shown in Figure 6. These exemplary profiles reflect the general trends of all 48 experiments of the DoE very well.

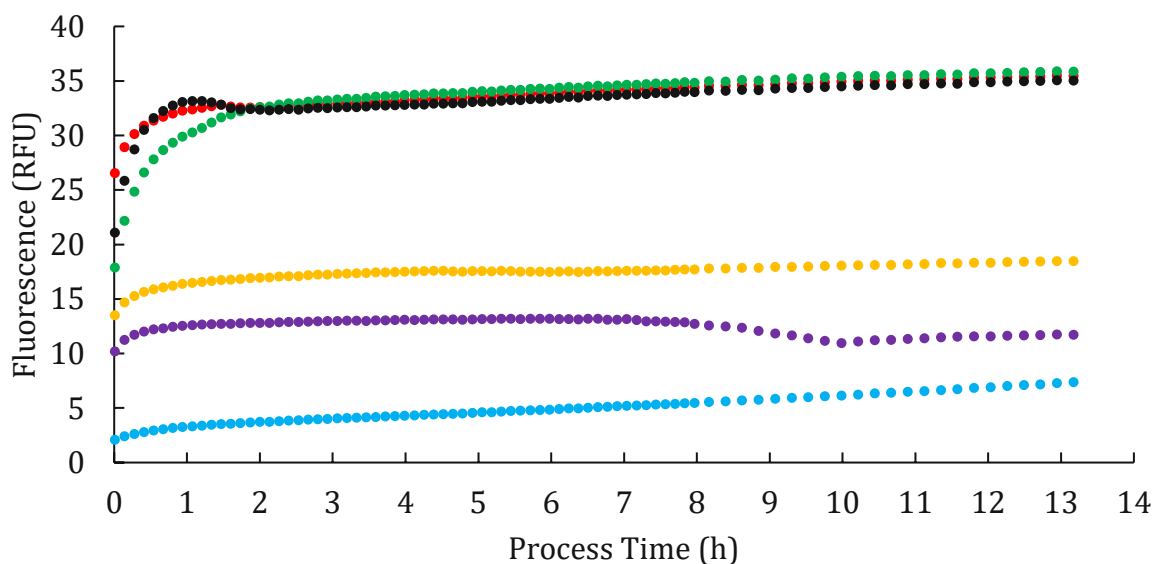


Figure 6: In-line fluorescence profiles of 6 screening experiments conducted in the BioLector® Pro.

The exemplary in-line fluorescence profiles match characteristics of previously reported GFP refolding experiments and the protein refolding process for experiments with high refolding yield is completed after approximately 3 h with more than 50 % of the final yield being reached after approximately 0.5 h [30, 31]. The initial phase of the refolding process cannot be observed in the in-line fluorescence profiles due to the long time required for solubilizate addition (approx. 40 min).

In Figure 7, the detected in-line and off-line fluorescence values after refolding are plotted against each other.

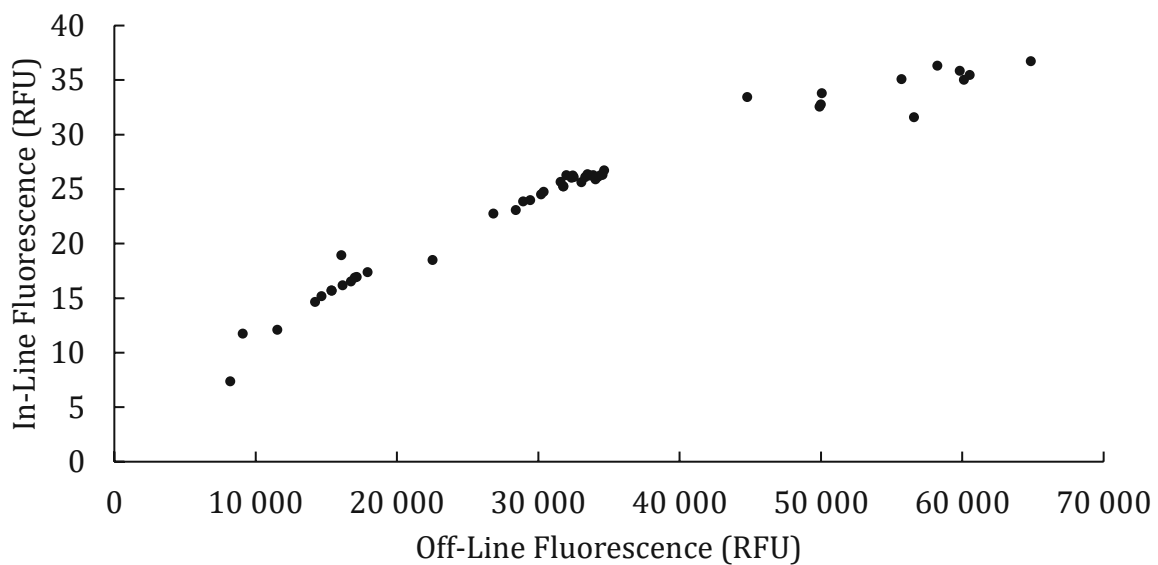


Figure 7: Plotted in-line and off-line fluorescence values of GFP screening experiments conducted with BioLector® Pro.

The in-line fluorescence values show a high correlation to the off-line fluorescence values after refolding with a comparable relative standard deviation of the replicates under 7 %. However, a flattening trend can be observed, hinting a skewed correlation either at low or high RFU. Since such trends typically occur when the linear range of analytical instruments is exceeded, the gain settings for the in-line fluorescence detection of the device were adjusted from level 1 to level 5, with the goal to correct the putative linear range.

Figure 8 illustrates the in-line fluorescence values of the GFP screening experiments, detected at gain levels 1 and 5.

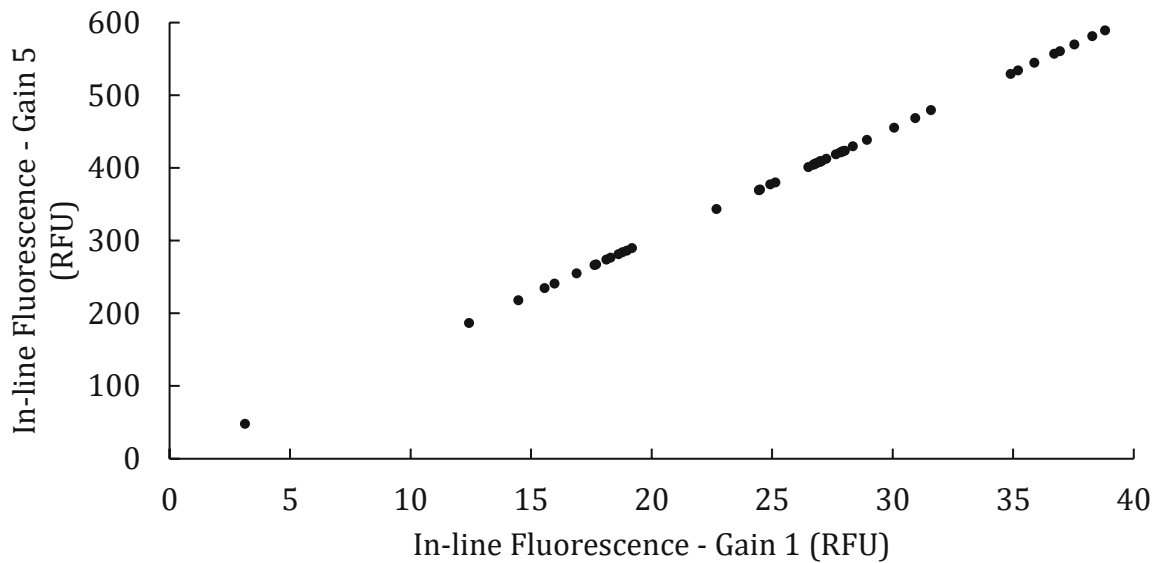


Figure 8: Plotted in-line fluorescence values detected at gain levels 1 and 5 with BioLector® Pro.

The plotted in-line fluorescence values at gain levels 1 and 5 correlated directly and the values at level 1 are simply multiplied with the factor 15.141 to reach the values detected at gain level 5. This implies that the gain setting adjustments only affect electronic data processing, and the issue of slightly skewed in-line fluorescence detection cannot be resolved by this approach. Inevitably, either low values are detected at too high levels or high values are detected at too low levels. This observation suggests that an MLR model, based on the in-line fluorescence values, will overestimate the impact of the factor initial protein concentration.

The contour plots of the MLR models based on the screening experiments with normalized in-line fluorescence as response are displayed in Figure 9 and the corresponding coefficient plots are depicted in Figure 10.

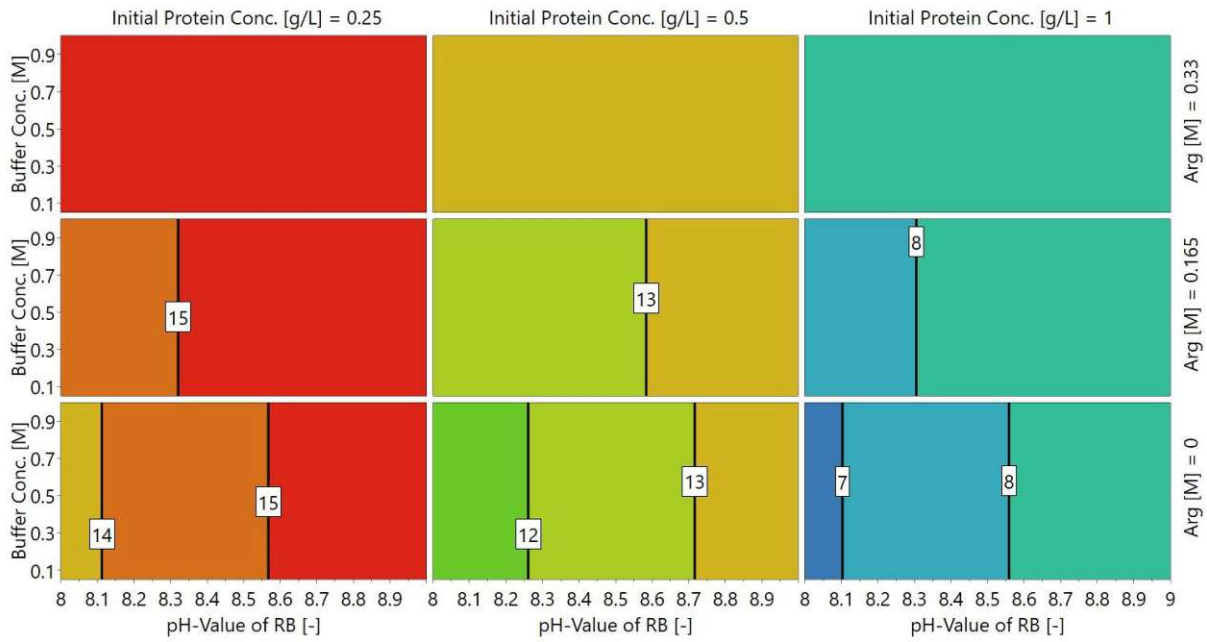


Figure 9: Contour plot of the MLR model based on the GFP screening experiments conducted using the BioLector® Pro. The response is the normalized in-line fluorescence (RFU) and the factors are the pH-value of the RB (-), the buffer substance concentration (M), the initial protein concentration (g/L) and the L-Arg concentration (M).

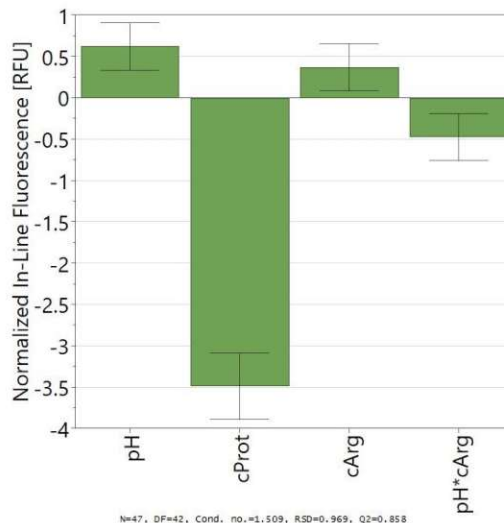


Figure 10: Coefficient plot of the MLR model based on the screening experiments conducted using the BioLector® Pro. The response is the normalized in-line fluorescence (RFU) and the factors are the pH value of the RB (-), the buffer substance concentration (M), the initial protein concentration (g/L) and the L-Arg concentration (M).

The MLR model based on in-line fluorescence data depicts similar trends as the MLR model based on off-line fluorescence data (Figure 1). But in contrast to the latter, the factor buffer substance concentration is insignificant, while the factors pH value and L-Arg concentration have a positive effect and the factor initial protein concentration has a negative effect on the response. The insignificance of one of the four factors and the low model coefficients of the others is caused by the excessive impact of the initial protein concentration on the model shown in the coefficient plot. This phenomenon originates from the problems described in the previous paragraph.



Moreover, aberrant in-line fluorescence profiles were detected exclusively for refolding experiments with RB containing 1 M Tris and 0.33 M L-Arg. The in-line fluorescence profiles of the six concerned experiments are illustrated in Figure 11.

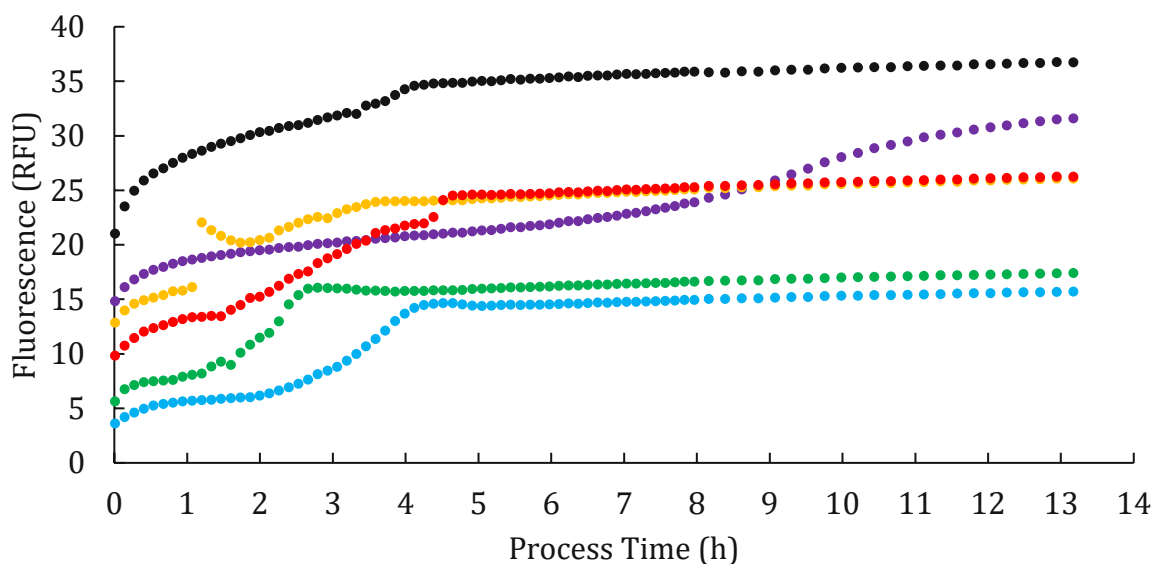


Figure 11: In-line fluorescence profiles of all six experiments of the DoE with the conditions 1 M Tris and 0.33 M L-Arg.

To rule out the possibility of erroneous measurements at certain positions of the MTP, the experiments were reiterated with a different MTP and well-layout. The results support the previous findings of aberrant in-line fluorescence profiles. Additionally, in-line fluorescence measurements were conducted for the RB with the conditions mentioned before, but without solubilizate addition, resulting in the absence of a fluorescence signal. Furthermore, the in-line fluorescence profiles of experiments conducted at 25 °C but at identical conditions using a plate reader, did not display the aberrant profiles detected using the BioLector® Pro (data not shown). Hence the obtained unusual in-line profiles are not well-dependent, are not caused by the RB itself and do not represent the actual refolding behavior. According to m2p-Labs, the high ionic strength caused by high concentrations does not interfere with in-line fluorescence detection. Thus, underlying reasons of this phenomenon cannot be explained and require further investigations.

### 7.3.2.2 In-Line pH Detection

First of all, the ability of the BioLector® system for in-line pH detection via optodes enables the identification of pH value changes due to solubilizate addition. In combination with the capability to apply a continuous feed, the control of the pH-value is possible. Furthermore, the implementation of this system has the potential to control the pH-dependent kinetics of redox systems during refolding. According to the datasheet of the utilized BOH2 round well plate, the dynamic range for pH detection is 3.7 - 8.0 with an accuracy of  $\pm 0.1$  in the pH range 4.7 - 7.0 and the temperature range is 15 - 50 °C. Since

the pH values of the screening experiments are in the range 7 - 10, and the working temperature is 10 °C, an offset and the necessity of an alternative calibration were anticipated.

### 7.3.2.2.1 Green Fluorescence Protein

Figure 12 displays the in-line pH value profiles of all 48 GFP screening experiments conducted with the BioLector® Pro.

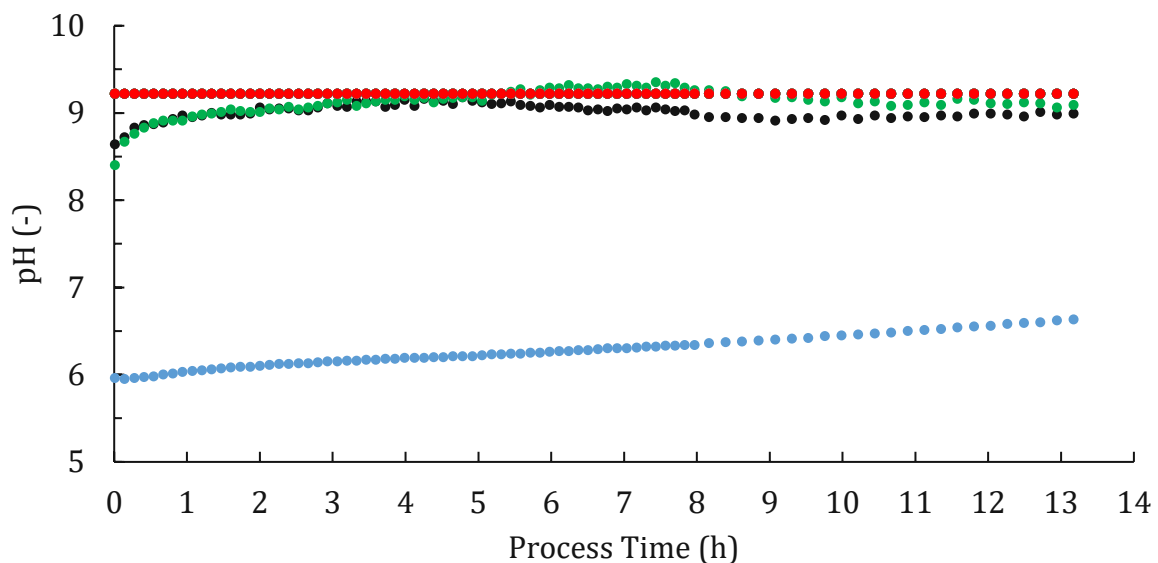


Figure 12: In-line pH value profiles of all 48 GFP screening experiments conducted with the BioLector® Pro.

45 of the experiments with preset pH-values of 8 and 9 are detected continuously at pH 9.22 (illustrated as red data points in Figure 12). The continuously identical pH-values indicate that the detected values are higher than the preset pH values of the experiments, exceeding the upper limit of the optode. This upward shift of the detected values in comparison to the preset values is presumably caused by the low temperature of 10 °C. All three of the 48 experiments that were detected below the limit, have an initial pH value of 8 and the lowest levels of buffer substance and L-Arg concentration (0.05 M Tris and 0 M L-Arg). Thus, the addition of the solubilizate (pH 2.5) cannot be compensated and lead to the severe drop of the pH value, especially for the experiment with an initial protein concentration of 1 g/L, requiring a high amount of solubilizate (illustrated as blue data points in Figure 12). Thus, the in-line pH value data for the GFP screening experiments reveal that the optodes for pH detection cannot detect pH values of 8 and higher at a temperature of 10 °C for the GFP screening experiments.

### 7.3.2.2.2 Horseradish Peroxidase

In Figure 13, the in-line pH profiles of all 48 HRP screening experiments, performed with standard dilution, are depicted. During the standard dilution, the solubilizate is added to the RB, while in the course of a reverse dilution the order is reversed. Although protein refolding has been shown to be inefficient using this dilution method, refolding does not affect the pH value and this dilution method allows to observe the pH value during and after solubilizate addition.

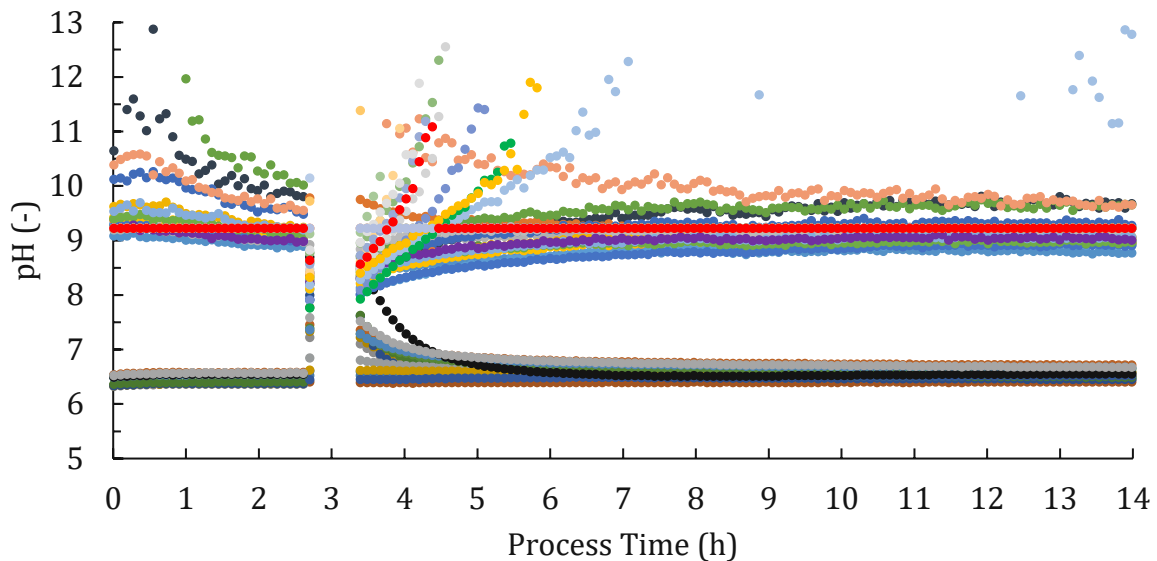


Figure 13: In-line pH profiles of all 48 HRP screening experiments conducted with the BioLector® Pro using the normal dilution method (HRP DoE 1).

The experiments with a preset pH value of 7 were detected in the range 6.5 - 6.7, while the experiments with preset pH values of 8.5 and 10 are detected in the range 8.9 - 9.8. The abrupt pH increase/decrease at 2.7 - 3.4 h process time is due to the addition of solubilizate with a divergent pH value in comparison to the pH value of the RB. But within one subsequent hour after solubilizate addition, the pH values converge towards the original level. Furthermore, many outliers can be observed in the pH range above 9.8.

Based on the observations of the previous paragraph, the experiments with a pH value of 8.5 and 10 are detected at or above the limit of the optode/detector, which is in the pH range 8.9 - 9.8. The experiments with a preset pH value of 7, are detected at slightly lower values, caused by the low temperature of 10 °C. Since the screening experiments conducted using the reverse dilution method were all performed at a RB pH value of 10, all detected in-line pH value profiles of those experiments clearly exceed the upper optode/detector limit, with all datapoints at pH 9.22, except for a few outliers (data not shown).

### 7.3.2.2.3 Summary

In conclusion, experiments with a pH value higher than 8 cannot be detected at all with the BioLector® Pro because the upper limit of the pH optode (with the dynamic range pH 3.7 - 8.0) is exceeded. This effect is especially distinctive for GFP, because all signals are detected continuously at pH 9.22 and no outliers are observable. It is hypothesized that the reason for this are cross interactions between the broad GFP fluorescence emission peak at a wavelength of 508 nm and the excitation (508 nm) and emission (550 nm) wavelengths of the pH optode of BOH2 well plates [38, 41].

On the other hand, experiments below the upper limit of the pH optode can be detected with only a slight downward pH shift due to the refolding temperature of 10 °C, which is 5 °C below the lower temperature limit of the pH optode. Since protein refolding is generally conducted at pH values above pH 7 in order to increase the reaction kinetics of established redox components, the use of the pH optode is severely limited due to its current measurement range [12, 69, 70].

### 7.3.2.3 In-Line dO<sub>2</sub> Detection

The in-line monitoring of dO<sub>2</sub> is suitable for tracking the oxygen consumption throughout the refolding process. Based on the capability of the BioLector® Pro for the in-line monitoring of dO<sub>2</sub>, there is a high potential to implement dO<sub>2</sub> monitoring for screening experiments in early DSP development, to gain specific insight into protein refolding and to facilitate the corresponding scale-up processes. According to the datasheet of the used BOH2 round well plate, the dynamic range for dO<sub>2</sub> detection is 0 – 100 % (air saturation) with an accuracy of ± 5 % and the temperature range is 10 - 40 °C. Thus, the experiments were performed within the temperature range of the dO<sub>2</sub> optode.

#### 7.3.2.3.1 Green Fluorescence Protein

Prior to the performance of the refolding screening experiments, the dO<sub>2</sub> profile of blanks (RB, without IBs and therefore no refolding reactions), was monitored at varying agitation levels. In Figure 14, the in-line dO<sub>2</sub> profiles of three replicates of a blank containing 0.5 M Tris, 0.33 M L-Arg at a pH of 8.5 are depicted. The agitation levels were increased by 200 rpm every 4 h, starting at 200 rpm.

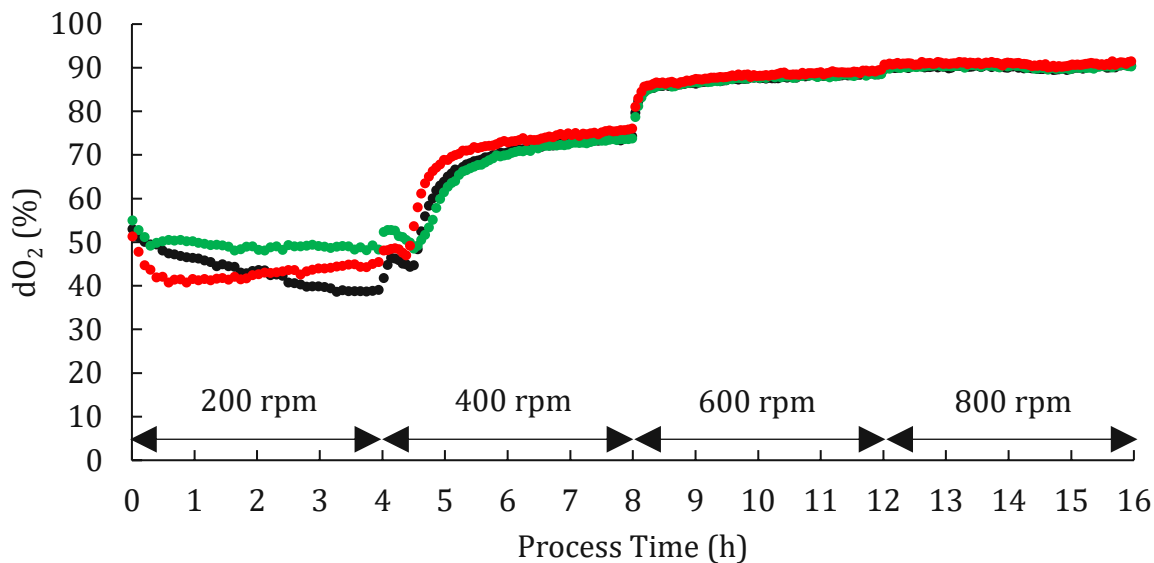


Figure 14: In-line  $dO_2$  profile of three blank replicates containing 0.5 M Tris, 0.33 M L-Arg at pH 8.5 at varying agitation levels.

Naturally, higher agitation causes increasing  $dO_2$  values based on increased oxygen transfer between the RB and the gas of reaction chamber of the BioLector<sup>®</sup> Pro (ambient air in this case). Accordingly, the  $dO_2$  level of the blank profiles increase each increment, approximately by 30 % after the first step, by 15 % after the second and merely 1 % after the third. The exceptionally long equilibration time of at least 1 h after the first increase of agitation at 4 h process time, in combination with the sudden rise and instant fall of the  $dO_2$  value at the moment of the change in agitation, suggests that during that period the reductant is oxidized quantitatively. The subsequent absence of the reducing agent leads to a drop in the oxygen consumption and thereby to an increase of  $dO_2$ . Hence, the  $dO_2$  level is hypothesized to be held down in the first phase until 5 h process time by the oxidation of the reducing agent. This oxidation reaction probably also causes the high initial absolute standard deviation of the replicates amounting to  $\pm 6.6$  %, which is slightly higher than the reference accuracy of the manufacturer but is approximately tenfold higher than the subsequent variation after 5 h process time.

In Figure 15 the in-line  $dO_2$  profiles of three refolding experiments each, with low and high final in-line fluorescence, are shown in combination with the corresponding fluorescence.

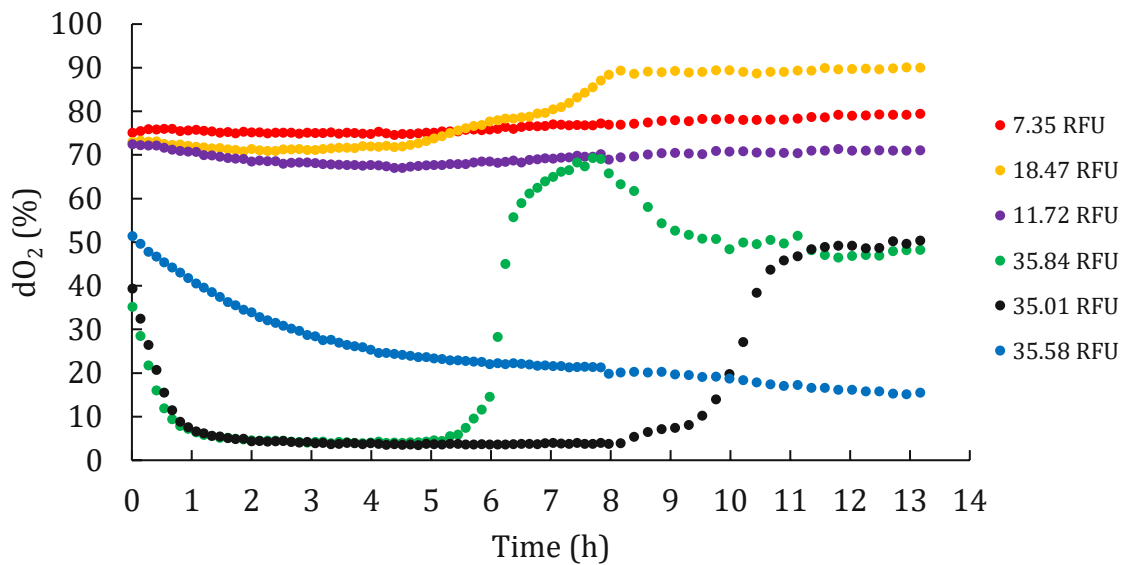


Figure 15: Exemplary  $dO_2$  profiles of three refolding experiments each with low and high final in-line fluorescence. The agitation level is changed from 400 rpm to 200 rpm at 8 h process time.

A moderate correlation between the  $dO_2$  profiles and the corresponding fluorescence values after refolding can be observed. Experiments with high final fluorescence and therefore high refolding yield, are subject to a significant drop of  $dO_2$  after the solubilizate addition. For most of these experiments, the  $dO_2$  value falls below 10 % and recovers at varying process times of up to 10 h without reaching a uniform level in the end. Experiments with a low final fluorescence and therefore low refolding yield, only experience a minor drop of  $dO_2$  with a faster recovery than other experiments. The profiles presented in Figure 15 are exemplary and represent the previous findings best, while some aberrant profiles exist that do not follow those general trends. Since the data is ambiguous there is only a moderate correlation.

Figure 16 illustrates the  $dO_2$  profiles of a refolding experiment and a blank at highly similar conditions. The refolding experiment was conducted with 0.5 M Tris, 0.33 M L-Arg at pH 9, while the blank contained identical Tris and L-Arg concentrations but had a slightly divergent pH of 8.5.

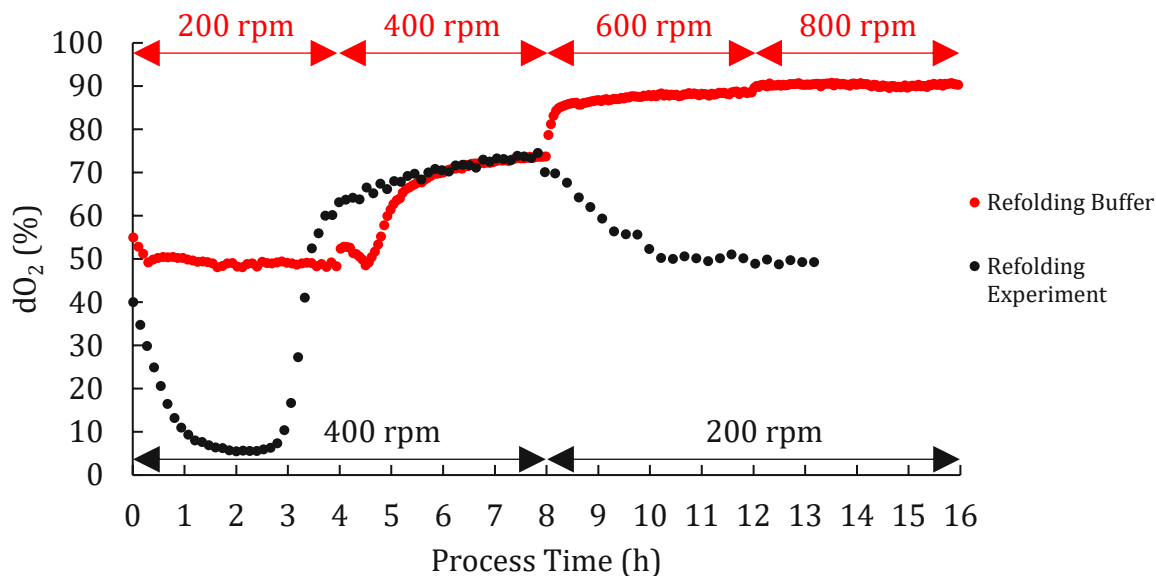


Figure 16: Comparison of the in-line  $dO_2$  profiles of a GFP refolding experiment and a blank with similar composition (refolding experiment: 0.5 M Tris, 0.33 M L-Arg, pH 9; blank: 0.5 M Tris, 0.33 M L-Arg, pH 8.5).

According to the previous findings, a clear drop of  $dO_2$  is observable in the profile of the refolding experiment in comparison to the blank without refolding reactions. Thus, the distinctive decline of the  $dO_2$  signal is clearly caused by refolding reactions and not by the buffer composition. Since the molecular refolding process is supported by reducing reactions, the time period for the quantitative oxidation of the reducing agent is shortened to 3 h in comparison to the 5 h required for the blank. After the reducing agent is completely oxidized in both experiments and the agitation level is identical, the  $dO_2$  levels align at ~70 % in the period 5.5 - 8 h. That underlines the comparability of the shown experiments and the validity of the results. The divergent  $dO_2$  profiles after 8 h process times are caused by deviating agitation levels. The different agitation levels impede the comparison of the two  $dO_2$  profiles and originate from an aberrant experiment design, but nevertheless the illustrated profiles are well suited for comparison.

A high reproducibility forms the basis for the in-line  $dO_2$  monitoring to be reasonably applied as a soft sensor for product quality and product yield. Therefore, the screening experiments of the DoE were reiterated two times to obtain triplicates and to assess the reproducibility. To differentiate between optimal and unsuitable refolding conditions, the  $dO_2$  profiles of three experiments each with a high and low final in-line fluorescence are depicted in Figure 17 and Figure 18.

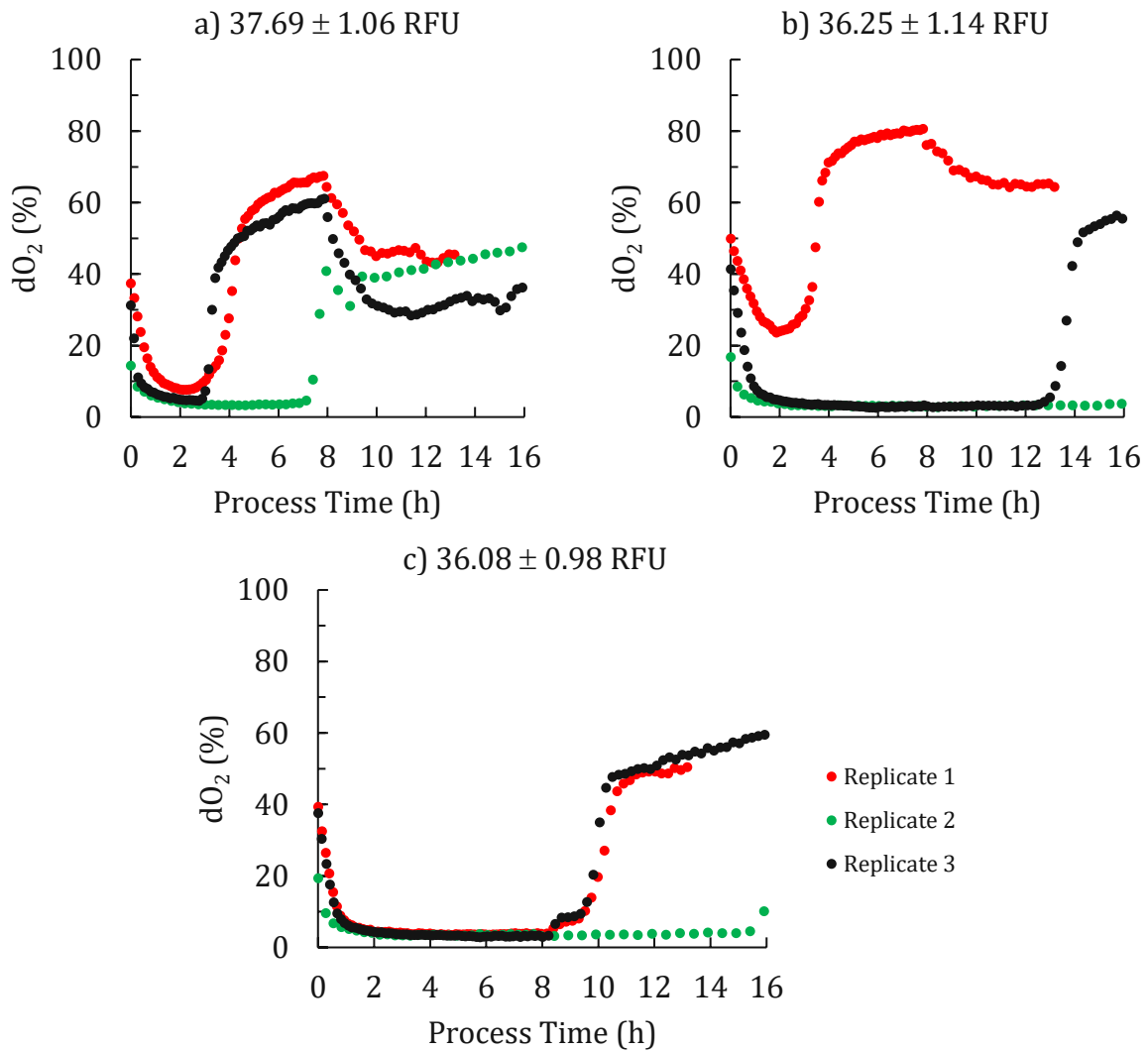


Figure 17: Comparison of the in-line  $dO_2$  profiles of three replicates each of three GFP refolding experiments that yield **high** in-line fluorescence after refolding. The average final in-line fluorescence values of the experiments are  $37.69 \pm 1.06$  RFU (a),  $36.25 \pm 1.14$  RFU (b) and  $36.08 \pm 0.98$  RFU (c).

The average final in-line fluorescence values of the three exemplary experiments shown in Figure 17 are  $37.69 \pm 1.06$  RFU (a),  $36.25 \pm 1.14$  RFU (b) and  $36.08 \pm 0.98$  RFU (c). It is clearly observable that the reproducibility for experiments with high refolding yield is very low in respect to the reproducibility of the buffer (Figure 14), albeit similar trends can be observed occasionally. Although, several confounding factors are present in the experiment design that impede the reproducibility. Due to different experiment layouts, the time required for solubilizate addition varies in the range  $\pm 0.5$  h possibly leading to an offset on the horizontal axis. Differences in agitation levels are present, with replicate 1 being agitated at 400 rpm for the initial 8 h, while the other replicates were continuously agitated at 200 rpm. Furthermore, replicate 3 was performed in a reused well plate and the impact of reused well plates on the in-line  $dO_2$  detection is not known.



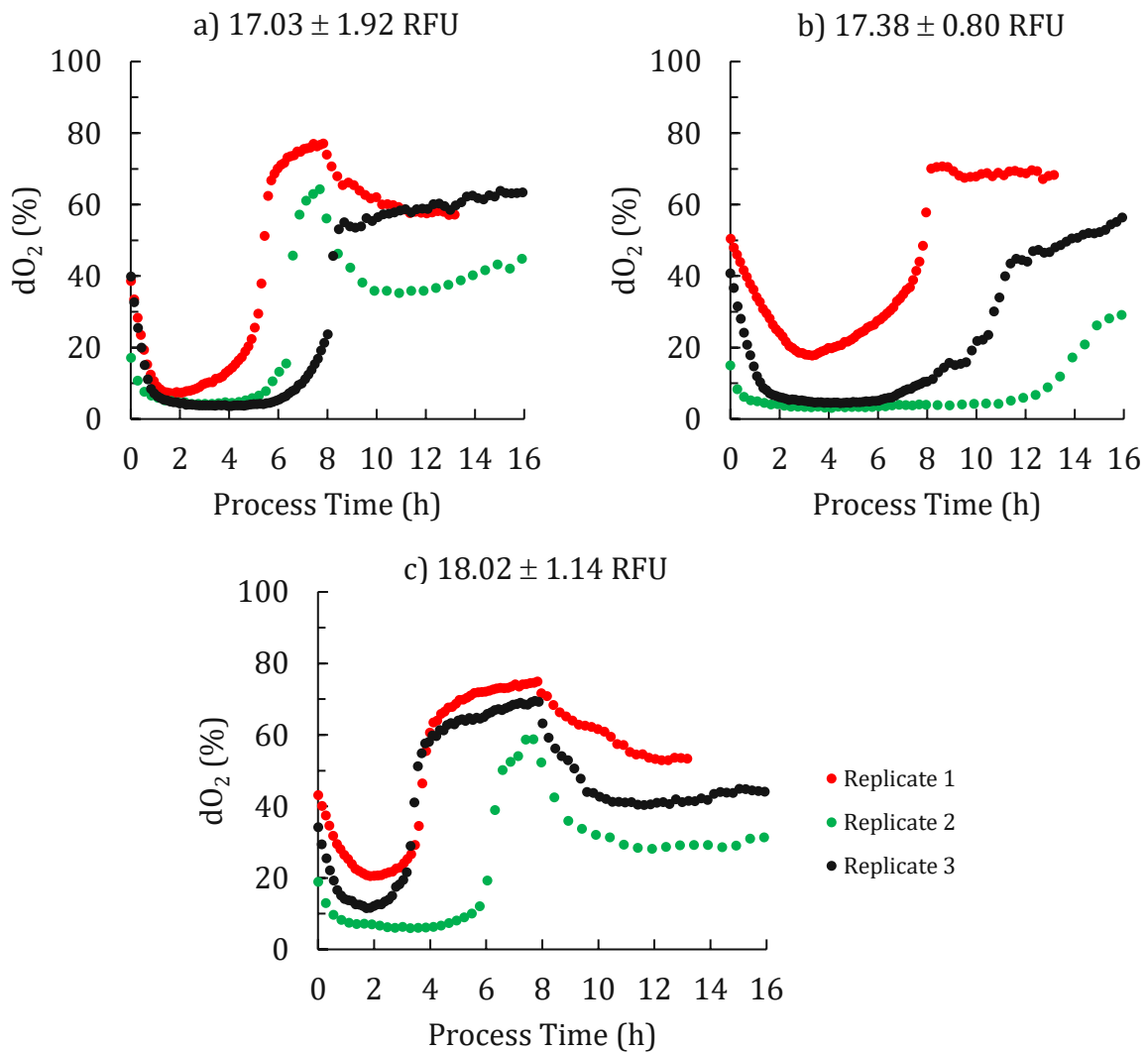


Figure 18: Comparison of the in-line  $dO_2$  profiles of three replicates each of three GFP refolding experiments that yield **low** in-line fluorescence after refolding. The average final in-line fluorescence values of the experiments are  $17.03 \pm 1.92$  RFU (a),  $17.38 \pm 0.80$  RFU (b) and  $18.02 \pm 1.14$  RFU (c).

The average final in-line fluorescence values of the three exemplary experiments shown in Figure 18 are  $17.03 \pm 1.92$  RFU (a),  $17.38 \pm 0.80$  RFU (b) and  $18.02 \pm 1.14$  RFU (c). Although the trends of the replicate profiles exhibit a higher similarity than the experiments with high final fluorescence, there are still substantial differences in the  $dO_2$  levels after the initial drop and in the time of recovery. The confounding factors are identical to the ones described in the last paragraph. Hence, the reproducibility of experiments with low refolding yield is also low, especially in respect to the reproducibility of the buffer (Figure 14). Furthermore, the exemplary  $dO_2$  profiles in Figure 18 show that several experiments defy the general moderate correlation between the  $dO_2$  profile and fluorescence after refolding, which has been illustrated in Figure 15.

#### 7.3.2.3.2 Horseradish Peroxidase

In analogy to the GFP experiments, the  $dO_2$  profiles of blanks were analyzed prior to the refolding screening experiments. However, in comparison to GFP, HRP has four disulfide bridges in its native tertiary structure, thus a redox system is required for refolding. This

increases the complexity of the buffer and the corresponding analysis. In Figure 19, the  $dO_2$  profiles of five blanks with RBs containing different ratios of reducing- and oxidizing agent are presented.

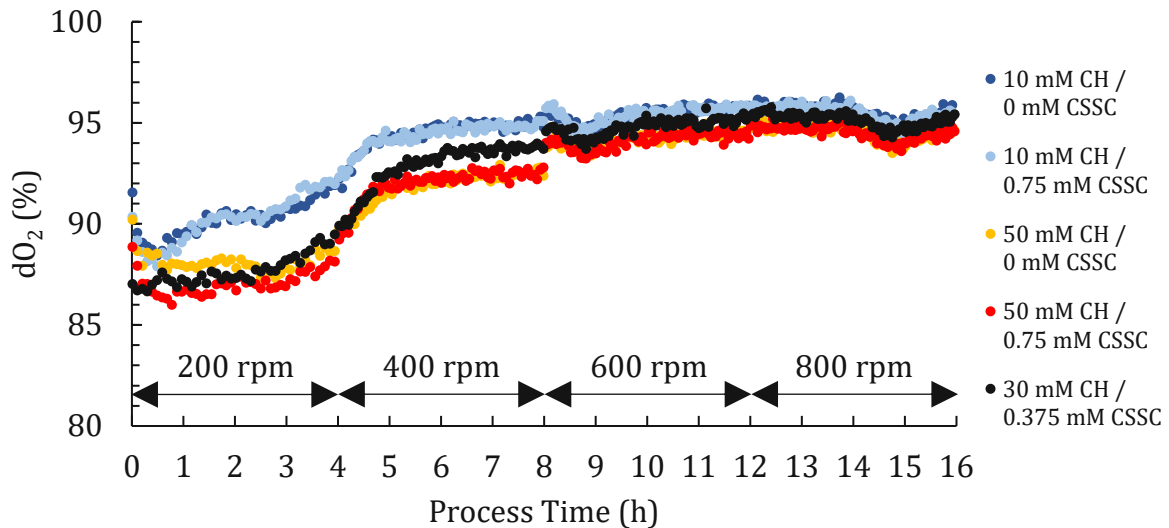


Figure 19: In-line  $dO_2$  profiles of five different blanks with varying CH and CSSC concentrations at pH 10 and varying agitation levels.

The  $dO_2$  values of the HRP blanks are notably higher and are detected in a smaller range, compared the blanks of GFP. Despite the low differences between the profiles throughout the process, a clear clustering based on the reducing agent (CH) concentration can be observed with an increasing amount of reductant leading to lower  $dO_2$  values. The differences persist until 8 h process time, at which the agitation speed is increased to 600 rpm and all profiles converge, leading to an absolute standard deviation of 2.2 %. The final  $dO_2$  level is reached at different times by the different blanks in accordance with their reducing agent concentration. Hence, the comprised amount of reducing agent is quantitatively oxidized after 5 h for blanks containing 10 mM CH and at approx. 8 h for blanks containing 30/50 mM CH. The seemingly simultaneous time for both blanks with higher reducing agent concentrations is hypothesized to be caused by an immediate and high oxygen transfer rate that is triggered by the increase of agitation speed to 600 rpm. Furthermore, the increments of the  $dO_2$  levels, initiated by the increase of agitation speed, are much lower than for the GFP blanks and the maximal level is already reached after 5 - 8 h, depending on the reducing agent concentration.

Figure 20 illustrates three blank replicates containing 10 mM CH in SB and 0.75 mM CSSC at SB pH 10 with varying agitation levels throughout the process.

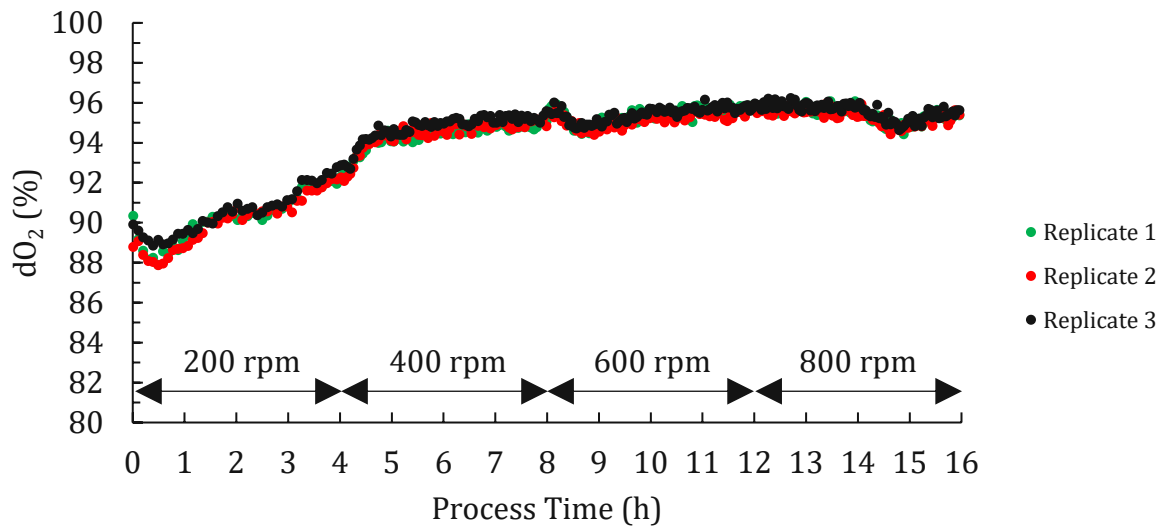


Figure 20:  $dO_2$  profiles of three blank replicates containing 10 mM CH (in SB), 0.75 mM CSSC at pH 10 and varying agitation levels.

The absolute standard deviation of the blank replicates is low throughout the whole process and amounts to 1.7 %, attesting a high reproducibility for blanks without refolding reactions. In Figure 21 exemplary  $dO_2$  profiles of three refolding experiments each with low and high final volumetric activity are displayed.

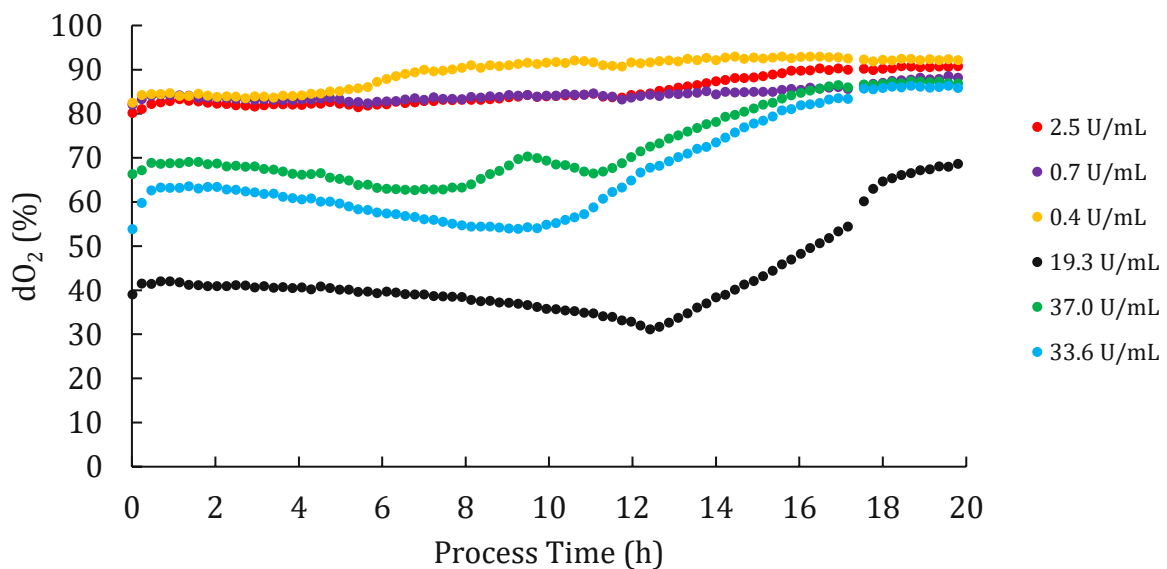


Figure 21: Exemplary  $dO_2$  profiles of three refolding experiments each with low and high final volumetric activity. The agitation speed is constantly at 200 rpm.

Analogously to the GFP experiments, a moderate correlation between the  $dO_2$  profiles and the corresponding volumetric activities after refolding can be observed. Experiments with high volumetric activity and therefore high refolding yield, are subject to a significant

drop of  $dO_2$  after the solubilizate addition, combined with long time periods for recovery. For most of these experiments, the  $dO_2$  value does not fall below 50 % and recovers at varying process times of up to 18 h without reaching a uniform level in the end. Experiments with a low final volumetric activity and therefore low refolding yield, only experience a minor drop of  $dO_2$  with a faster recovery than other experiments. But there are some experiments which defy the previously described trends. Hence, the described correlation is ambiguous.

Figure 22 shows the  $dO_2$  profiles of a refolding experiment with a high final volumetric activity and a blank at identical conditions (30 mM CH in SB, 0.375 mM CSSC, SB pH 10) but with diverging agitation levels throughout the process.

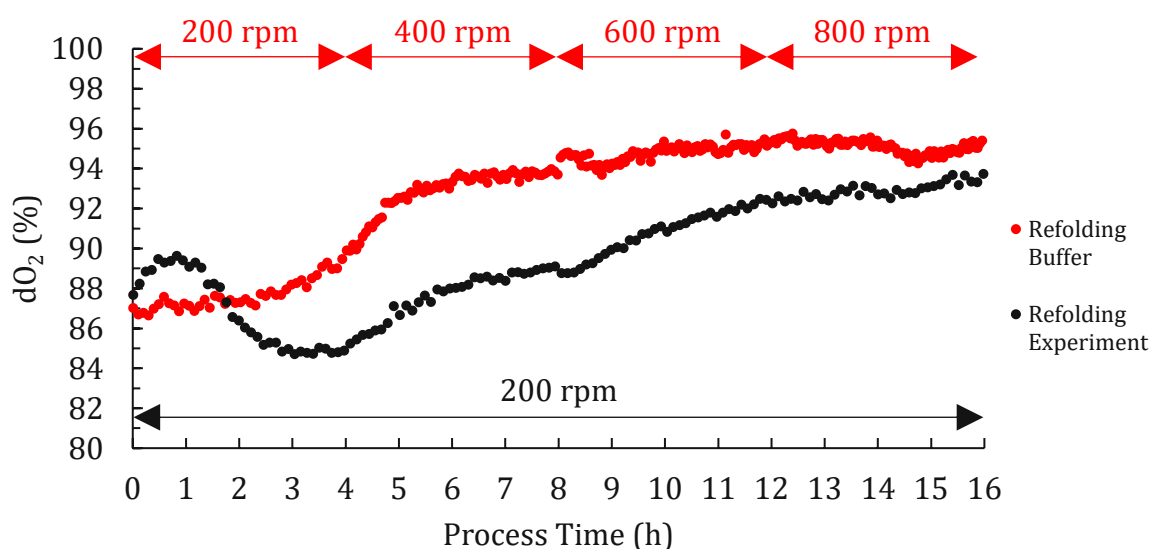


Figure 22: Comparison of the in-line  $dO_2$  profiles of a refolding experiment and a blank with identical composition (30 mM CH in SB, 0.375 mM CSSC in RB, SB pH 10).

During the initial 4 h of the process, the  $dO_2$  profile of the refolding experiment falls below the profile of the blank, underlining the fact that the distinctive decline of the  $dO_2$  signal is caused by refolding reactions and not by the buffer composition. The drop of ~5 % is remarkably lower than for GFP experiments with a high refolding yield (drop of >35 %), which is probably caused by the slower refolding kinetics of HRP and additionally indicates that the  $dO_2$  profile during refolding is highly dependent on the POI. Since the  $dO_2$  levels of the blanks are also lower for GFP, the different reducing agents are believed to have an influence on the magnitude of the drop. After the recovery of the  $dO_2$  level of the refolding experiment at 11 h, the  $dO_2$  values are still below the level of the blank due to divergent agitation levels.

Analogously to the GFP experiments, the HRP experiments were reiterated to assess the reproducibility of the in-line  $dO_2$  measurements. To differentiate between optimal and unsuitable refolding conditions, the  $dO_2$  profiles of three experiments each, with a high and low final volumetric activity, are illustrated in Figure 23 and Figure 24.

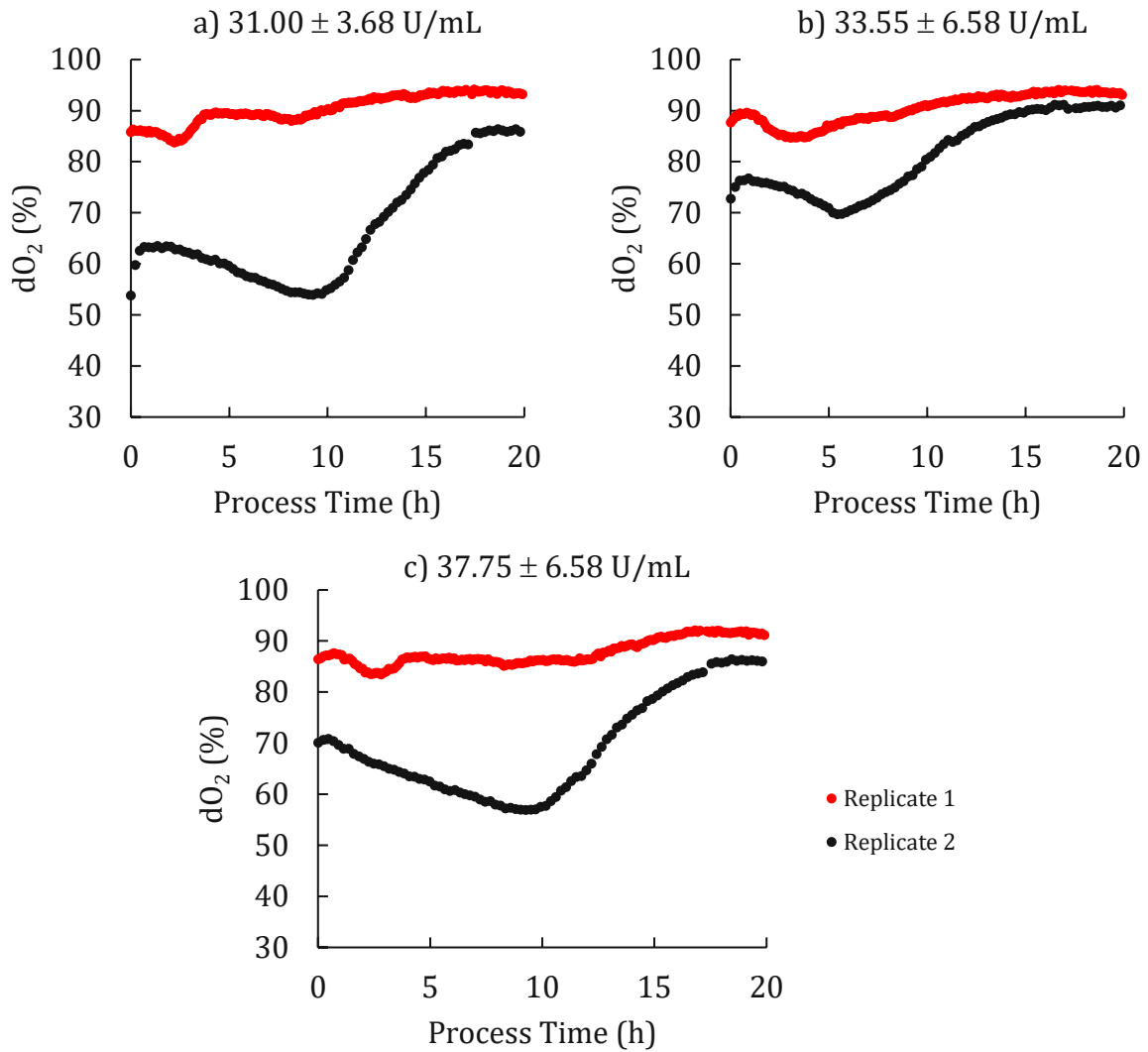


Figure 23: Comparison of the in-line  $dO_2$  profiles of three replicates each of three HRP refolding experiments that yield **high** volumetric activity after refolding. The average final volumetric activity values of the experiments are  $31.00 \pm 3.68$  U/mL (a),  $33.55 \pm 6.58$  U/mL (b),  $37.75 \pm 6.58$  U/mL (c).

The average final volumetric activity values of the three exemplary experiments shown in Figure 23 are  $31.00 \pm 3.68$  U/mL (a),  $33.55 \pm 6.58$  U/mL (b),  $37.75 \pm 6.58$  U/mL (c). The relative standard deviation of the volumetric activity is several times higher than the relative standard deviation of the in-line- or off-line fluorescence, which are used to quantify the refolding of GFP. It is hypothesized that this is partly because of the more complex refolding process of HRP, caused by its more intricate native tertiary structure, and partly because the many parameters that are involved in the execution of ABTS assays and are thereby increasing the measurement inaccuracy. Therefore, the direct comparison of the  $dO_2$  profiles of the two replicates needs to be considered cautiously. In regard to the relatively small  $dO_2$  range in which the profiles for HRP are detected and the extremely high reproducibility of the blank runs, the reproducibility needs to be classified as low. Although, similar confounding factors play a role as for GFP. Due to different experimental layouts, the time required for solubilizate addition varies in the range  $\pm 0.5$  h possibly leading to an offset on the horizontal axis and replicate 2 was conducted in a reused well plate. The impact of reused well plates on the in-line  $dO_2$  detection is not known.

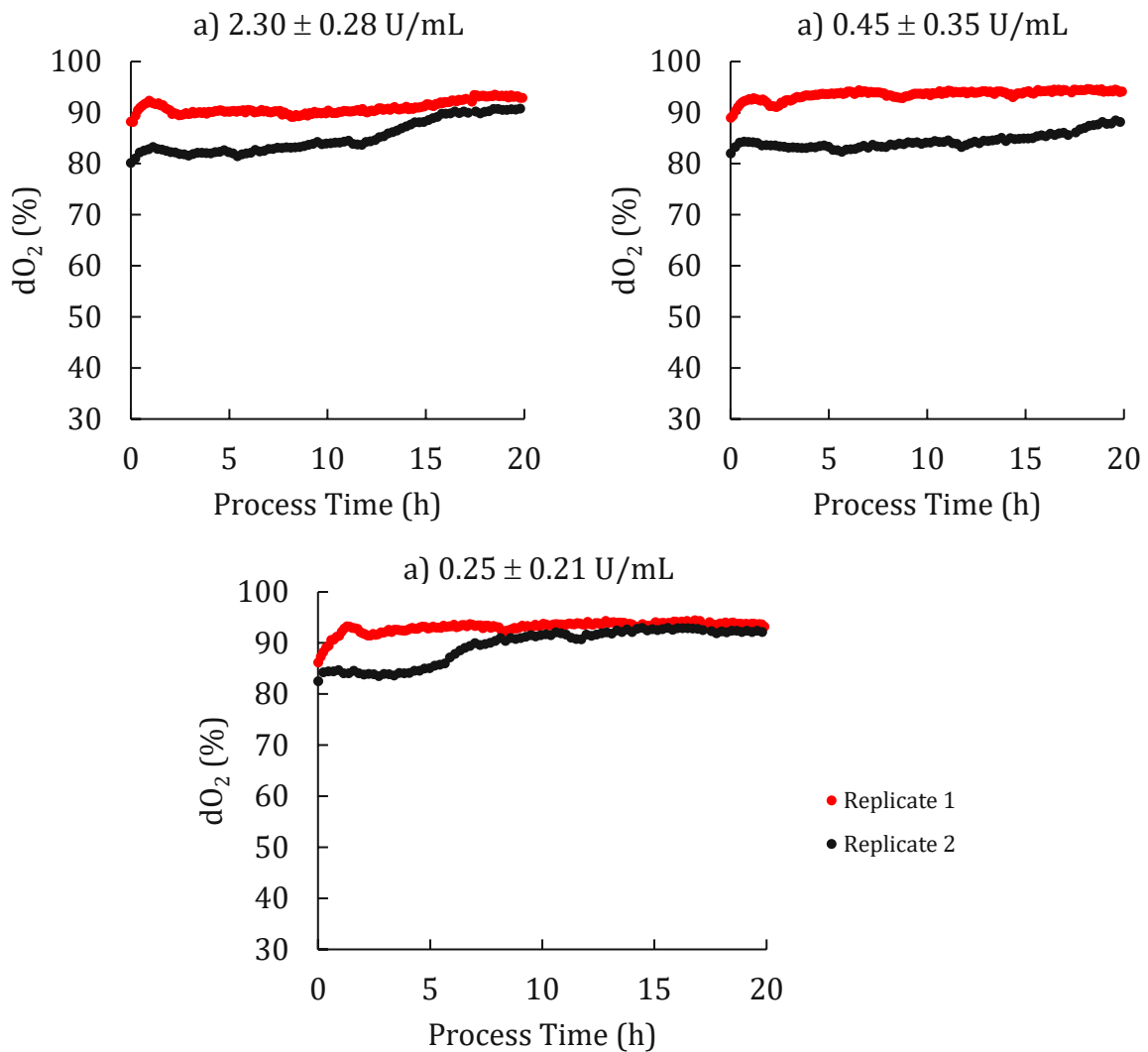


Figure 24: Comparison of the in-line  $dO_2$  profiles of three replicates each of three HRP refolding experiments that yield **low** volumetric activity after refolding. The average final volumetric activity values of the experiments are  $2.30 \pm 0.28$  U/mL (a),  $0.45 \pm 0.35$  U/mL (b),  $0.25 \pm 0.21$  U/mL (c).

The average final volumetric activity values of the three exemplary experiments shown in Figure 24 are  $2.30 \pm 0.28$  U/mL (a),  $0.45 \pm 0.35$  U/mL (b),  $0.25 \pm 0.21$  U/mL (c). Although the profiles show a higher similarity than the profiles of experiments with high final volumetric activity, the differences are considerable and therefore, the reproducibility low. Especially in respect to the marginally low obtained volumetric activities, the small  $dO_2$  range in which the profiles for HRP are detected and the extremely high reproducibility of the blank runs. Additionally, identical confounding factors apply as for the experiments described in the previous paragraph. Because of different experimental layouts, an offset of  $\pm 0.5$  h on the horizontal axis is possible and replicate 2 was performed in a reused well plate.

### 7.3.2.3.3 Summary

In conclusion, the in-line monitoring of  $dO_2$  has only a limited benefit for protein refolding screening experiments. Since no mechanistic link between protein refolding and  $dO_2$  has been reported previously, a moderate empiric correlation was established. It is shown

that refolding reactions lead to a drop of the detected  $dO_2$  values. The extent of the decline, in combination with the time period required for the recovery to a higher continuous level, are directly correlated to the refolding yield, which was quantified by fluorescence for GFP and by volumetric activity for HRP. However, this correlation is not universally applicable. Additionally, the agitation-dependent  $dO_2$  levels and the range in which shifts occur, have been shown to be highly specific for the POI and the corresponding RB composition. Although, the comparison of experiments with blanks showed that the distinctive decline of the  $dO_2$  signal is clearly caused by refolding reactions and not by the buffer composition.

Furthermore, it is hypothesized that because of the highly specific and empiric nature of the  $dO_2$  profiles of refolding experiments, the reported robustness and reproducibility of the  $dO_2$  signal during the refolding of human vascular endothelial growth factor could not be observed for GFP and HRP [14]. Hence, further investigations into mechanistic links between protein refolding and  $dO_2$  are required for the universal application of  $dO_2$  as a soft sensor for product quality and product yield. Since the purpose of screening experiments is the optimization of parameters for proteins, whose refolding properties are unknown, universally applicable knowledge on the correlation between  $dO_2$  and the protein refolding process is necessary to apply the in-line  $dO_2$  monitoring abilities of the BioLector<sup>®</sup> Pro reasonably for protein refolding.

A direct correlation between the refolding yield and the redox potential has been reported for HRP [67]. Moreover, the complementary application of the redox potential to  $dO_2$  was implemented as a soft sensor for product quality and product yield. All these observations, in combination with the fact that the redox- and  $dO_2$  profiles exhibit remarkably similar trends imply a link between the two parameters in respect to protein refolding [14]. This link between the two parameters and their relation to protein refolding bears high potential for further investigations.

### 7.3.3 Advantages of a Continuous Feed for Screening of Protein Refolding

The microfluidic technology of the BioLector<sup>®</sup> Pro was expected to be the most substantial advantage of the system over conventional screening approaches, since it enables the application of a continuous feed for protein refolding screening experiments, which is not possible with the previously reported conventional approaches [12, 33, 34].

Unfortunately, it was not possible to obtain a stable pump pressure for the membrane valves caused by a malfunction of the external pump module of the BioLector<sup>®</sup> Pro at 4 °C ambient temperature. Thus, it was not possible to investigate the application of a continuous feed for protein refolding experiments. This is an unexpected but possible outcome of a feasibility study, which this thesis constitutes. No previous reports on the subject of the application of the BioLector<sup>®</sup> for protein refolding and for the application of the device at reduced ambient temperature could be obtained beforehand.

Nevertheless, experiments related to several aspects of a continuous feed were planned. First, the ability to apply a continuous feed in combination with an automatic IPM and IPC

of the pH value could have been tested to counteract changes in the pH value, caused by the addition of solubilizate. Second, the utilization of the IPC of the pH value could have been evaluated for the control of pH-dependent kinetics of redox systems during refolding. This could lead to an expansion of possibilities for screening experiments and form the basis for the implementation of a fine tuning of redox kinetics for protein refolding. Third, the effect of various continuous feed profiles of denatured protein or buffer components on protein refolding could have been investigated and compared to pulsed feed profiles. Aside from positive linear or -exponential functions with various coefficients, also atypical negative linear and -exponential functions could have been explored.



## 8 Conclusions of the Thesis

The application of the BioLector<sup>®</sup> Pro for the screening of protein refolding was thoroughly assessed. Keeping the nature of this thesis as a feasibility study in mind, the results are satisfying and form a far-ranging basis for further studies. On the basis of the results, the four goals defined at the beginning of this thesis are evaluated in the course of the following chapters.

### 8.1 Goal One

As a prerequisite for the screening of protein refolding conditions, an at-line RPLC method for the IPM and IPC of the solubilization process was established. The goal of the IPM, a precise prediction of the refolding yield using the monomeric HRP concentration, was met, exceeding the accuracy of the prevalent SDS-PAGE tool. Additionally, the goal of the IPC, the adjustment of protein concentration during refolding to compensate for USP deviations and thereby improve the robustness of the refolding, was fulfilled.

### 8.2 Goal Two

The conventional protocol for the screening of protein parameters was adapted and established for the characteristics of the BioLector<sup>®</sup> Pro, utilizing a reverse dilution method. Furthermore, screening experiments were designed for the two model proteins, with the goal to compare the results of the BioLector<sup>®</sup> Pro and a conventional screening approach. The results have shown to be fundamentally different for HRP, which represents industrially relevant proteins of a complex tertiary structure, requiring redox systems during refolding. It is hypothesized that the main underlying reason is the controlled and constant oxygen input of the BioLector<sup>®</sup> that leads to a shift in the required redox system. Since the oxygen input in large-scale stirred tank reactors can be controlled, the ability of to control and include this factor into the design of screening experiments is a remarkable advantage for the scale-up process. That enables the comparison of this crucial process parameter between different scales and increases the robustness of the experiments. The capability of the BioLector<sup>®</sup> system to control the oxygen input via the gas composition within the reaction chamber and to monitor it via in-line dO<sub>2</sub> detection is unprecedented. Since the BioLector<sup>®</sup> Pro additionally has the ability to control the refolding temperature precisely, its results are believed to be more accurate and useful for the main purpose of small-scale screening experiments, which is the optimization of process parameters for industrial scale refolding.

### 8.3 Goal Three

The benefits of the in-line detection of fluorescence, pH and dO<sub>2</sub> of the BioLector<sup>®</sup> Pro for the screening of protein refolding parameters was comprehensively assessed for GFP and HRP.

The detected in-line fluorescence profiles match characteristics of previously reported GFP refolding experiments. But the fluorescence values are shown to be skewed, leading to an overestimation of the impact of the initial protein concentration in the resulting MLR models. However, the obtained results were similar to the ones derived from the off-line detected fluorescence values. Unfortunately, the number of fluorescent proteins of industrial relevance is low. Hence the demand for in-line fluorescence detection for protein refolding is negligible but has promising potential to be combined with labelling techniques using fluorescent chromophores [17].

The in-line monitoring of the pH value proved to be unsuitable for protein refolding experiments in its current form. pH values of higher than 8 cannot be detected at all with the BioLector® Pro because the upper limit of the dynamic range of the pH optode is exceeded. The fact that experiments below the upper limit of the optode can be monitored with only a slight downward shift, caused by the reduced temperature, is of little avail since refolding is generally conducted at rather high pH values above pH 7, to increase the reaction kinetics of established redox components.

The in-line monitoring of  $dO_2$  is of a limited benefit for protein refolding experiments. It is shown that refolding reactions lead to a drop of detected  $dO_2$  values and the extent of the decline, in combination with the time period required for the recovery to a higher continuous level, are directly correlated to the refolding yield. But this correlation is not universally applicable and highly specific for the POI. Furthermore, a very low reproducibility of the  $dO_2$  profile was observed. In regard to the high impact of the oxygen input on refolding and to the demonstrated effect of refolding reactions on  $dO_2$  values, the ability for the in-line detection of  $dO_2$  during screening experiments bears a high potential to improve the scale-up of refolding processes. Despite the missing mechanistic links between  $dO_2$  profiles and refolding yields, an improved reproducibility would open up possibilities for the empirical application of this parameter for scale-up processes.

## 8.4 Goal Four

The benefits of a constant feed for the screening of protein refolding parameters could not be evaluated due to a malfunction of the external pump module of the BioLector® Pro at 4 °C ambient temperature. This is an undesirable but conceivable outcome of a feasibility study, which this thesis constitutes.

## 9 Outlook

The fundamental scheme of the application of the BioLector<sup>®</sup> system for protein refolding, presented in this thesis, is the following: a system that has been designed for screening experiments in the field of fermentations is diverted to the field of protein refolding. However, based on the extensive experiments conducted for this thesis, two categorical problems of this approach could be identified. First, essential process parameters (e.g. temperature, pH value) differ between the two mentioned fields of application. This leads to problems, which were observed and are discussed throughout this thesis. For instance, the upper limit of the pH optode at pH 8 is not high enough to cover the pH range that is generally used for the refolding of proteins that require redox systems. Moreover, the low ambient temperature of approx. 4°C, that was required to reach the refolding temperature within the reaction chamber of the BioLector<sup>®</sup>, presumably led to the malfunction of the external pump module and impeded the application of the promising microfluidic technology. Second, the range of in-line analytical tools are not optimal for protein refolding. While the in-line detection of fluorescence, pH and dO<sub>2</sub> are at least partially of interest for protein refolding, the ability for biomass detection via light scattering is needless, while the possibility for the detection of redox potential is not existent but would be beneficial.

For the solution of the problems that were identified in the scope of this thesis, two approaches are possible. The first, and potentially more feasible, approach is the design of a high-throughput screening system, which is implicitly dedicated for the needs of protein refolding. The simplicity and subsequent cost-efficiency of such a system is potentially higher than for a multi-purpose device that is efficiently designed for both, the screening of fermentation and protein refolding. The second approach is to expand key functions and parameters of the current BioLector<sup>®</sup> system and add features, with the goal to create a multi-purpose device.

For the purpose of the adaption of the BioLector<sup>®</sup> system for the screening of protein refolding, six proposals can be formulated on the basis of the findings of this thesis:

- i. Establishment of the microfluidic technology to investigate the benefits of a continuous feed for protein refolding, either by implementing an external pump module that is functional at low temperatures around 4 °C or by implementing an active cooling system for the reaction chamber of the BioLector<sup>®</sup> system. The latter seems to be the more efficient solution since it would make the installation of the BioLector<sup>®</sup> device in a cold room dispensable and therefore simplify many aspects of the handling of the device. But on the other hand, the issue of condensation water will need to be managed.
- ii. Implementation of an oxygen and nitrogen source within a cold room for the investigation of the benefits and possibilities of a controlled oxygen input for protein refolding. An active cooling system, explicitly for the reaction chamber, would simplify the execution of this proposal.
- iii. Development of a pH optode with an extended upper limit, to be capable to monitor pH values at least up to pH 11.

- iv. Investigation of the reasons for the low reproducibility and the high protein specificity of in-line  $dO_2$  profiles during protein refolding. Additionally, the general mechanistic links between protein refolding and the parameters  $dO_2$  and redox potential needs to be investigated for a reasonable application of in-line  $dO_2$  detection for screening experiments.
- v. Development of an optode for the in-line detection of the redox potential, which has been reported to be beneficial for the characterization of refolding processes, especially in addition to the already available in-line  $dO_2$  detection [14].
- vi. Investigation of the reasons for the skewed in-line fluorescence detection as described in chapter 7.3.2.1. Furthermore, the investigation of labelling techniques using fluorescent chromophores for the quantification of protein refolding is necessary, in order to expand the field of application of in-line fluorescence detection for non-fluorescent proteins.

## 10 References

1. Kaur, J., A. Kumar, and J. Kaur, *Strategies for optimization of heterologous protein expression in E. coli: Roadblocks and reinforcements*. Int J Biol Macromol, 2018. **106**: p. 803-822.
2. Baneyx, F. and M. Mujacic, *Recombinant protein folding and misfolding in Escherichia coli*. Nat Biotechnol, 2004. **22**(11): p. 1399-408.
3. Rinas, U., et al., *Bacterial Inclusion Bodies: Discovering Their Better Half*. Trends Biochem Sci, 2017. **42**(9): p. 726-737.
4. Humer, D. and O. Spadiut, *Wanted: more monitoring and control during inclusion body processing*. World J Microbiol Biotechnol, 2018. **34**(11): p. 158.
5. Gatti-Lafranconi, P., et al., *Concepts and tools to exploit the potential of bacterial inclusion bodies in protein science and biotechnology*. FEBS J, 2011. **278**(14): p. 2408-18.
6. Rathore, A.S., et al., *Refolding of biotech therapeutic proteins expressed in bacteria: review*. Journal of Chemical Technology & Biotechnology, 2013. **88**(10): p. 1794-1806.
7. Yamaguchi, H. and M. Miyazaki, *Refolding techniques for recovering biologically active recombinant proteins from inclusion bodies*. Biomolecules, 2014. **4**(1): p. 235-51.
8. Yamaguchi, S., et al., *Protein refolding using chemical refolding additives*. Biotechnol J, 2013. **8**(1): p. 17-31.
9. Eggenreich, B., et al., *Production strategies for active heme-containing peroxidases from E. coli inclusion bodies - a review*. Biotechnol Rep (Amst), 2016. **10**: p. 75-83.
10. Eiberle, M.K. and A. Jungbauer, *Technical refolding of proteins: Do we have freedom to operate?* Biotechnol J, 2010. **5**(6): p. 547-59.
11. Vallejo, L.F. and U. Rinas, *Strategies for the recovery of active proteins through refolding of bacterial inclusion body proteins*. Microb Cell Fact, 2004. **3**(1): p. 11.
12. Humer, D., J. Ebner, and O. Spadiut, *Scalable High-Performance Production of Recombinant Horseradish Peroxidase from E. coli Inclusion Bodies*. Int J Mol Sci, 2020. **21**(13).
13. Bulaj, G., *Formation of disulfide bonds in proteins and peptides*. Biotechnol Adv, 2005. **23**(1): p. 87-92.
14. Pizarro, S.A., et al., *Biomanufacturing process analytical technology (PAT) application for downstream processing: Using dissolved oxygen as an indicator of product quality for a protein refolding reaction*. Biotechnol Bioeng, 2009. **104**(2): p. 340-51.
15. Palmer, I. and P.T. Wingfield, *Preparation and extraction of insoluble (inclusion-body) proteins from Escherichia coli*. Curr Protoc Protein Sci, 2004. **Chapter 6**: p. Unit 6 3.
16. Pramod, K., et al., *Pharmaceutical product development: A quality by design approach*. Int J Pharm Investig, 2016. **6**(3): p. 129-38.
17. Pauk, J.N., et al., *Advances in monitoring and control of refolding kinetics combining PAT and modeling*. Appl Microbiol Biotechnol, 2021. **105**(6): p. 2243-2260.

18. Singh, S.M., et al., *Solubilization of inclusion body proteins using n-propanol and its refolding into bioactive form*. Protein Expr Purif, 2012. **81**(1): p. 75-82.
19. Sasse, J. and S.R. Gallagher, *Staining proteins in gels*. Curr Protoc Mol Biol, 2009. **Chapter 10**: p. Unit 10 6.
20. Kopp, J., et al., *Development of a generic reversed-phase liquid chromatography method for protein quantification using analytical quality-by-design principles*. J Pharm Biomed Anal, 2020. **188**: p. 113412.
21. Sandra, K., I. Vandenheede, and P. Sandra, *Modern chromatographic and mass spectrometric techniques for protein biopharmaceutical characterization*. Journal of Chromatography A, 2014. **1335**: p. 81-103.
22. Fekete, S. and D. Guillarme, *Ultra-high-performance liquid chromatography for the characterization of therapeutic proteins*. TrAC Trends in Analytical Chemistry, 2014. **63**: p. 76-84.
23. Fekete, S., J.-L. Veuthey, and D. Guillarme, *Modern Column Technologies for the Analytical Characterization of Biopharmaceuticals in Various Liquid Chromatographic Modes*. Advances in Biopharmaceutical Analysis, 2015. **34**: p. 6-13.
24. Baca, M., et al., *A comprehensive study to protein retention in hydrophobic interaction chromatography*. J Chromatogr B Analyt Technol Biomed Life Sci, 2016. **1032**: p. 182-188.
25. Fekete, S., et al., *Size Exclusion Chromatography of Protein Biopharmaceuticals: Past, Present and Future*. American Pharmaceutical Review, 2018: p. 1-4.
26. Kochling, J., et al., *A platform analytical quality by design (AQbD) approach for multiple UHPLC-UV and UHPLC-MS methods development for protein analysis*. J Pharm Biomed Anal, 2016. **125**: p. 130-9.
27. Fekete, S., J.L. Veuthey, and D. Guillarme, *New trends in reversed-phase liquid chromatographic separations of therapeutic peptides and proteins: theory and applications*. J Pharm Biomed Anal, 2012. **69**: p. 9-27.
28. Mannall, G.J., N.J. Titchener-Hooker, and P.A. Dalby, *Factors affecting protein refolding yields in a fed-batch and batch-refolding system*. Biotechnol Bioeng, 2007. **97**(6): p. 1523-34.
29. Singh, A., et al., *Protein recovery from inclusion bodies of Escherichia coli using mild solubilization process*. Microb Cell Fact, 2015. **14**: p. 41.
30. Pan, S., et al., *Continuous protein refolding in a tubular reactor*. Chemical Engineering Science, 2014. **116**: p. 763-772.
31. Pan, S., et al., *Engineering batch and pulse refolding with transition of aggregation kinetics: An investigation using green fluorescent protein (GFP)*. Chemical Engineering Science, 2015. **131**: p. 91-100.
32. Malavasi, N.V., et al., *The effect of temperature on protein refolding at high pressure: Enhanced green fluorescent protein as a model*. Process Biochemistry, 2014. **49**(1): p. 54-60.

33. Wang, Y., et al., *A Systematic Protein Refolding Screen Method using the DGR Approach Reveals that Time and Secondary TSA are Essential Variables*. *Sci Rep*, 2017. **7**(1): p. 9355.
34. Vincentelli, R., et al., *High-throughput automated refolding screening of inclusion bodies*. *Protein Sci*, 2004. **13**(10): p. 2782-92.
35. Funke, M., et al., *Microfluidic biolector-microfluidic bioprocess control in microtiter plates*. *Biotechnol Bioeng*, 2010. **107**(3): p. 497-505.
36. Blesken, C., et al., *The microfluidic bioreactor for a new era of bioprocess development*. *Engineering in Life Sciences*, 2016. **16**(2): p. 190-193.
37. Battistutta, R., A. Negro, and G. Zanotti, *Crystal structure and refolding properties of the mutant F99S/M153T/V163A of the green fluorescent protein*. *Proteins: Structure, Function and Genetics*, 2000. **41**(4): p. 429-437.
38. Yang, F., L.G. Moss, and J. George N. Phillips, *The Molecular structure of green fluorescent protein*. *Nature Biotechnology*, 1996. **14**.
39. Shimomura, O., F.H. Johnson, and Y. Saiga, *Extraction, Purification and Properties of Aequorin, a Bioluminescent Protein from the Luminous Hydromedusan, Aequorea*. *Journal of Cellular and Comparative Physiology*, 1962. **59**(3): p. 223-239.
40. Remington, S.J., *Green fluorescent protein: a perspective*. *Protein Sci*, 2011. **20**(9): p. 1509-19.
41. Chalfie, M., et al., *Green Fluorescent Protein as a Marker for Gene Expression*. *Science*, 1994. **263**(5148): p. 802-805.
42. Veitch, N.C., *Horseradish peroxidase: a modern view of a classic enzyme*. *Phytochemistry*, 2004. **65**(3): p. 249-59.
43. Welinder, K.G., *Covalent structure of the glycoprotein horseradish peroxidase (EC 1.11.1.7)*. *FEBS Letters*, 1976. **72**(1): p. 19-23.
44. Gajhede, M., et al., *Crystal structure of horseradish peroxidase C at 2.15Å resolution*. *Nature Structural Biology*, 1997. **4**(12): p. 1297-1032.
45. Wuhler, M., C.H. Hokke, and A.M. Deelder, *Glycopeptide analysis by matrix-assisted laser desorption/ionization tandem time-of-flight mass spectrometry reveals novel features of horseradish peroxidase glycosylation*. *Rapid Commun Mass Spectrom*, 2004. **18**(15): p. 1741-8.
46. Wuhler, M., et al., *New features of site-specific horseradish peroxidase (HRP) glycosylation uncovered by nano-LC-MS with repeated ion-isolation/fragmentation cycles*. *Biochim Biophys Acta*, 2005. **1723**(1-3): p. 229-39.
47. Yakovleva, J., et al., *Microfluidic enzymeimmunoassay using silicon microchip with immobilized antibodies and chemiluminescence detection*. *Analytical Chemistry*, 2002. **74**: p. 2994-3004.
48. Van Gijlswijk, R.P.T., E.G.; Peekel, I.; Bloem, J.; Van Velzen, M.A.; Heetebrij, R.J.; Tanke, H.J. , *Use of horseradish peroxidase-and fluorescein-modified cisplatin derivatives for simultaneous labeling of nucleic acids and proteins*. *Clinical Chemistry*, 2002. **48**: p. 1352-1359.

49. Moody, M.D., et al., *Array-Based ELISAs for High-Throughput Analysis of Human Cytokines*. Biotechniques, 2001. **31**: p. 186-194.
50. Alonso Lomillo, M.A., J.G. Ruiz, and F.J.M. Pascual, *Biosensor based on platinum chips for glucose determination*. Analytica Chimica Acta, 2005. **547**(2): p. 209-214.
51. Azevedo, A.M., et al., *Ethanol biosensors based on alcohol oxidase*. Biosens Bioelectron, 2005. **21**(2): p. 235-47.
52. Vasileva, N., et al., *Application of immobilized horseradish peroxidase onto modified acrylonitrile copolymer membrane in removing of phenol from water*. Int J Biol Macromol, 2009. **44**(2): p. 190-4.
53. Bhunia, A., S. Durani, and P.P. Wangikar, *Horseradish peroxidase catalyzed degradation of industrially important dyes*. Biotechnology and Bioengineering, 2001. **72**: p. 562-567.
54. Colonna, S., et al., *Horseradish peroxidase catalysed sulfoxidation is enantioselective*. Journal of the Chemical Society, Chemical Communications, 1992. **4**: p. 357-358.
55. Sakai, S., et al., *Horseradish peroxidase-catalyzed formation of hydrogels from chitosan and poly(vinyl alcohol) derivatives both possessing phenolic hydroxyl groups*. Carbohydr Polym, 2014. **111**: p. 404-9.
56. Ebner, J., et al., *At-Line Reversed Phase Liquid Chromatography for In-Process Monitoring of Inclusion Body Solubilization*. Bioengineering, 2021. **8**(6).
57. Wiedenmann, J., F. Oswald, and G.U. Nienhaus, *Fluorescent proteins for live cell imaging: opportunities, limitations, and challenges*. IUBMB Life, 2009. **61**(11): p. 1029-42.
58. Gao, Y.-G., et al., *Refolding of Lysozyme at High Concentration in Batch and Fed-batch Operation*. Korean Journal of Chemical Engineering, 2002.
59. S., K. and K. Y., *Continuous refolding of lysozyme with fed-batch addition of denatured protein solution*. Process Biochemistry, 2000.
60. DeLisa, M.P., et al., *Monitoring GFP-Operon Fusion Protein Expression During High Cell Density Cultivation of Escherichia coli Using an On-line Optical Sensor*. Biotechnology and Bioengineering, 1999. **65**(1): p. 54-64.
61. Slouka, C., et al., *Monitoring and control strategies for inclusion body production in E. coli based on glycerol consumption*. J Biotechnol, 2019. **296**: p. 75-82.
62. Slouka, C., et al., *Custom made inclusion bodies: impact of classical process parameters and physiological parameters on inclusion body quality attributes*. Microb Cell Fact, 2018. **17**(1): p. 148.
63. Kopp, J., et al., *Impact of Glycerol as Carbon Source onto Specific Sugar and Inducer Uptake Rates and Inclusion Body Productivity in E. coli BL21(DE3)*. Bioengineering (Basel), 2017. **5**(1).
64. Kopp, J., et al., *Boosting Recombinant Inclusion Body Production-From Classical Fed-Batch Approach to Continuous Cultivation*. Front Bioeng Biotechnol, 2019. **7**: p. 297.
65. Childs, R.E. and W.G. Bardsley, *The Steady-State Kinetics of Peroxidase with 2,2'-Azine-di-(3-ethyl-benzthiazoline-6-sulphonic acid) as Chromogen*. Biochemical Journal, 1975. **145**(1): p. 93-103.



66. Chen, J., et al., *Different Effects of L-Arginine on Protein Refolding: Suppressing Aggregates of Hydrophobic Interaction, Not Covalent Binding*. Biotechnology Progress, 2008.
67. Ebner, J., *Development of a refolding and capture protocol for HRP IBs produced in E. coli*. 2021, Vienna University of Technology: Vienna.
68. Asad, S., et al., *Studies on the refolding process of recombinant horseradish peroxidase*. Mol Biotechnol, 2013. **54**(2): p. 484-92.
69. Liu, D.K. and S.G. Chang, *Kinetic study of the reaction between cystine and sulfide in alkaline solutions*. Can. J. Chem., 1986. **65**.
70. Gorin, G., P.A. Martic, and G. Doughty, *Kinetics of the Reaction of N-Ethylmaleimide with Cysteine and Some Congeners*. Archives of Biochemistry and Biophysics, 1966. **115**: p. 593-597.
71. Duursma, E.K. and M.P.R.M. Bioisson, *Global oceanic and atmospheric oxygen stability considered in relation to the carbon cycle and to different time scales*. Oceanologica Acta, 1994. **17**: p. 117-141.